Etudes sur la matrice de mélange leptonique et sur la matière noire

F. Palorini

N° d'ordre 131-2008

Thèse

présentée devant

l'Université Claude Bernard Lyon-1

pour l'obtenition du

DIPLOME de DOCTORAT

(arrêté du 7 août 2006)

par

Federica PALORINI

Études sur la matrice de mélange leptonique et sur la matière noire

Soutenue le 15 septembre 2008
devant la Commission d'Examen

Jury :	Mme	L.	Covi	Rapporteur
	Mme	S.	Davidson	Directrice de thèse
	M.	A.	Deandrea	Co-directeur de thèse
	M.	G.	Isidori	Rapporteur
	M.	C.	Savoy	Président du jury

REMERCIEMENTS

Je remercie d'abord Monsieur Bernard Ille, Directeur de l'Institut de Physique Nucléaire, et Aldo Deandrea, Responsable du Groupe de Physique Théorique, pour m'avoir accueillie dans ce laboratoire.

Ma gratitude s'adresse aussi aux membres de mon jury de thèse, Laura Covi, Sacha Davidson, Aldo Deandrea, Gino Isidori et Carlos Savoy, pour les échanges très enrichissants.

Une gratitude particulière est destinée à mon directeur de thèse Sacha Davidson, qui m'a permis d'accroître mes connaissances scientifiques et de découvrir des points de vue originaux sur l'activité de recherche.

Je remercie également Laura Covi, qui m'a introduite dans le monde de la cosmologie, et mes collaborateurs, Carola F. Berger, Julia Garayoa, Sabine Kraml et Nuria Rius. Sans leur expertise, ce travail n'aurait pas été possible.

Mon séjour à l'IPNL a été rendu agréable par l'amitié des doctorants et par le soutien du Groupe de Physique Théorique et des Services Techniques.

CONTENTS

ABSTRACT

Neutrino oscillations, the baryon asymmetry and dark matter are important evidences of new physics beyond the Standard Model.

Neutrino oscillations imply neutrino masses and a lepton mixing matrix that can contribute to flavour violating processes and CP violation at low energies, accessible to next experiments, and to the CP violation necessary for baryogenesis. Among the most interesting implications, is flavour violation in the lepton sector, but it has only been observed in neutrino oscillations. By analogy with quarks, it is then possible to deduce a principle of minimal flavour violation for leptons. Since such formulation is not straightforward in the lepton sector, we discuss different possibilities. Then we propose a definition which could be applied to various models and could help us in selecting between the possible neutrino mass generating mechanisms.

Furthermore, if the seesaw mechanism describes neutrino masses, we can have a natural explanation to the baryon asymmetry of the universe with leptogenesis. In the context of leptogenesis including flavour effects, we demonstrate that the baryon asymmetry of the universe is insensitive to the low energy CP violating phases. This study is performed in the minimal extension of the Standard Model, with the introduction of 3 right-handed neutrinos and type-1 seesaw, only, and it is extended, in a following study, to the supersymmetric case. Since the seesaw parameter space is quite large, the numerical study is developed with the Markov Chain Monte Carlo method.

In relation to dark matter, we study a scenario with very weakly coupled candidates and their production through the decay of a charged long-lived scalar particle. We compute the scalar particle number density, evaluating its gauge interactions, and compare it with Big-Bang Nucleosynthesis bounds. Then, we apply our results to the Minimal Supersymmetric Standard Model scenario with axino or gravitino as Lightest Supersymmetric Particle and stau or stop as Next to Lightest Supersymmetric Particle.

First Part:
Introduction

I

EVIDENCES OF NEW PHYSICS

I.1 Neutrino oscillations

The Standard Model (SM) of particle physics contains 3 left-handed neutrinos ν_e, ν_μ, ν_τ that are weakly-interacting particles and have null mass. This choice is in agreement with the analysis of the invisible Z-boson width at LEP [1], from which we deduce three "active" neutrinos with masses below the Z mass. These left-handed neutrinos do not mix, therefore, neither flavour changes nor neutrino oscillations are predicted in the SM.

Nevertheless, there are now many different data supporting the hypothesis of neutrino oscillations which come from experiments measuring fluxes of neutrinos produced in the Sun, in the atmosphere, in accelerators and nuclear reactors. The first hint to neutrino oscillations was given by solar and atmospheric neutrino experiments. A deficit in the neutrino solar flux was already found in the Homestake experiment [2]. The flux of electron neutrinos from the Sun was $\sim 1/3$ the value predicted by the Standard Solar Model (SSM) [3]. But the most important confirmation to the so-called "solar anomaly" arrived with the SNO experiment. It was in fact able to distinguish the electron neutrino flux ϕ_{ν_e} from the total neutrino flux ϕ_t via charged and neutral current neutrino interactions in the detector. In 2001 it found a ratio $\phi_{\nu_e}/\phi_t \sim 0.34$ compatible with $\nu_{\mu,\tau}$ appearance, and a value for the total flux $\phi_t \sim 4.94\ 10^{-6} cm^{-2} s^{-1}$ in agreement with the SSM predictions [4]. KamLAND, confirmed the solar anomaly discovering disappearance of $\overline{\nu}_e$ from terrestrial reactors [5]. In the meantime, SuperKamiokande found a second neutrino anomaly, analysing fluxes of atmospheric

neutrinos, that was confirmed in 2004 by the reactor neutrino experiment K2K. It observed a dependence on the zenith angles in the muon neutrino flux, correlated with the distance covered by neutrinos. These data were consistent with ν_μ disappearance [6].

All those results are now interpreted with flavour change in the lepton sector. The simplest way to include it in the SM is to introduce a neutrino mass matrix which is not diagonalized in the charged lepton mass basis. It implies flavour change and controls neutrino oscillations. The oscillation probability between two flavours a, b is indeed given by:

$$\begin{aligned} P(\overset{(-)}{\nu}_a \to \overset{(-)}{\nu}_b) &= |\sum_i U^*_{ai} e^{-im_i^2 L/2E} U_{bi}|^2 = \\ &= \delta_{ab} - 4\sum_{i>j} \Re(U^*_{ai}U_{bi}U_{aj}U^*_{bj}) \sin^2(\Delta m^2_{ij}\frac{L}{4E}) \\ &\overset{(+)}{(-)} \; 2\sum_{i>j} \Im(U^*_{ai}U_{bi}U_{aj}U^*_{bj}) \sin(\Delta m^2_{ij}\frac{L}{2E}) \end{aligned} \tag{I.1}$$

where U is the mixing matrix relating the neutrino and charged lepton mass bases, m_i the neutrino mass eigenstates, L the distance covered by the neutrino beam and E its energy.

The solar and atmospheric anomalies are approximately two flavour oscillations. The solar one is interpreted as an oscillation $\nu_e \to \nu_{\mu,\tau}$, governed by a mass square difference $\Delta m^2_\odot \sim 7.6\ 10^{-5}\ eV^2$ and a mixing angle $\sin^2\theta_\odot \sim 0.32$, while the atmospheric anomaly as an oscillation $\nu_\mu \to \nu_\tau$ with $\Delta m^2_{atm} \sim 2.4\ 10^{-3}\ eV^2$ and a mixing angle $\sin^2\theta_{atm} \sim 0.5$. Those 2 flavour oscillation probabilities are approximations of a 3 flavour mixing, governed by a 3×3 unitary mixing matrix, usually referred to as U_{MNS} [1]. This matrix contains 3 mixing angles and 1 phase, if neutrinos are Dirac particles. However, neutrinos are neutral particles and can be Majorana, i.e. identical to their anti-particle. In this scenario, two more phases must be added to the MNS lepton mixing matrix.

[1] There are still two anomalies in neutrino data that are not understood in the 3 oscillation picture, from LSND [7] and low energy data in MinibooNE [8].

The lepton mixing matrix is usually parametrized in the following way:

$$U_{MNS} = \begin{bmatrix} c_{12}c_{13} & s_{12}c_{13} & s_{13}e^{-i\delta} \\ -s_{12}c_{23} - c_{12}s_{23}s_{13}e^{i\delta} & c_{12}c_{23} - s_{12}s_{23}s_{13} & s_{23}c_{13} \\ s_{12}s_{23} - c_{12}c_{23}s_{13}e^{i\delta} & -c_{12}s_{23} - s_{12}c_{23}s_{13}e^{i\delta} & c_{23}c_{13} \end{bmatrix} \times \begin{bmatrix} e^{i\alpha} & 0 & 0 \\ 0 & e^{i\beta} & 0 \\ 0 & 0 & 1 \end{bmatrix}$$

The Dirac phase δ can be evaluated in neutrino oscillations, since it implies a difference between neutrino or anti-neutrino oscillation probabilities, as we can see from eq. (I.1). Notice that this phase always appears in the U_{MNS} with $\sin\theta_{13}$, which induces $\nu_\mu \leftrightarrow \nu_e$ oscillations at the atmospheric frequency. The value of θ_{13}, not known at the moment but constrained to be $\lesssim 10^\circ$ [9], therefore determines the capability of future experiments to detect CP violation in neutrino oscillations. While the α and β Majorana phases can be measured in experiments sensitive to lepton number violation, like neutrinoless double beta decays [10]. However, in this case it is hard to extract a value for those phases because of the uncertainties on nuclear matrices involved in the reaction.

Oscillation experiments are insensitive to the determination of the absolute neutrino mass scale. Laboratory bounds can be given in measurements of tritium beta decay, where they have set a limit on $m_{\nu_e} = (\sum_i |U_{ei}|^2 m_i^2)^{1/2} < 2.2$ eV [11, 12], in future experiments they are expected to reach a sensitivity of 0.2 eV [13]. In case of Majorana neutrinos, neutrinoless double beta decays give a bound on $|m_{ee}| = |\sum_i U_{ei}^2 m_i| < (0.44 \div 0.66) h_N$ eV , where h_N takes into account the uncertainties on the nuclear matrices [14]. While from cosmology, the WMAP collaboration gives a bound $\sum_i m_i < 0.61$ eV by a combination of data from WMAP 5-year run on Cosmic Microwave Background (CMB) anisotropies, Baryon Acoustic Oscillations (BAO) and Type Ia Supernovae data [15]. Observations of CMB thermal fluctuations give the best determinations of various cosmological parameters, as we can see in the following. A comprehensive explanation of the more recent developments in cosmology can be found in [16]. With respect to neutrino physics, an updated overview of neutrino experiments is given in [17].

I.2 The baryon asymmetry of the universe

Observations tell us that the known universe is made of matter. Indeed we do not see γ rays from particle and anti-particle annihilations so that we can deduce there is an excess of matter over anti-matter. Visible matter is mainly composed by atoms, implying a baryon asymmetry:

$$Y_B = \frac{n_B - n_{\overline{B}}}{s} \neq 0 \tag{I.2}$$

where n_B and $n_{\overline{B}}$ are the number density of baryons and anti-baryons respectively, and s is the entropy. Measurements of the baryon number density come from the estimation of Big-Bang Nucleosynthesis (BBN) [18] relic densities and from measurements of the CMB thermal fluctuations . Those independent measurements are compatible. The WMAP results, combined with BAO and Supernovae, give: $Y_B \sim 8.75 \pm 0.23 \times 10^{-11}$ [15]. We have no definite information on the lepton asymmetry, however there is an undetectable CMB of neutrinos which could contain a large lepton asymmetry.

There are strong motivations to believe that a dynamical mechanism at the early universe is necessary to explain the present value of the baryon asymmetry. Indeed, even if the universe was born with a baryon asymmetry, this would have been diluted during its period of exponential expansion, called inflation. Therefore, in order to have a baryogenesis at the origin, when the universe is repopulated by a hot thermal plasma after inflation, the three Sakharov must be satisfied:

1. B violation, to evolve from a state with $B = 0$ to a state with $B \neq 0$;

2. C and CP violation, in order to have a different behaviour of particles and anti-particles;

3. Out-of-equilibrium dynamics, indeed CPT conservation implies that particles and anti-particles have the same mass and, thus, the same abundance if in equilibrium.

In the Standard Model of particle physics all the conditions are present. Indeed, even if baryon number is conserved at three level, B violation is provided by quantum anomalies and non-perturbative processes. C and CP violation are included in the CKM matrix and the out-of-equilibrium dynamics is provided at the electroweak phase transition. Nevertheless, the two last conditions are not successful, since CP violation

provided by the CKM matrix is too small and the Higgs potential, inducing the out-of-equilibrium, is too smooth for Higgs masses bigger than 70 GeV [19]. Therefore, an extension of the Standard Model scenario is inevitable.

I.3 Dark matter

Cosmology and astronomy provide another strong evidence of new physics. Observations suggest that most of the mass in the Universe is some non luminous dark matter, of a yet unknown composition. This dark matter does not emit or absorb electromagnetic radiation at every known wavelength, while its gravitational interactions dominate on scales from tiny galaxies, to the largest scales observed.

The cosmological matter density is usually quoted by using the matter fraction of the critical energy density $\Omega_m = \rho_m/\rho_c$ multiplied by h^2, where $h \equiv H_0/100$ km s^{-1} Mpc^{-1} = 0.701 ± 0.013 is the present Hubble parameter. Ω_m could be evluated by determining the mass-to-light ratio $\Upsilon = M/L$ of some system and then multiplying this by the average luminosity density of the universe, so $\Omega_{vis} = \Upsilon\mathcal{L}/\rho_c$, where ρ_c is the critical density. The value of Ω_m obtained with these measurements, corresponding to mass associated with light, provides less than 1% of the critical density, $\Omega_{vis} \lesssim 0.01$. While, as we will see below, from other kinds of determinations there is strong evidence that $\Omega_m \simeq 0.3$, thus supporting the idea that such a kind of dark matter exists.

Evidences for dark matter are provided at very different scales. The earliest indication for dark matter came at galactic scales from the observation that various luminous objects (stars, gas clouds, globular clusters, or entire galaxies) move faster then one would expect if they only felt the Newtonian gravitational attraction of other visible objects. An important example is the measurement of the *rotation curves* of spiral galaxies, namely the graph of circular velocities of stars and gas as a function of their distance from the galactic centre. Observed rotation curves, usually exhibit a characteristic flat behavior at large distances, that is outside the edge of the visible disk. This leads to a lower bound on the dark matter density, $\Omega_m \gtrsim 0.1$.

Moving to larger scales, the methods of determining Ω_m involve observation of clusters of galaxies. These observations include measurements of the peculiar velocities of galaxies in the cluster, which are a measure of their potential energy if the cluster

satisfies the virial theorem; measurements of the X-ray gas temperatures in the cluster, which again correlate with the gravitational potential felt by the gas; and, most directly, studies of gravitational lensing of background galaxies on the cluster. These measurements are consistent with a value of $\Omega_m \sim 0.2-0.3$. A recent spectacular proof comes from a weak lensing observation of a unique cluster merger. Due to the collision of two clusters, the X-ray emitting plasma is spatially segregated from the collisionless dark matter galaxies. The gravitational lensing reconstruction shows a spatial offset of the centre of the total mass from the center of the baryonic peaks [20].

However, the observations discussed above do not allow us to determine the *total* amount of dark matter in the universe. The currently most accurate determination of Ω_{DM} comes from global fits of cosmological parameters to a variety of observations. For the most recent measurements of the anisotropy of the CMB provided by WMAP 5-year run, combined with data from Baryon Acoustic Oscillations and Type Ia Supernovae, the dark matter density is set to [15]:

$$\Omega_m h^2 = 0.1143 \pm 0.0034. \tag{I.3}$$

Since ordinary matter is baryonic, the first proposal was to assume also this composition for dark matter. The main baryonic candidates are MAssive Compact Halo Objects (MACHOs) nevertheless, as we have seen in the chapter before, the measurements on BBN relic densities and from CMB are consistent and set a limit to the number of baryons that can exist in the universe. Expressed in baryon density over critical density data from WMAP 5 year only give $0.02149 \leq \Omega_b h^2 \leq 0.02397$. Hence, the baryon density is clearly too small to account for the whole dark matter in the universe, then we have to focus our attention on non-baryonic candidates.

Candidates for non-baryonic dark matter must satisfy several conditions: they must be stable on cosmological time scales, otherwise they would have decayed by now, they must interact very weakly with electromagnetic interaction, otherwise they wouldn't qualify as *dark* matter, and they must have the right relic density. Furthermore, from studies of galaxy formations, they must be "cold", that is non relativistic at the time galaxies just started to form. Hot dark matter cannot cluster on galaxy scales until it has cooled to non-relativistic speeds and, so, gives rise to a considerably different primordial fluctuation. The leading SM dark matter candidate could be the neutrino, but it is very light and can contribute only to the hot dark matter density. Therefore,

also the requirement of non-baryonic cold dark matter implies an extension of the SM.

References

[1] W. M. Yao *et al.* [Particle Data Group], J. Phys. G **33** (2006) 1.

[2] B. T. Cleveland *et al.*, Astrophys. J. **496** (1998) 505.

[3] J. N. Bahcall, M. H. Pinsonneault and S. Basu, Astrophys. J. **555** (2001) 990 [arXiv:astro-ph/0010346]. J. N. Bahcall, Phys. Rev. C **65** (2002) 025801 [arXiv:hep-ph/0108148].

[4] B. Aharmim *et al.* [SNO Collaboration], Phys. Rev. C **72** (2005) 055502 [arXiv:nucl-ex/0502021].

[5] T. Araki *et al.* [KamLAND Collaboration], Phys. Rev. Lett. **94** (2005) 081801 [arXiv:hep-ex/0406035].

[6] Y. Ashie *et al.* [Super-Kamiokande Collaboration], Phys. Rev. Lett. **93** (2004) 101801 [arXiv:hep-ex/0404034]. E. Aliu *et al.* [K2K Collaboration], Phys. Rev. Lett. **94** (2005) 081802 [arXiv:hep-ex/0411038].

[7] A. Aguilar *et al.* [LSND Collaboration], Phys. Rev. D **64** (2001) 112007 [arXiv:hep-ex/0104049].

[8] A. A. Aguilar-Arevalo *et al.* [The MiniBooNE Collaboration], Phys. Rev. Lett. **98** (2007) 231801 [arXiv:0704.1500 [hep-ex]].

[9] M. Apollonio *et al.* [CHOOZ Collaboration], Phys. Lett. B **466** (1999) 415 [arXiv:hep-ex/9907037].

[10] H. V. Klapdor-Kleingrothaus *et al.*, Eur. Phys. J. A **12** (2001) 147 [arXiv:hep-ph/0103062].

[11] V. M. Lobashev, Nucl. Phys. A **719** (2003) 153.

[12] C. Kraus *et al.*, Eur. Phys. J. C **40** (2005) 447 [arXiv:hep-ex/0412056].

[13] A. Osipowicz *et al.* [KATRIN Collaboration], arXiv:hep-ex/0109033.

[14] A. Strumia and F. Vissani, Nucl. Phys. B **726** (2005) 294 [arXiv:hep-ph/0503246].

[15] J. Dunkley *et al.* [WMAP Collaboration], arXiv:0803.0586 [astro-ph]. E. Komatsu *et al.* [WMAP Collaboration], arXiv:0803.0547 [astro-ph].

[16] S. Dodelson *Modern Cosmology*, Academic Press.

[17] A. Strumia and F. Vissani, arXiv:hep-ph/0606054.

[18] R. H. Cyburt, B. D. Fields, K. A. Olive and E. Skillman, Astropart. Phys. **23** (2005) 313 [arXiv:astro-ph/0408033]. G. Steigman, Int. J. Mod. Phys. E **15** (2006) 1 [arXiv:astro-ph/0511534]. G. Steigman, Ann. Rev. Nucl. Part. Sci. **57** (2007) 463 [arXiv:0712.1100 [astro-ph]].

[19] A. D. Dolgov, Phys. Rept. **222** (1992) 309.

[20] D. Clowe, M. Bradac, A. H. Gonzalez, M. Markevitch, S. W. Randall, C. Jones and D. Zaritsky, Astrophys. J. **648** (2006) L109 [arXiv:astro-ph/0608407].

II

THE FLAVOUR PROBLEM

II.1 SM flavour symmetry

As we said in section I.1, in the Standard Model of particle physics we do not expect flavour violation in the lepton sector. The kinetic lagrangian for the SM leptons is given by:

$$L_c = \overline{\ell} \not{D} \, \ell + \overline{e}_R \not{D} \, e_R. \tag{II.1}$$

where the $SU(2)$ lepton doublet, ℓ, is repeated over the three families, and the right-handed neutrinos are not included. This lagrangian has an accidental global flavour symmetry under the action of the group $G_{SMl} = U_\ell(3) \times U_e(3)$. That is, if we consider the three component vector ℓ, the kinetic term is invariant under the application $\ell \to V\ell$, where $V \in U_\ell(3)$. To this kinetic term we add the renormalizable yukawa coupling:

$$L_Y = \overline{\ell} \mathbf{Y_e} H_u^c e_R + h.c. \tag{II.2}$$

that breaks the symmetry group into the group $U_{L_e}(1) \times U_{L_\mu}(1) \times U_{L_\tau}(1)$. This residual symmetry is large and can be identified with the three family lepton number conservations. Therefore, we do not have mixing between lepton families, and neutrino oscillations or flavour violating processes are not predicted in the Standard Model.

Nevertheless, some new physics beyond the SM should exist if we want to explain dark matter, neutrino oscillations and baryon asymmetry. This new physics is surely flavoured in the lepton sector and must behaves in agreement with present strong bounds on lepton flavour violating processes. Neutrino oscillations are indeed explained

with the introduction of a neutrino mass matrix $[m_\nu]$ in the lepton doublet space which is not simultaneously diagonalised with the $Y_e Y_e^\dagger$ operator already present. As a consequence, it reduces the residual flavour symmetry and implies a mixing between lepton families that, besides neutrino oscillations, allows flavour violating processes. These processes have not been seen yet and the strongest upper bound is given on $\mu \to e\gamma$, with $BR < 1.2\times10^{-11}$ [1]. However, the introduction of the neutrino matrix opens new questions. An adequate neutrino mass generation mechanism should explain the smallness of neutrino masses or the Dirac or Majorana neutrino nature, furthermore, it would be really interesting to find a scenario were also baryon asymmetry and/or dark matter are explained. There are theoretical motivations to believe that this new physics should be visible at energies accessible to LHC. Indeed it could preserve the theory from an hierarchy problem and, in some extension of the Standard Model, could also provide a dark matter candidate. Since, as we have seen, flavour is not a symmetry for leptons, this new physics can be flavoured and encounter the so called "flavour problem" described in the following.

II.2 The non-renormalizable flavour violating operator

The effects of new physics at the electroweak scale are parametrised by non renormalizable operators, O_n^d, built by the known fields:

$$L_{SM} = L_{gauge}(\psi_i, A) + L_{Higgs}(\psi_i, A, \phi) + \sum_{d\geq 5} \frac{c_n}{\Lambda^{d-4}} O_n^d(\psi_i, A, \phi). \tag{II.3}$$

The high energy experiments completely determine the form of such operators thanks to the direct production of new particles. However, even before attaining the necessary energies, we can deduce some of their properties starting from the low energy data. At present, very strong bounds exist on lepton flavour violating processes. At low energy, flavour violating decays of charged leptons are described by a dimension six operator of the form:

$$\frac{O_{e\gamma}^{\alpha\beta} v}{m_{NP}^2} \bar{e}_\alpha \sigma^{\mu\nu} P_R e_\beta F_{\mu\nu} + h.c. \tag{II.4}$$

where $O_{e\gamma}^{\alpha\beta}$ is a dimensionless coefficient and m_{NP}^2 is the new physics (matching) scale. The flavour off-diagonal elements give flavour violating radiative decays for charged leptons:

$$\Gamma(l_\alpha \to l_\beta \gamma) = \frac{e^2 m_\alpha^5}{16\pi}(|A_L^{\alpha\beta}|^2 + |A_R^{\alpha\beta}|^2) \tag{II.5}$$

with $m_\alpha A_{R,L} = 2O_{e\gamma}^{\alpha\beta,*\beta\alpha} v/m_{NP}^2$.

The present bounds on flavour violating processes put strong constraints on the form of the coefficients $A_{L,R}$, that can be translated into a strong lower bound on the new physics scale if we take $O_{e\gamma}^{\alpha\beta}$ of order $O(1)$. Indeed, defining the branching ratio as:

$$BR \equiv \frac{\Gamma(l_\alpha \to l_\beta \gamma)}{\Gamma(l_\alpha \to l_\beta \nu \bar{\nu})} \simeq \frac{192\pi^3 \alpha v^2}{G_F^2 m_\alpha^2} \frac{(|O_{e\gamma}^{\alpha\beta}|^2 + |O_{e\gamma}^{\beta\alpha}|^2)}{m_{NP}^4} \tag{II.6}$$

and considering the process $\mu \to e\gamma$, which has the strongest bound, we obtain:

$$m_{NP} \gtrsim 10^4 \text{TeV} \times (|O_{e\gamma}^{\mu e}|^2 + |O_{e\gamma}^{e\mu}|^2). \tag{II.7}$$

The form of the coefficients $A_{L,R}$ is specified by the high-energy physics scenario. In order to respect the present bounds on flavour violating processes and allow some new physics at the TeV scale, we need a principle of minimal flavour violation for leptons that restricts the form of the non-renormalizable operators.

II.3 Minimal flavour violation

Minimal Flavour Violation (MFV) is a principle that was first proposed in the quark sector [2, 3], where the flavour and CP violation of the CKM matrix are observed in many different ways. We can determine the CKM angles at the tree level and the measured loop effects on flavour changing neutral currents (FCNC) are those predicted by the Standard Model. Thus, the new effects in loops coming from new physics should be smaller than the SM ones [4]. Similarly to the situation explained above for the leptons sector, we have two possible scenarios. Either the new degrees of freedom carrying flavour appear at very high energy, and they are not early testable. Or, at the TeV scale the flavour changing couplings are suppressed by a MFV symmetry principle.

So, Minimal Flavour Violation is a principle introduced in the quark sector in order to suppress new particle interactions and respect present data. This principle

becomes a useful tool in model building at the TeV scale since it is very predictive and contemporarily includes the most part of models in accord with quark flavour physics. In [2] they define minimal flavour violation where the SM yukawas are the only source of quark flavour symmetry breaking. With this definition flavour change and CP violation in the quark sector are proportional to the CKM matrix and the quark eigenvalues. Thus, MFV becomes a predictive framework that encompasses many models. As we have seen before, the lepton sector differs sensibly. A new physics must exist to accommodate neutrino oscillations but flavour change has not been seen in flavour violating processes yet. Thus we do not know if the lepton mixing matrix controls neutrino oscillations and flavour violation.

In our work reproduced in Chapter 1 we discuss the possibility of defining a principle of minimal flavour violation in the lepton sector, where the lepton mixing matrix angles are not measured with a precision comparable with the CKM one [5] and strong upper bounds on lepton flavour violating processes exist. A first definition of minimal lepton flavour violation has been proposed by Cirigliano et al. [6], where they allow only the operators Y_e and $[m_\nu]$ to define a basis in the lepton doublet space. In that case, the scenario is very predictive and flavour violation is driven by the U_{MNS} matrix. Some variations have been studied in subsequent papers [7, 8]. However, we look for a more extensive definition which could be applied to various models and could help us in selecting between the possible neutrino mass generating mechanisms. We will see that various definitions of minimal flavour violation for leptons can be deduced and, in particular, in the case of Majorana neutrinos, where the light neutrino mass operator is non renormalizable at the electroweak scale. We propose a definition that could encompass many models, where flavour violating processes are not necessarily controlled by the U_{MNS} mixing matrix.

References

[1] W.-M. Yao et al., *J. Phys.* **G 33**, 1 (2006). M. L. Brooks *et al.* [MEGA Collaboration], Phys. Rev. Lett. **83** (1999) 1521 [arXiv:hep-ex/9905013]. U. Bellgardt *et al.* [SINDRUM Collaboration], Nucl. Phys. B **299** (1988) 1.

[2] G. D'Ambrosio, G. F. Giudice, G. Isidori and A. Strumia, Nucl. Phys. B **645** (2002) 155 [arXiv:hep-ph/0207036].

[3] A. J. Buras, P. Gambino, M. Gorbahn, S. Jager and L. Silvestrini, Phys. Lett. B **500** (2001) 161 [arXiv:hep-ph/0007085]. C. Bobeth, M. Bona, A. J. Buras, T. Ewerth, M. Pierini, L. Silvestrini and A. Weiler, Nucl. Phys. B **726** (2005) 252 [arXiv:hep-ph/0505110].

[4] see *e.g.* A. J. Buras, arXiv:hep-ph/0505175.

[5] S. Antusch, C. Biggio, E. Fernandez-Martinez, M. B. Gavela and J. Lopez-Pavon, arXiv:hep-ph/0607020.

[6] V. Cirigliano, B. Grinstein, G. Isidori and M. B. Wise, Nucl. Phys. B **728** (2005) 121 [arXiv:hep-ph/0507001].

[7] V. Cirigliano and B. Grinstein, [arXiv:hep-ph/0601111].

V. Cirigliano, G. Isidori and V. Porretti, [arXiv:hep-ph/0607068].

[8] V. Porretti, arXiv:hep-ph/0610194.

III

LEPTOGENESIS AND CP VIOLATION

III.1 The Seesaw mechanism

In our studies reported in Chapters 2 and 3 we have considered the type-1 seesaw extension of the Standard model. It is a very attractive scenario, since it can naturally explain the smallness of neutrino masses and give a dynamical production of the baryon asymmetry of the universe, through leptogenesis, without inducing proton decay [1].

We have focused our attention on the CP violation provided by the seesaw mechanism. As we have seen in section I.1, CP violation has not been discovered in the lepton sector yet. Nevertheless, in the seesaw scenario we consider, CP violation is provided by 6 phases. And, some combination of those phases can contribute to the U_{MNS} matrix and be measurable in future experiments. We recall that in neutrino oscillations we can measure only the Dirac phase, while some constraints on the Majorana phases can be set in neutrinoless double beta decays.

The type-1 seesaw extension of the Standard Model contains three heavy ($M \gtrsim 10^9$ GeV) Majorana neutrinos N_I in addition to the SM particles. The Lagrangian at the N_I mass scale is given by:

$$\mathcal{L} = \overline{e_R}^j \mathbf{Y_e}_{ij} H_d \ell^i + \overline{N}^J \lambda_{iJ} H_u \ell^i + \overline{N}^J \frac{\mathbf{M}_{JK}}{2} N^{cK} + h.c. \qquad \text{(III.1)}$$

where the flavour index order on the Yukawa matrices $\mathbf{Y_e}$, λ is left-right, and $H_u = i\sigma_2 H_d^*$. This Lagrangian contains 21 parameters, among them the 6 CP violating phases.

In the basis where the charged lepton yukawas are diagonal (D_{Y_e}), the seesaw can be parametrized in different ways, where the CP violating phases appear in different combinations:

- *Top-down parametrization*, the usual one, at $\Lambda > M_i$, with inputs from the right-handed neutrino sector. The neutrino yukawa coupling is bi-diagonalized by two unitary matrices $\lambda = V_L^\dagger D_\lambda V_R$. So that, the input parameters are the 9 eigenvalues of D_M, D_λ and the 6 mixing angles and 6 phases of V_L and V_R.

- *Bottom-up parametrization* [2], with inputs from the left-handed sector. At low energy the heavy degrees of freedom are integrated out and the effective light neutrino mass matrix can be written:

$$[m_\nu] \simeq \lambda M^{-1} \lambda^T v_u^2 = U D_\nu U^T \tag{III.2}$$

  where U is the lepton mixing matrix and D_ν is the diagonal neutrino light mass matrix. We are then left with the SM seesaw measurable parameters. The remaining ones can be the taken to be the yukawa eigenvalues D_λ and V_L.

- *Intermediate parametrization*, proposed by Casas and Ibarra [3]. The neutrino yukawa couplings are written in terms of the lepton mixing matrix U and of a complex orthogonal matrix R:

$$\lambda = U D_\nu^{1/2} R D_M^{1/2} / v_u \tag{III.3}$$

  And the other inputs are the 6 light and heavy neutrino masses D_ν and D_M.

The two last parameterizations make manifest the role of the 3 low energy U_{MNS} phases and are, therefore, convenient to follow the role of the 3 measurable CP violating phases also at high energy.

III.2 Flavoured leptogenesis

CP violation provided by the seesaw mechanism can be an important ingredient for the production of the baryon asymmetry of the universe (BAU). For clarity we briefly recall, here, the leptogenesis SM seesaw scenario, while in our work we have also considered

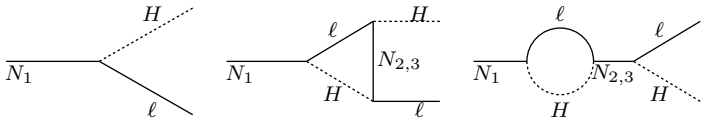

Figure III.1: CP violating decay of the lightest right-handed neutrino N_1.

its supersymmetric extension. In this context, BAU is provided by the CP violating decays of the lightest right-handed neutrino N_1, which populates the thermal plasma at temperatures $T \sim M_1$. In this case, hierarchical N masses are assumed: $M_1 \sim 10^9$ GeV $\ll M_2,\ M_3$. A population of N_1 is produced, mainly by scattering processes, at $T \sim M_1$. Then, the N_1 decay violating CP producing a lepton asymmetry [4]:

$$\epsilon_{\alpha\alpha} = \frac{\Gamma(N_1 \to \ell_\alpha H) - \Gamma(N_1 \to \overline{\ell}_\alpha \overline{H})}{\Gamma(N_1 \to \ell H) + \Gamma(N_1 \to \overline{\ell H})} \simeq \frac{3M_1}{8\pi v_u^2 \left[\lambda^\dagger \lambda\right]_{11}} \mathrm{Im}\left\{[\lambda]_{\alpha 1}[m_\nu^\dagger \lambda]_{\alpha 1}\right\}, \qquad \text{(III.4)}$$

where α specifies the flavour of the lepton doublet in the final state. The flavour indices are explicitly written since, recently, has been suggested that flavours can have a role in leptogenesis [5, 6, 7]. Indeed if the interactions involving charged lepton yukawas are in equilibrium, flavours become distinguishable and the lepton asymmetry evolutions in each flavour must be considered separately. If inverse decays and scattering processes that erase the lepton asymmetries are out of equilibrium, then the asymmetries can survive. The effect of those processes is included in the efficiency parameter η_α, equal to:

$$\eta_\alpha \simeq \left[\left(\frac{m_*}{2|A_{\alpha\alpha}|\tilde{m}_{\alpha\alpha}}\right)^{-1.16} + \left(\frac{|A_{\alpha\alpha}|\tilde{m}_{\alpha\alpha}}{2m_*}\right)^{-1}\right]^{-1}, \qquad \text{(III.5)}$$

in strong wash-out regime. Where $A_\alpha \sim 2/3$ and $\tilde{m}$ are the N_1 (rescaled) decay rates:

$$\widetilde{m} = \sum_\alpha \widetilde{m}_{\alpha\alpha} = \sum_\alpha \frac{|\lambda_{\alpha 1}|^2}{M_1} v_u^2. \qquad \text{(III.6)}$$

The lepton asymmetry is then converted into baryon asymmetry by non-perturbative processes. The central quantities for leptogenesis are then the lepton asymmetry $\epsilon_{\alpha\alpha}$ and the wash-out factors η_α, so that the final baryon number density can be written as

$$Y_B \simeq -\frac{12}{37}\frac{1}{3g_*}\sum_\alpha \epsilon_{\alpha\alpha}\ \eta_\alpha, \qquad \text{(III.7)}$$

where $g_\star \sim 106.75$ in the SM and 12/37 takes into account non-perturbative effects to convert the lepton asymmetry into baryon asymmetry. For a detailed review on flavoured leptogenesis see [8].

III.3 CP violation

Here we concentrate on the role of CP violating phases. The phenomenological question we want to answer, in the context of thermal leptogenesis, can be formulated in the following way:

Given the measured value of the baryon asymmetry,
can an allowed range for the U_{MNS} phases be predicted?

The inclusion of flavour effects has changed the standard scenario. Following the Casas-Ibarra parametrization, see Eq. (III.3), the low-energy measurable phases are explicitely visible in the lepton asymmetry ϵ:

$$\epsilon_{\alpha\alpha} = -\frac{3M_1}{16\pi v^2}\frac{\Im(\sum_{\beta\rho} m_\beta^{1/2} m_\rho^{3/2} U^*_{\alpha\beta} U_{\alpha\rho} R_{\beta 1} R_{\rho 1})}{\sum_\beta m_\beta |R_{1\beta}|^2} \quad . \tag{III.8}$$

Therefore, without including flavour effects $Y_B \propto \epsilon\eta = \sum_\alpha \epsilon_{\alpha\alpha} \sum_\alpha \eta_\alpha$ and, because of the U_{MNS} unitarity, the low-energy phases disappear from the total lepton asymmetry:

$$\epsilon = -\frac{3M_1}{16\pi v^2}\frac{\Im(\sum_\rho m_\rho^2 R_{\rho 1}^2)}{\sum_\beta m_\beta |R_{1\beta}|^2}. \tag{III.9}$$

We can than easily conclude that the baryon asymmetry, in leptogenesis without flavours, is *insensitive* to the low energy phases. This result was first found by [9]. Nevertheless, this simple argument cannot be applied in flavoured leptogenesis, where the lepton asymmetry in each flavour evolves independently and must be considered with its own washout factor: $Y_B \propto \sum_\alpha \epsilon_{\alpha\alpha}\eta_{\alpha\alpha}$.

In the two publications reproduced in Chapters 2 and 3, we show that leptogenesis is insensitive to the low energy phases even if flavour effects are taken into account.

In Chapter 2 we discuss the simplest extension of the SM with 3 right-handed neutrinos and the type-1 seesaw mechanism. We look for an area of the unmeasurable parameter space where we have enough baryon asymmetry and Y_B independent of low

energy phases. It is found analytically, in strong washout regime, with a simple choice of the unmeasurable R matrix defined in the Casas-Ibarra parameterization. The study is completed by a numerical analysis, where we provide a random selection of points, in the seesaw parameter space, with large enough baryon asymmetry for any value of the low energy phases.

The subsequent publication, in Chapter 3, extends this work to the supersymmetric seesaw scenario. This framework is particularly attractive since it stabilizes the hierarchy between the leptogenesis scale and the electroweak one. In this context we have preferred a phenomenological bottom-up parameterization since, besides the usual measurable low-energy parameters U and D_ν, also D_λ and V_L can have physical relevance in supersymmetry. They indeed may contribute to the renormalization group running of the slepton mass matrix and, so, to the enhancement of flavour violating processes, that could in that case be measurable in the next experiments [10]. The analysis is performed numerically by a Markov Chain Monte Carlo scan. This method is particularly efficient in case of a large parameter space, since it samples through a fast random walk a representative subset of points, according to a given probability distribution [11, 12].

References

[1] M. Fukugita and T. Yanagida, Phys. Lett. **B174** (1986) 45.

[2] S. Davidson and A. Ibarra, JHEP **0109** (2001) 013 [arXiv:hep-ph/0104076].

[3] J. A. Casas and A. Ibarra, Nucl. Phys. B **618** (2001) 171 [arXiv:hep-ph/0103065].

[4] L. Covi, E. Roulet and F. Vissani, Phys. Lett. B **384** (1996) 169 [arXiv:hep-ph/9605319].

[5] A. Abada, S. Davidson, A. Ibarra, F. X. Josse-Michaux, M. Losada and A. Riotto, JHEP **0609** (2006) 010 [arXiv:hep-ph/0605281].

[6] E. Nardi, Y. Nir, E. Roulet and J. Racker, JHEP **0601**, 164 (2006) [arXiv:hep-ph/0601084];

[7] A. Abada, S. Davidson, F. X. Josse-Michaux, M. Losada and A. Riotto, JCAP **0604** (2006) 004 [arXiv:hep-ph/0601083].

[8] S. Davidson, E. Nardi and Y. Nir, arXiv:0802.2962 [hep-ph].

[9] G. C. Branco, T. Morozumi, B. M. Nobre and M. N. Rebelo, Nucl. Phys. B **617** (2001) 475 [arXiv:hep-ph/0107164].

[10] F. Borzumati and A. Masiero, Phys. Rev. Lett. **57** (1986) 961.

[11] D. J. C. MacKay, "Information Theory, Inference, and Learning Algorithms", Cambridge University Press.

[12] W. R. Gilks, S. Richardson and D. J. Spiegelhalter, "Markov Chain Monte Carlo in Practice", Chapman and Hall.

IV

PARTICLES AND THE EARLY UNIVERSE

IV.1 The hot Big-Bang

All the cosmological processes we have discussed so far rely on the standard cosmological model for the evolution of our universe, which has its foundations on Einstein's General Relativity theory. The most compelling idea is the so-called Big-Bang: our universe was once very hot and dense and has expanded and cooled to its present state. The first idea of a Big-Bang model was formulated in order to account for the possibility that the abundances of light-elements, e.g. D and ^4He, had a cosmological origin. Then the presence of a relic background radiation (CMB) with a temperature of a few K was predicted. It was found many years later giving the first confirmation for the hot Big-Bang model [1].

At the origin, the universe was hot and dense and populated by particles maintained in equilibrium by very fast interactions. However the universe expanded and cooled, thus the initial equilibrium condition was no longer maintained and particles started leaving the thermal plasma (freeze-out). The particles left the equilibrium when their interactions with the plasma were not fast enough if compared with expansion of the universe. This happened at different temperatures for different particles depending on their interaction couplings and their thermal masses. A review over the standard cosmological model can be found in [2] and, with recent developments on cosmological perturbations, in [3].

IV.2 Very weakly interacting dark matter

Dark matter could have been produced in the primordial thermal plasma. If stable on cosmological scales, once frozen out of the thermal plasma, its relic density has not changed. Then, if produced in the right amount at the origin, it could provide for the dark matter amount observed today.

The non-baryonic cold dark matter candidates are basically elementary particles which have not been discovered yet, like axions and Weakly Interacting Massive Particles (WIMPs). In the context of the dark matter problem, supersymmetric theories seem to give an elegant solution, see e.g. [4]. The supersymmetric extensions of the Standard Model which include the conservation of a new quantity, the R-parity, lead to the appearance of an appealing candidate which could be the main constituent of dark matter. This candidate is the lightest supersymmetric particle, the LSP, which is absolutely stable in these models and, so, could have been produced at the origin of our universe and now be still present and be the main constituent of matter. Between the supersymmetric particles the dark matter candidates are those electrically neutral. The most studied is the weakly interacting neutralino, which is the fermionic superpartner of SM gauge and Higgs bosons and is present in the minimal supersymmetric extensions of the SM (MSSM).

In our work we are mainly interested to dark matter candidates that have "very" weakly interactions with the ordinary particles. Two interesting examples from supersymmetry are the gravitino [6] and the axino [5]. The gravitino, superpartner of the graviton, is present in supersymmetric theories that include also gravity. Its mass depends strongly on the supersymmetry breaking scheme and can vary between many orders of magnitude. It is very weakly coupled since its interactions are suppressed by the Planck scale. The axino, instead, is present in supersymmetric models that include the axion as dynamical solution to the strong CP problem. A new chiral symmetry $U(1)$ is introduced and then spontaneously broken at a very large scale $f_a \sim 10^{11}$ GeV. The axion is the Goldstone boson of such a broken symmetry and the axino its superpartner. The axino coupling to matter is suppressed by the f_a symmetry breaking scale and its mass can be set at different energy scales.

Thus, gravitino and axino are massive particles whose interactions with ordinary matter are strongly suppressed. If one of them is the LSP, it can be an interesting

candidate for cold dark matter.

IV.3 Charged relics

The LSP can be thermally produced from scattering processes with particles in the thermal bath at the origin of the universe. But it can also be produced non-thermally, in decay processes of particles which are already out of equilibrium. This mechanism involves two steps, the freeze out of the next-to-lightest-supersymmetric particle (NLSP) from the thermal bath and, then, its decay into the LSP. In order for a two step process to occur, the decay width of the NLSP must be sufficiently small to allow for the decoupling in the first place. On the other hand, the lifetime of the NLSP cannot be too large, otherwise the decay into axinos and ordinary particles would take place too late, during or after nucleosynthesis, and it could destroy predictions for the abundance of light elements. The R parity conservation implies that all the NLSP decoupled from the thermal bath must decay into the LSP, thus for each NLSP a LSP is produced. In this non-thermal production, the abundance of the NLSP is then strictly correlated with the abuundance of the dark matter candidate.

In the study reported in Chapter A, we have studied the general case of a scalar charged thermal relic. We have computed its number density and compared it with BBN bounds. In the first part of the analysis we have considered its gauge interactions, in both abelian and non-abelian case at the leading order in perturbation theory. They are often the dominant interaction channels and allow a more "model independent" analysis, since they depend on only a few parameters, the mass of the interacting particle and its charge or representation. The strength of those gauge interactions is enhanced by the Sommerfeld effect, that takes into account non perturbative effects at the threshold, where the expansion in terms of the coupling is inadequate. In the second part of the paper we apply our results to the MSSM scenario with axino or gravitino LSP and stau or stop NLSP.

References

[1] A. Einstein, *Ann. Phys.* **69** (1922) 436. G. Gamow, *Phys. Rev.* **70** (1946) 572. R. A. Alpher, H. Bethe and G. Gamow, *Phys. Rev.* **73** (1948) 803. R. A. Alpher and R. C. Herman, *Phys. Rev.* **74** (1948) 1737. R. A. Alpher and R. C. Herman, *Phys. Rev.* **75** (1949) 1089. A. A. Penzias and R. W. Wilson, *Astrophys. J.* **142** (1965) 419. R. H. Dicke, P. J. E. Peebles, P. G. Roll, D. T. Wilkinson, *Astrophys. J.* **142** (1965) 414.

[2] E. W. Kolb and M. S. Turner *The Early Universe*, Addison-Wesley.

[3] S. Dodelson *Modern Cosmology*, Academic Press.

[4] G. Jungman, M. Kamionkowski and K. Griest, Phys. Rept. **267** (1996) 195 [arXiv:hep-ph/9506380].

[5] L. Covi, J. E. Kim and L. Roszkowski, Phys. Rev. Lett. **82** (1999) 4180 [arXiv:hep-ph/9905212]; L. Covi, H. B. Kim, J. E. Kim and L. Roszkowski, JHEP **0105** (2001) 033 [arXiv:hep-ph/0101009]. A. Brandenburg and F. D. Steffen, JCAP **0408** (2004) 008 [arXiv:hep-ph/0405158]. K. Y. Choi, L. Roszkowski and R. Ruiz de Austri, JHEP **0804** (2008) 016 [arXiv:0710.3349 [hep-ph]]. H. Baer and H. Summy, arXiv:0803.0510 [hep-ph].

[6] J. L. Feng, A. Rajaraman and F. Takayama, Phys. Rev. Lett. **91** (2003) 011302 [arXiv:hep-ph/0302215]; J. R. Ellis, K. A. Olive, Y. Santoso and V. C. Spanos, Phys. Lett. B **588** (2004) 7 [arXiv:hep-ph/0312262]; J. L. Feng, S. f. Su and F. Takayama, Phys. Rev. D **70** (2004) 063514 [arXiv:hep-ph/0404198]; J. L. Feng, S. Su and F. Takayama, Phys. Rev. D **70** (2004) 075019 [arXiv:hep-ph/0404231]; L. Roszkowski, R. Ruiz de Austri and K. Y. Choi, JHEP **0508** (2005) 080 [arXiv:hep-ph/0408227]. D. G. Cerdeno, K. Y. Choi, K. Jedamzik, L. Roszkowski and R. Ruiz de Austri, JCAP **0606** (2006) 005 [arXiv:hep-ph/0509275]. J. L. Feng, B. T. Smith and F. Takayama, Phys. Rev. Lett. **100** (2008) 021302 [arXiv:0709.0297 [hep-ph]].

Second Part:
Publications

1

VARIOUS DEFINITIONS OF MINIMAL FLAVOUR VIOLATION FOR LEPTONS

AUTHORS: Sacha Davidson and F.P.

IPNL, Université CB Lyon-1, 4 rue Enrico Fermi, 69622 Villeurbanne, France

PUBLISHED IN: Physics Letters B 642 (2006) 72 [1]

Neutrino masses imply the violation of lepton flavour and new physics beyond the Standard Model. However, flavour change has only been observed in oscillations. In analogy with the quark sector, we could deduce the existence of a principle of Minimal Flavour Violation also for Leptons. Such an extension is not straightforward, since the mechanisms generating neutrino masses are unknown and many scenarios can be envisaged. Thus, we explore some possible definitions of MFVL and propose a notion that can include many models. We build an R-parity violating neutrino mass model in agreement with our preferred definition of MFVL, and show that flavour violating processes are not neccessarily controlled by the MNS mixing matrix.

1.1 Introduction

Minimal flavour violation[1, 2] in the quark sector, is a useful framework in which to construct TeV-scale models of New Physics. It is predictive, and includes many or

[1] pre-print arXiv:hep-ph/0607329

most models that are consistent with quark flavour data. Recently, a definition of Minimal Flavour Violation (MFV) has been introduced for leptons [3]. The proposed formulation is predictive—it implies that lepton flavour violation is determined by the light neutrino mass matrix— but includes few of the many neutrino mass models [4, 5, 6, 7, 8, 9] that are consistent with current observations.

The flavour-changing mixing angles of the leptonic sector (MNS matrix), are not measured with the overconstrained precision of the CKM matrix. So MFV is not strongly suggested for leptons, as it is for quarks. However, if one *assumes* that there is new physics at the TeV-scale, that satisfies MFV or a similar principle in the quark sector, then it is reasonable to expect a similar principle to apply for leptons. So it is interesting to explore different possible definitions of minimal flavour violation for leptons (MFVL), and in particular to study whether it implies that lepton flavour violation is controlled by the MNS matrix and the light neutrino masses.

In this paper, we take the principle of MFV to limit the number of flavour structures allowed to the renormalisable couplings of the theory. This flexible definition can be applied to many models, but is less predictive than [3]. We explicitly construct an R-parity violating neutrino mass model that is "minimally flavour violating", in agreement with observation, and where the lepton flavour violation is not controlled by the light neutrino mass matrix.

In section 1.2, we review minimal flavour violation for the quarks, and classify neutrino mass generation mechanisms. In section 1.3, we discuss the purpose of Minimal Flavour Violation for leptons, and various possible implementations which we apply to some neutrino mass models. In section 1.4, we build an R-parity violating neutrino mass model, using the λLLE^c coupling, that satisfies our preferred definition of MFVL. In the Appendix is sketched a model satisfying a more restrictive definition of MFVL.

1.2 Review

Beyond-the-Standard-Model physics, in the form of new particles or new interactions, must exist at some scale, to explain observations such as dark matter, neutrino masses, the baryon asymmetry and the temperature fluctuations in the Cosmic Microwave Background. New physics at the TeV-scale (such as, for instance, supersymmetry)

is particularily desirable because it could be discovered at the LHC, and would be theoretically welcome to address the hierarchy problem. However, if there are new flavoured TeV-scale particles, as one would like, it is puzzling that their footprints have not been seen in rare flavoured and CP violating processes. So Minimal Flavour Violation is introduced as a constraint on the interactions of such new particles, to suppress their contributions to flavoured observables.

We follow the approach to Minimal Flavour Violation of [1], which starts from the flavour transformation properties of various terms in the SM Lagrangian. We define the SM to have massless neutrinos. In three generations, the fermionic kinetic terms

$$\overline{q}_L \not{D}\, q_L + \overline{u}_R \not{D}\, u_R + \overline{d}_R \not{D}\, d_R + \overline{\ell} \not{D}\, \ell + \overline{e}_R \not{D}\, e_R \tag{1.1}$$

have a global $U_q(3) \times U_u(3) \times U_d(3) \times U_\ell(3) \times U_e(3)$ flavour symmetry. For instance, q_L is a three component vector in quark doublet flavour space, whose kinetic term is invariant under $q_L \to V_q q_L$, where $V_q \in U_q(3)$. This large symmetry group is broken to $U_B(1) \times U_{L_e}(1) \times U_{L_\mu}(1) \times U_{L_\tau}(1)$ by the Yukawa couplings

$$\overline{q}_L \mathbf{Y_u} H_u u_R + \overline{q}_L \mathbf{Y_d} H_u^c d_R + \overline{\ell} \mathbf{Y_e} H_u^c e_R + h.c. \tag{1.2}$$

where H_u is the SM Higgs, and the index order on Yukawa matrices is left-right. In the lepton sector, there is one "symmetry-breaking" operator, or "spurion" in the language of [1], per vector space: $\mathbf{Y_e}\mathbf{Y_e}^\dagger$ in ℓ_L space, $\mathbf{Y_e}^\dagger\mathbf{Y_e}$ in e_R space. These hermitian matrices can be diagonalised, and are uniquely identified by their eigenvalues in the eigenbasis. So we will sometimes say the operators can "choose a basis", and discuss interchangeably the matrix, the spurion and the basis of eigenvectors who are normalised to have length^2 = the eigenvalue. In the presence of $\mathbf{Y_e}$ (and the absence of other "basis choosing" operators in the lepton sector), there are three remaining global $U(1)$s. The three conserved quantum numbers can be taken as the individual lepton flavours [2]. So in our restricted definition of the SM, neutrinos are massless and lepton flavours are conserved. We add neutrino masses at the end of the section.

In the quark sector, $\mathbf{Y_d}\mathbf{Y_d}^\dagger$ and $\mathbf{Y_d}^\dagger\mathbf{Y_d}$ choose respectively a basis in the q_L and the d_R flavour spaces. Similarly, $\mathbf{Y_u}\mathbf{Y_u}^\dagger$ and $\mathbf{Y_u}^\dagger\mathbf{Y_u}$ choose respectively a basis in

[2]The three $U(1)$s can also be taken to correspond to the three diagonal generators of $U(3) = \{I, \lambda_3, \lambda_8\}$, acting simultaneously on the ℓ_L and e_R flavour spaces. In this case one conserves the total lepton number $L_e + L_\mu + L_\tau$, and the flavoured asymmetries $L_e - L_\mu$ and $L_e + L_\mu - 2L_\tau$

the q_L and the u_R flavour spaces. So there are two operators in q_L space, $\mathbf{Y_d Y_d}^\dagger$ and $\mathbf{Y_u Y_u}^\dagger$, who are not simultaneously diagonalisable. Flavour is therefore not conserved, and the misalignment between the two eigenbases is parametrised by the CKM matrix.

The mixing angles and phase of the quark sector are over-determined in many flavour-changing, flavour-conserving and CP violating processes of the quark sector. For instance, the CKM angles can be obtained in tree level processes, and used to predict rates that are mediated by loops in the Standard Model. To date, the experimentally measured rates agree with these predictions, implying that the new physics contribution in loops should be smaller than the SM. For new particles with generic flavour-changing couplings, this is a strong constraint, placing the mass above 10-100 TeV [10].

Minimal Flavour Violation was introduced to allow New Physics to have TeV-scale masses, and be consistent with precision flavoured data from the quark sector. It is a restriction on the flavour structure of new interactions. The only operators allowed in the "flavour-spaces" are those of the SM (and the identity matrix). So flavour-change and CP violation in the quarks are proportional to the CKM matrix and quark Yukawa eigenvalues, eg to $\mathbf{Y_d Y_d}^\dagger$ in the mass basis of up-type doublet quarks. MFV is therefore a predictive framework, and encompasses many of the models that fit the data.

Flavour-changing processes are also observed in the lepton sector, in neutrino oscillations. The weakly intereacting neutrinos are observed to have small mass differences, and large mixing angles with respect to the charged leptons. That is, in the lepton doublet space, there are two operators that break the flavour $U_\ell(3)$ symmetry. These are the charged lepton and neutrino mass matrices, which "choose bases" related by the MNS matrix U. In the charged lepton mass eigenstate basis (referred to as the "flavour" basis), the light neutrino mass matrix satisfies

$$[m_\nu][m_\nu]^\dagger = U^* D^2_{m_\nu} U^T \tag{1.3}$$

where $D^2_{m_\nu} = \mathrm{diag}\{m_1^2, m_2^2, m_3^2\}$. To date, only flavour changing charged current processes (mediated by W exchange) are observed in the lepton sector, and MFV is not "required" for the leptons. Four elements of the MNS matrix are measured—the remainder being obtained from unitarity[11]—and CP violation is not observed. This means new leptonic physics is not stringently constrained to agree with SM predictions

for CP violation, as is the case in the quark sector. Rates for unobserved FCNC lepton processes (*e.g.* $\mu \to e\gamma$) can be calculated using the MNS matrix and neutrino masses, and are well below the current experimental sensitivity. So new leptonic physics is only constrained to be less than the experimental rates, and not, as in the quark sector, to be smaller than the prediction one obtains using observed masses.

The neutrino masses can be lepton number conserving ("Dirac") or not ("Majorana"). In the Dirac case one could define MFV in the lepton sector as an exact copy of the quarks, so in this paper, we consider Majorana neutrino masses, which arise from a dimension five operator

$$(\ell_j H_u)\mathbf{K}^{jk}(\ell_k H_u) \quad . \tag{1.4}$$

Two classes of new physics generating this operator can be distinguished. One possibility is that it is generated by new flavoured particles, in a new flavour space. These new particles should be heavy or weakly coupled, since they have not been observed. The canonical example is the seesaw, where one adds, *e.g.*, 3 generations of ν_R, and the flavour symmetry group of the kinetic terms is enlarged to $U(3)^6$. The second possibility is that the all flavoured particles live in the 5 flavour spaces of the SM, and some new lepton number- or flavour-changing interactions are included. This is the case for neutrino masses generated in the R-parity violating MSSM.

1.3 Minimal Flavour Violation for Leptons?

We *assume* that there are new flavoured particles at the TeV scale, and hope that this is verified soon at the LHC. A definition of Minimal Flavour Violation in the lepton sector [3] could then be interesting for various reasons. Firstly, MFV in the quark sector is well motivated by the experimental observations. So one could conclude it reflects some principle or symmetry of the underlying theory, and should apply in the lepton sector as well. Secondly, in the lepton sector, we know there must be Beyond the Standard Model physics at some scale, because we observe neutrino masses. We can hope to use MFV as a tool in distinguishing among the multitude of candidate models for new physics in the lepton sector [3]. Minimal Flavour Violation for leptons

[3]Taking a principle of MFV to apply to the neutrino mass generation mechanism is a more ambitious implementation of MFV than in the quark sector. For quarks, one hopes for new TeV-scale

should therefore be applicable to most models, and be predictive, so we can test the hypothesis and/or differentiate models.

A predictive definition of MFV for the lepton sector has recently been introduced in [3], and further studied in [12]. It supposes that the three light neutrinos are Majorana, with the required lepton number violation occuring at some high scale Λ_{LN}. Two classes of models are considered: those whose particles transform according to the $U^5(3)$ flavour transformations of the SM, and a second scenarino with three (heavy) right-handed neutrinos.

In this work, we also take the light neutrino masses to be Majorana. If they were Dirac, MFV could be defined for leptons by copying the quark definition. Models that generate Majorana neutrino masses can be divided into two cases [3]:
• case A: models whose particles transform according to the $U^5(3)$ flavour transformations of the SM, and
• case B: models with a flavour transformation group that is larger than that of the SM (*e.g.* the seesaw, where the kinetic terms of the three ν_R have a $U(3)$ symmetry).

1.3.1 Larger flavour transformation group

Suppose there are a several generations of a new particle, *e.g.* three right-handed neutrinos. The kinetic terms therefore have an enlarged flavour symmetry group, which is $U^6(3)$ when 3 ν_R are added to the SM. The renormalisable Lagrangian for the SM + the new particle will contain the SM Yukawas, and some number of additional spurions corresponding to the interactions of the new particle. In the case of the seesaw, the Lagrangian is

$$\mathcal{L}_{SM} + \overline{\ell}_j \mathbf{Y}_\nu{}^{jK} H_u N_K + \frac{1}{2}\overline{N_J^c}\mathbf{M}_{JJ} N_J + h.c. \tag{1.5}$$

and there are potentially two "basis-choosing" interactions, or spurions, in ν_R space: $\mathbf{Y}_\nu{}^\dagger\mathbf{Y}_\nu$ and $\mathbf{M}$. There are a variety of potential definitions of MFV, which we illustrate

particles (for instance to address the hierarchy problem), in which case MFV is almost required to describe the Lagrangian up to scales ~ 100 TeV. In the lepton sector, we know there is New Physics, and it should have some connection to flavour because it generates neutrino masses. However, this new physics could be at a high scale ($\sim 10^{10} - 10^{16}$ GeV in the seesaw?), so in assuming that MFV applies to the interactions that generate the neutrino masses, we may be applying it across many more orders of magnitude than in the quark sector.

with the seesaw example.

1. one could impose that the new physics may not introduce new spurions in the Standard Model flavour spaces. In the case of the seesaw, this means that $\mathbf{Y}_\nu \mathbf{Y}_\nu{}^\dagger$ should be diagonal in the lepton doublet flavour basis (charged lepton mass eigenstate basis). No restrictions are imposed on the number of bases chosen in the flavour space of the new particles. In the seesaw case, $\mathbf{Y}_\nu{}^\dagger \mathbf{Y}_\nu$ and $\mathbf{M}$ could have different eigenbases, and must do so to reproduce the correct neutrino mixing angles. This definition of MFV for leptons is predictive but unattractive, because it implies that lepton flavour violation amoung charged leptons is suppressed by neutrino masses.

2. CGIW [3] define MFV for the seesaw by allowing the renormalisable interactions of eqn (1.5) to choose a second basis in ℓ space, but impose restrictions on the spurions in ν_R space. They study the case where the ν_R are degenerate of mass M, and CP is a symmetry of the right-handed neutrino sector [13]. (So there is only one eigenbasis in ν_R space.)

   In this case $\mathbf{K} = \mathbf{Y}_\nu \mathbf{M^{-1}} \mathbf{Y}_\nu^{\mathbf{T}} = \mathbf{Y}_\nu \mathbf{Y}_\nu{}^T / M$. The two "basis-choosing" coupling matrices in ℓ space, that are relevant for lepton number conserving flavour violation, are

   $$\mathbf{Y_e} \mathbf{Y_e}^\dagger \quad , \quad \mathbf{Y}_\nu \mathbf{Y}_\nu{}^\dagger = \frac{M}{v^2} \mathbf{U}^* \mathbf{D}_{m_\nu} \mathbf{U}^T \tag{1.6}$$

   If there is no CP violation in the lepton sector (the case studied by CGIW), then $\mathbf{Y}_\nu \mathbf{Y}_\nu{}^\dagger = M\mathbf{K}$. In either case, lepton flavour violation is controlled by parameters from the light neutrino sector. The predictions of this scenario should be similar to the SUSY seesaw with degenerate ν_R [14].

3. The more generic (and less predictive) definition of MFV for the seesaw would be to allow all renormalisable interactions to be independent spurions, as one allows for SM constituents (equivalently, one could allow up to two spurions per vector space). In the case of the ν_R, with the seesaw Lagrangian of eqn (1.5), the Majorana mass matrix $\mathbf{M}$ and the Yukawa coupling $\mathbf{Y}_\nu{}^\dagger \mathbf{Y}_\nu$ are independent spurions in the ν_R flavour space. Similarly to $\mathbf{Y}_\nu \mathbf{Y}_\nu{}^\dagger$ and $\mathbf{Y_e} \mathbf{Y_e}^\dagger$ in ℓ space, they have unrelated eigenbases. This is the "usual" type-1 seesaw, whose supersymmetric

flavour-changing predictions have been extensively studied in the literature [15]. It is well known that in the SUSY seesaw, the rates for flavour-changing processes among the charged leptons are not related to the neutrino masses or the MNS matrix [16].

1.3.2 Standard Model flavour transformations

Consider now neutrino mass models whose particles transform according to the $U^5(3)$ flavour transformations of the SM. In the quark sector, MFV restricts the bases chosen by flavour-dependent new interactions to be those of the SM Yukawas. That is, there are two allowed bases (spurions) in q_L space, and one in u_R and d_R spaces respectively.

1. CGIW define MFV for leptons, in this case, to allow two spurions ("basis-choosing" operators) in the doublet lepton (ℓ) space, which are $\mathbf{K}$ and $\mathbf{Y_e Y_e}^\dagger$. The $\mathbf{K}$ is the dimensionful coefficient of a lepton number violating operator, so lepton flavour changing processes, that conserve lepton number, are controlled by the dimensionless $\Lambda_{LN}^2 \mathbf{K K}^\dagger$. Rates for lepton flavour violating processes (*e.g.* $\mu \to e\gamma$) are proportional to the unknown Λ_{LN}^2, but ratios of LFV processes are predicted to be controlled by $\mathbf{K K}^\dagger$. This describes for instance the SUSY triplet model [9, 3, 12].

2. Alternatively one could suppose that MFV is a restriction on *renormalisable* couplings. This is reasonable firstly because MFV is a recipe for extrapolating in scale. We know how renormalisable couplings evolve, whereas we cannot guess, in a bottom up approach, when a non-renormalisable interaction becomes renormalisable. Secondly, one could expect that flavour is introduced into the theory at some high scale, (M_{GUT}?), and comes to us via renormalisable couplings.
   • One could hope to define MFV, by analogy with the quark sector, as restricting all new interactions to be aligned with the SM Yukawas. But then it is difficult to obtain the large mixing angles of the MNS matrix. A model attempting to satisfy this ideal can be found in Appendix A. This version of MFV would predict that lepton flavour changing amplitudes must contain the neutrino mass to some power, or lepton number violation. Notice that this differs from the CGIW prediction; in the present case, lepton flavour violation is suppressed by the small

neutrino mass scale.

• A more realistic definition of MFV, that includes some models, would allow (at least) one other basis in ℓ space. New renormalisable interactions can choose one, and only one, new basis for ℓ space, and no new bases for $\{e_R, u_R, d_R, q_L\}$ spaces. That is, we take MFV as a statement about renormalisable interactions, that allows two bases in the q_L and ℓ spaces, one in the u_R, d_R and e_R spaces. The question then arises: is lepton flavour violation among charged leptons controlled by the light neutrino mass matrix? If yes, then this definition of MFVL is equivalent to that of CGIW. If the lepton flavour violating rates are independent, one could hope they give information about the neutrino mass generation mechanism.

Some renormalisable, lepton number violating interactions involving ℓ, that can be used to construct the neutrino mass matrix, are

$$\frac{1}{2}M_T\vec{T}\cdot\vec{T}^\dagger + g_\phi M_T H_u^c \vec{\tau} H_u^c \cdot \vec{T} + g_{ij}\overline{\ell}_i^c \vec{\tau}\ell_j\cdot\vec{T} \qquad \text{(triplet)} \tag{1.7}$$

$$\mu_i L_i H_u + \lambda'_{jrs} L_j Q_r D_s^c + \frac{1}{2}\lambda^n_{ij} L_i L_j E_n^c \qquad \text{(R parity Violating)} \tag{1.8}$$

where H_u is the Standard Model doublet Higgs, T is an SU(2) triplet scalar, and the second line is in superfield notation, so are renormalisable interactions in supersymmetry. Under the $U(3)$ flavour transformations of ℓ space, g transforms as a symmetric $\mathbf{6}$, λ' and μ as $\bar{\mathbf{3}}$, and the antisymmetric λ as a $\mathbf{3}$.

In the triplet model of eqn (1.7), the exchange of $\vec{T}$ induces the neutrino mass operator (1.4). The light neutrino mass matrix is therefore $[m_\nu]_{\alpha\beta} \propto g_{\alpha\beta}$, and flavour violation among the charged leptons is controlled by the light neutrino mass matrix [9]. In this model, this definition of MFV based on renormalisable couplings, agrees with the definition of CGIW based on mass matrices.

It seems not possible to generate observed light neutrino masses with the λ' coupling, if we implement strictly this definition of MFV. The λ' must respect MFV in the quark sector:

$$\sum_{\ell,d}\lambda'_{\ell qd}\lambda'^*_{\ell pd} \propto [\mathbf{Y_d}\mathbf{Y_d}^\dagger]_{qp} \qquad \sum_{\ell,q}\lambda'_{\ell qd}\lambda'^*_{\ell qf} \propto [\mathbf{Y_d}^\dagger\mathbf{Y_d}]_{df}$$

so the eigenvalues of λ' are those of the $\mathbf{Y_d}$. This hierarchy, when combined with quark masses to obtain m_ν, gives too steep a neutrino mass hierarchy. In the

following section, we construct a neutrino mass model that satisfies this definition of MFV, using the λ interaction.

1.4 The λ model

The aim of this section is to construct a neutrino mass model that has two features. It should be minimally flavour violating, in the sense that the new renormalisable interaction λ only introduces one new basis, or spurion, which is in ℓ_L space. And the model should agrees with current bounds on lepton flavour violating processes ($\mu \to e\gamma$, etc), *but* the predictions for these processes should not be determined by the light neutrino mass matrix.

We take the light neutrino masses to be generated entirely by the RPV λ coupling, so we neglect λ' and bilinear RPV. In the charged lepton mass eigenstate basis, the light neutrino mass matrix can be written [17]

$$[m_\nu]_{ij} = \sum_{m,n,p,q} \lambda^m_{in}\lambda^q_{pj} m_{e_n} \delta^n_q \tilde{A}^{mp} I(m_{\tilde{E}_m}, m_{\tilde{L}_m}) + (i \leftrightarrow j) \quad , \tag{1.9}$$

where the A-term $\tilde{\mathbf{A}}^{mp} = -((\mathbf{Y_e A})^{mp}\frac{v_d}{\sqrt{2}} + \mu\frac{v_u}{\sqrt{2}}\mathbf{Y_e}^{mp})$ is taken flavour diagonal and included in the mass insertion approximation, the mass matrices for the sleptons $\tilde{E}_m$ and $\tilde{L}_m$ are taken diagonal in the flavour basis (which is consistent with MFV), and

$$I(m_1, m_2) = -\frac{1}{16\pi^2}\frac{m_1^2}{m_1^2 - m_2^2}\ln\frac{m_1^2}{m_2^2} \quad . \tag{1.10}$$

The λ^n_{ij} is an antisymmetric matrix on its doublet indices i, j, so corresponds to a plane in ℓ_L space. It is convenient to rewrite it as a single index object in ℓ_L space (the vector orthogonal to the plane), using the antisymmetric ϵ tensor

$$\tilde{\lambda}_{nk} = \frac{1}{2}\epsilon_{ijk}\lambda^n_{ij}. \tag{1.11}$$

The ϵ_{ijk} is SU(3) invariant, but not $U(3)$ invariant, so this renaming has some peculiar consequences. Consider the case where $\lambda^n_{ij} \propto \epsilon_{ijn}$, so $\tilde{\lambda}$ is "flavour diagonal". However, since it transforms under $SU_\ell(3) \times SU_e(3)$ as ℓe_R, it is not invariant, and the flavour differences $L_e - L_\mu$ and $L_e + L_\mu - 2L_\tau$ are conserved mod 2 in four fermion interactions.

The "MFV" constraint is that $\sum_j \tilde{\lambda}_{sj}\tilde{\lambda}^*_{tj}$ should be diagonal in the singlet charged lepton mass basis, with eigenvalues proportional to the charged lepton Yukawas [4]. We will permute the $\mu-\tau$ eigenvalues, that is $\sum_{ij} \lambda^e_{ij}\lambda^{e*}_{ij} \propto m_e^2/v^2$, but $\sum_{ij} \lambda^\mu_{ij}\lambda^{\mu*}_{ij} \propto m_\tau^2/v^2$, and $\sum_{ij} \lambda^\tau_{ij}\lambda^{\tau*}_{ij} \propto m_\mu^2/v^2$. On its doublet indices

$$V_\lambda^\dagger \tilde{\lambda}\tilde{\lambda}^\dagger V_\lambda = \mathrm{diag}\{m_e^2, m_\tau^2, m_\mu^2\}/v^2 \tag{1.12}$$

where V_λ is a unitary matrix transforming from the charged lepton basis to the eigenbasis of $\tilde{\lambda}$. The observed light neutrino parameters, with masses in the inverse hierarchy, can be obtained from

$$V_\lambda^\dagger = \begin{bmatrix} -c\epsilon & \frac{1+s\epsilon}{\sqrt{2}} & -\frac{1-s\epsilon}{\sqrt{2}} \\ s & \frac{c}{\sqrt{2}} & \frac{c}{\sqrt{2}} \\ c & -\frac{s-\epsilon}{\sqrt{2}} & -\frac{s+\epsilon}{\sqrt{2}} \end{bmatrix} \tag{1.13}$$

where $c = \cos(\pi/4+\delta)$. This corresponds to

$$\begin{aligned} \lambda^e_{\alpha\beta} &\propto \frac{m_e}{v} \sim 0 \\ \lambda^\mu_{\mu\tau} = s\frac{m_\tau}{v} \qquad \lambda^\mu_{e\tau} &= \frac{c}{\sqrt{2}}\frac{m_\tau}{v} \qquad \lambda^\mu_{e\mu} = \frac{c}{\sqrt{2}}\frac{m_\tau}{v} \\ \lambda^\tau_{\mu\tau} = c\frac{m_\mu}{v} \qquad \lambda^\tau_{e\tau} &= -\frac{s-\epsilon}{\sqrt{2}}\frac{m_\mu}{v} \qquad \lambda^\tau_{e\mu} = -\frac{s+\epsilon}{\sqrt{2}}\frac{m_\mu}{v} \end{aligned} \tag{1.14}$$

For $\theta = \pi/4$, $\epsilon = 0$ and degenerate sleptons, eqn (1.9) gives exactly degenerate neutrinos ν_e and $\nu_{\mu-\tau}$, whose mass varies inversely with the slepton mass. The observed neutrino mass differences and mixing angles, in the inverse hierarchy, can be obtained by including small perturbations. e difference between the square of the slepton masses $\tilde{m}_\mu^2 - \tilde{m}_\tau^2$ and the small mixing angle ϵ contribute to splitting the ν_1 and ν_2 masses, while the parameter δ of the V_λ matrix seems to control the solar mixing angle.

In Figure (1.4) we show the behaviour of two physical parameters, $\tan^2\theta_{12}$ and the ratio $\Delta m^2_{sol}/\Delta m^2_{atm}$, when the parameters δ and ϵ vary. For both the plots, we have considered only those points in agreement with the experimental bounds on the remaining set of neutrino parameters. From the intersection between the dark and the light region we can deduce the range of availability for ϵ and δ. (The slepton mass difference in these plots is fixed at a value that could be generated by renormalisation group running.)

[4]Since the SM has only one eigenbasis in e_R space, it is not required of new interactions that they have the same eigenvalues as $\mathbf{Y_e}^\dagger\mathbf{Y_e}$, provided that they have the same eigenvectors.

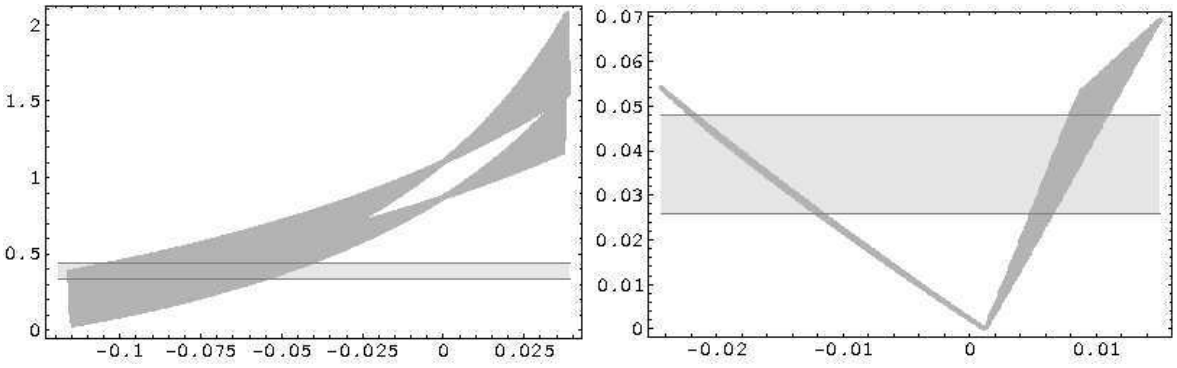

Figure 1.1: For slepton masses at $\sim$ 300 GeV and $\tan\beta \sim 25$, on the left we plot our prediction for the "solar" mixing parameter $\tan^2\theta_{12}$ as a function of the model parameter δ (see eqn (1.13)); where we have choosen an ϵ such that the other parameters ($\Delta m^2_{sol}/\Delta m^2_{atm}$, $\tan^2\theta_{23}$, $\sin^2\theta_{13}$) satisfy the experimental bounds. On the right we plot the ratio $\Delta m^2_{sol}/\Delta m^2_{atm}$ as a function of ϵ, with δ consistent with the experimental bounds on the other physical parameters ($\tan^2\theta_{12}$, $\tan^2\theta_{23}$, $\sin^2\theta_{13}$). In both cases the horizontal light gray band represents the experimentally allowed parameter space [18].

This λ model, then, satisfies our requests. The neutrino masses are generated by a renormalisable operator $\tilde{\lambda}$, whose eigenbasis is related with the charged lepton mass eigenbasis by a matrix $V_\lambda^\dagger$ different from the MNS mixing matrix. The matrix $V_\lambda^\dagger$, then, has become the operator that guides flavour violating processes, whose amplitudes are now determined by the λ couplings. In particular, we can see in (1.14) that the order of magnitude of each λ coupling is determined by its upper index, which is related with the flavour of the right-handed particle involved in the vertex. As we can see in Table 1.1 the experimental bounds on FV decays are satisfied in this λ model, in agreement with our definition of MFV.

The strongest experimental constraints on FV processes are given for the muon decay into three electrons and the $\mu \to e\gamma$ decay [19, 20, 21]. The flavour violating decays with charged leptons in the initial and final states, like $\mu^- \to e^-e^+e^-$, appear at the tree level and are mediated by the exchange of a left-handed sneutrino $\tilde{\nu}_i$. So, it can be easily understood why the decay rates of muon, but also tau, into three electrons are so low. In addition to the suppression due to the sneutrino mass, in each diagram appears a vertex $\tilde{\nu}ee$, whose amplitude is determined by a coupling of the form $\lambda^e_{\alpha\beta}$

	Expected value	**Experimental bound**
$BR(\mu^- \to e^- e^+ e^-)$	$\sim 10^{-17} \left(\frac{100\ GeV}{m_{\tilde{\nu}}}\right)^4$	$< 1.0\ 10^{-12}$
$BR(\mu^- \to e^- \gamma)$	$\sim 10^{-12} \left(\frac{100\ GeV}{m_{\tilde{\nu}}}\right)^4$	$< 1.2\ 10^{-11}$
$BR(\tau^- \to e^- e^+ e^-)$	$\sim 10^{-19} \left(\frac{100\ GeV}{m_{\tilde{\nu}}}\right)^4$	$< 2.9\ 10^{-6}$
$BR(\tau^- \to e^- \mu^+ \mu^-)$	$\sim 10^{-10} \left(\frac{100\ GeV}{m_{\tilde{\nu}}}\right)^4$	$< 1.8\ 10^{-6}$
$BR(\tau^- \to e^+ \mu^- \mu^-)$	$\sim 10^{-12} \left(\frac{100\ GeV}{m_{\tilde{\nu}}}\right)^4$	$< 1.5\ 10^{-6}$
$BR(\tau^- \to \mu^- e^+ e^-)$	$\sim 10^{-12} \left(\frac{100\ GeV}{m_{\tilde{\nu}}}\right)^4$	$< 1.7\ 10^{-6}$
$BR(\tau^- \to \mu^+ e^- e^-)$	0	$< 1.5\ 10^{-6}$
$BR(\tau^- \to \mu^- \mu^+ \mu^-)$	$\sim 10^{-11} \left(\frac{100\ GeV}{m_{\tilde{\nu}}}\right)^4$	$< 1.9\ 10^{-6}$

Table 1.1: Table of the branching ratios for flavour violating processes. In the second column appear the branching ratios predicted in the λ model, while in the third column are indicate the experimental bounds at 90% of confidence level [19].

which is proportional to the small electron mass, since right-handed sneutrinos are not present in the model.

The $\mu \to e\gamma$ decay [20], instead, appears at a loop level, mediated by a charged lepton and slepton. In this case the main contribution comes from the diagram with vertices proportional to $\lambda^{\mu}_{\mu\tau}\lambda^{\mu}_{e\tau} \propto m_\tau^2/v^2$, whose large contribution is somewhat compensated by the loop suppression. We estimate the decay branching ratio in our model to be $\sim 6 \times 10^{-13}$, and we can notice that, although this value respects the present experimental constraint, it could be accessible in the next experiments.

1.5 Summary

In the lepton sector, new beyond-the-Standard-Model (BSM) interactions are required to generate neutrino masses. If these masses are Majorana, they arise from a dimension five operator whose flavour structure (eigenvalues, eigenvectors in lepton doublet space) may not be the same as the (renormalisable) BSM interactions. In this context, it is not obvious to define Minimal Flavour Violation for leptons. One can take the "minimal" scenario to be that flavour-change in the lepton sector is controlled by the neutrino mass matrix, which is in part known. This predictive approach was taken in [3].

However, there are neutrino mass generation mechanisms that do not make this prediction, since flavour change may be proportional to a different combination of renormalisable couplings than enters m_ν. In this paper, we explore various possible definitions of "minimally flavour violating", based on the renormalisable interactions in the Lagrangian. We suppose that Minimal Flavour Violation is a restriction on the number of inequivalent eigenbases that *renormalisable* flavour-dependent interactions can choose. The most minimal possibility would be to restrict the new interactions to align themselves with the charged lepton Yukawa, but then it is difficult to obtain MNS mixing angles (without enlarging the flavour transformation group, for instance by adding right-handed neutrinos). The leptonic masses and mixing angles can be obtained in more models (*e.g.* triplet, R-parity violation) by allowing two eigenbases in doublet lepton space. The second basis may be other than the neutrino mass basis; we construct a model where flavour violation among charged leptons is not predictable from the light neutrino mass matrix.

Data in the quark sector suggest that new particles and interactions at the TeV-scale should satisfy Minimal Flavour Violation. Data in the lepton sector do not require a minimal flavour violation principle, but one could imagine it is there, by analogy with the quarks. Unfortunately, there are many possible definitions, which seem either predictive, or able to include many models. A compelling definition of MFV, giving different predictions for different neutrino mass generation mechanisms, could be useful in attempting a bottom-up reconstruction of the neutrino mass mechanism [22] from lepton flavour violating rates.

1.6 Appendix A

The aim of this appendix is to obtain an acceptable neutrino mass matrix, using new interactions that are diagonal in the charged lepton mass basis. We consider an RPV model, with lepton number violating terms in the superpotential

$$\frac{1}{2}\lambda^k_{ij} L_i L_j E^c_k + \mu_i H_u L_i \tag{1.15}$$

an $\not{L}$ soft term $B_i H_u L_i$, and we estimate the light neutrino mass matrix from the formulae in [23]. It seems possible to obtain degenerate light neutrinos ($m_\nu \sim 0.2$ eV), and an MNS matrix in agreement with observations [5].

This peculiar result arises by taking

$$\lambda^k_{ij} = \lambda \epsilon_{ijk} \quad , \quad \mu_\mu = \delta_\mu \mu_0 \quad , \quad B_\tau = \delta_B B_0 \tag{1.16}$$

and all other $\not{R}_p$ couplings to be zero. The usual μ_0 and B_0 terms are $\mu_0 H_u H_d$ in the superpotential and $B_0 H_u H_d$ among the soft breaking terms, and we will later solve for the desired values of δ_μ, δ_B. We claim that $\lambda \propto \epsilon_{ijk}$ is "flavour-diagonal", insofar as it is an SU(3) invariant (see discussion after eqn (1.11)). We can obtain off-diagonal contributions to the neutrino mass matrix, by combining it with the "bilinear" $\not{R}_p$ interactions B_τ and μ_μ.

The leading contributions to the neutrino mass matrix, in the charged lepton mass basis, can be estimated as [23]

$$[m_\nu] \simeq \frac{1}{8\pi^2 m_{SUSY}} \begin{bmatrix} \lambda^2 m_\mu m_\tau & \lambda\delta_B m_\tau (h_\mu m_\mu - h_e m_e) & \lambda\delta_\mu m_\mu (h_e m_e - h_\tau m_\tau) \\ \lambda\delta_B m_\tau (h_\mu m_\mu - h_e m_e) & 8\pi^2 |\delta_\mu|^2 m^2_{SUSY} & g^2 \delta_\mu \delta_B m^2_{SUSY}/8 \\ \lambda\delta_\mu m_\mu (h_e m_e - h_\tau m_\tau) & g^2 \delta_\mu \delta_B m^2_{SUSY}/8 & g^2 \delta_B^2 m^2_{SUSY}/8 \end{bmatrix} \tag{1.17}$$

where $m_{SUSY} \sim 300$ GeV is of order the slepton and neutralino masses.

We can match this onto the neutrino mass matrix for degenerate light neutrinos, with $\theta_{13} = 0$. Concentrating first on the $\mu\tau$ submatrix, we obtain

$$\delta_\mu \simeq \sqrt{\frac{m_1}{m_{SUSY}}} \qquad \delta_B \simeq \frac{8\pi}{g}\sqrt{\frac{m_1}{m_{SUSY}}} \tag{1.18}$$

[5] we did not scan parameter space, more realistic masses could be possible. Our example requires delicate fine-tuning.

and get the large atmospheric mixing by taking m_1, the lightest mass of the degenerate neutrinos, to be $\sqrt{4\pi\Delta m^2_{atm}/g^2} \simeq .2$ eV.

The first row has a desirable sign difference between the $e\mu$ and $e\tau$ entries, and can be adjusted to give the solar mass difference and mixing angle by taking $\lambda \sim .02$ and $\tan\beta \gtrsim 10$ ($\tan\beta$ enters via the charged lepton Yukawas).

Acknowledgements

We thank Aldo Deandrea, Gino Isidori, and Alessandro Strumia for discussions.

References

[1] G. D'Ambrosio, G. F. Giudice, G. Isidori and A. Strumia, Nucl. Phys. B **645** (2002) 155 [arXiv:hep-ph/0207036].

[2] A. J. Buras, P. Gambino, M. Gorbahn, S. Jager and L. Silvestrini, Phys. Lett. B **500** (2001) 161 [arXiv:hep-ph/0007085]. C. Bobeth, M. Bona, A. J. Buras, T. Ewerth, M. Pierini, L. Silvestrini and A. Weiler, Nucl. Phys. B **726** (2005) 252 [arXiv:hep-ph/0505110].

[3] V. Cirigliano, B. Grinstein, G. Isidori and M. B. Wise, Nucl. Phys. B **728** (2005) 121 [arXiv:hep-ph/0507001].

[4] K. S. Babu and C. N. Leung, Nucl. Phys. B **619** (2001) 667 [arXiv:hep-ph/0106054]. M. C. Gonzalez-Garcia and Y. Nir, Rev. Mod. Phys. **75** (2003) 345 [arXiv:hep-ph/0202058].

[5] P. Minkowski, Phys. Lett. B **67** (1977) 421; M. Gell-Mann, P. Ramond and R. Slansky, *Proceedings of the Supergravity Stony Brook Workshop*, New York 1979, eds. P. Van Nieuwenhuizen and D. Freedman; T. Yanagida, *Proceedinds of the Workshop on Unified Theories and Baryon Number in the Universe*, Tsukuba, Japan 1979, ed.s A. Sawada and A. Sugamoto; R. N. Mohapatra, G. Senjanovic, *Phys.Rev.Lett.* **44** (1980)912.

[6] H.P. Nilles and N. Polonsky, Nucl. Phys. **B499** (1997) 33. T. Banks, Y. Grossman, E. Nardi and Y. Nir, Phys. Rev. **D52** (1995) 5319. L. Hall

and M. Suzuki. *Nucl. Phys.*, B231:419, 1984. Y. Grossman and H. Haber, *Phys. Rev. Lett.* **78** (1997) 3438; *Phys.Rev.* **D59** 093008; hep-ph/9906310. R. Hempfling *Nucl.Phys.* **B478** (1996) 3. Eung Jin Chun, Sin Kyu Kang, *Phys.Rev.* **D61** (2000) 075012, M. Hirsch, M.A. Diaz, W. Porod, J.C. Romao, J.W.F. Valle, hep-ph/0004115.

[7] A. Zee, Phys. Lett. B **93** (1980) 389 [Erratum-ibid. B **95** (1980) 461].

[8] G. B. Gelmini and M. Roncadelli, Phys. Lett. B **99** (1981) 411. J. Schechter and J. W. F. Valle, Phys. Rev. D **25** (1982) 774. A. Santamaria, Phys. Rev. D **39** (1989) 2715. K. Choi and A. Santamaria, Phys. Lett. B **267** (1991) 504. C. Wetterich, Nucl. Phys. B **187** (1981) 343.

[9] A. Rossi, Phys. Rev. D **66** (2002) 075003 [arXiv:hep-ph/0207006].

[10] see *e.g.* A. J. Buras, arXiv:hep-ph/0505175.

[11] S. Antusch, C. Biggio, E. Fernandez-Martinez, M. B. Gavela and J. Lopez-Pavon, arXiv:hep-ph/0607020.

[12] V. Cirigliano and B. Grinstein, arXiv:hep-ph/0601111. V. Cirigliano, G. Isidori and V. Porretti, arXiv:hep-ph/0607068.

[13] G. C. Branco, M. N. Rebelo and J. I. Silva-Marcos, Phys. Rev. Lett. **82** (1999) 683 [arXiv:hep-ph/9810328].

[14] J. Hisano, T. Moroi, K. Tobe and M. Yamaguchi, Phys. Rev. D **53** (1996) 2442 [arXiv:hep-ph/9510309].

[15] an incomplete selection of papers studying LFV in the seesaw (see also [14]):
J. Hisano and D. Nomura, Phys. Rev. D **59** (1999) 116005 [arXiv:hep-ph/9810479].
S. Lavignac, I. Masina and C. A. Savoy, Nucl. Phys. B **633** (2002) 139 [arXiv:hep-ph/0202086].
J. A. Casas and A. Ibarra, Nucl. Phys. B **618** (2001) 171 [arXiv:hep-ph/0103065].

[16] S. Davidson and A. Ibarra, JHEP **0109** (2001) 013 [arXiv:hep-ph/0104076].

[17] S. Davidson and M. Losada, Phys. Rev. D **65** (2002) 075025 [arXiv:hep-ph/0010325].

[18] B. Aharmim *et al.* [SNO Collaboration], Phys. Rev. C **72** (2005) 055502 [arXiv:nucl-ex/0502021]. T. Araki *et al.* [KamLAND Collaboration], Phys. Rev. Lett. **94** (2005) 081801 [arXiv:hep-ex/0406035]. J. Nelson, for the Minos Experiment, talk at Neutrino'06, Santa Fe. Y. Ashie *et al.* [Super-Kamiokande Collaboration], "A measurement of atmospheric neutrino oscillation parameters by Phys. Rev. D **71** (2005) 112005 [arXiv:hep-ex/0501064].

[19] W.-M. Yao et al., *J. Phys.* **G 33**, 1 (2006)

[20] M. L. Brooks *et al.* [MEGA Collaboration], Phys. Rev. Lett. **83** (1999) 1521 [arXiv:hep-ex/9905013].

[21] U. Bellgardt *et al.* [SINDRUM Collaboration], Nucl. Phys. B **299** (1988) 1.

[22] M. Pospelov, A. Ritz and Y. Santoso, Phys. Rev. Lett. **96** (2006) 091801 [arXiv:hep-ph/0510254]. E. J. Chun, AIP Conf. Proc. **805** (2006) 145 [arXiv:hep-ph/0510318].

[23] S. Davidson and M. Losada, JHEP **0005**, 021 (2000) [arXiv:hep-ph/0005080].

2

SENSITIVITY OF THE BARYON ASYMMETRY PRODUCED BY LEPTOGENESIS TO LOW ENERGY CP VIOLATION

AUTHORS: Sacha Davidson[1], Julia Garayoa[2], F.P.[1] and Nuria Rius[2]

(1) *IPN de Lyon, Université Lyon 1, CNRS, 4 rue Enrico Fermi, Villeurbanne, 69622 cedex France*

(2) *Depto. de Física Teórica and IFIC, Universidad de Valencia-CSIC, Valencia, Spain*

PUBLISHED IN: Physical Review Letters 99 (2007) 161801 [1]

If the baryon asymmetry of the Universe is produced by leptogenesis, CP violation is required in the lepton sector. In the seesaw extension of the Standard Model with three hierarchical right-handed neutrinos, we show that the baryon asymmetry is *insensitive* to the PMNS phases: thermal leptogenesis can work for any value of the observable phases. This result was well-known when there are no flavour effects in leptogenesis; we show that it remains true when flavour effects are included.

[1]pre-print arXiv:0705.1503 [hep-ph]

2.1 Introduction

CP violation is required to produce the puzzling excess of matter (baryons) over anti-matter (anti-baryons) observed in the Universe[1]. If this Baryon Asymmetry of the Universe (BAU) was made via leptogenesis [2], then CP violation in the lepton sector is needed. So any observation thereof, for instance in neutrino oscillations, would support leptogenesis by demonstrating that CP is not a symmetry of the leptons. It is interesting to explore whether a stronger statement can be made about this tantalising link between low-energy observable CP violation and the BAU.

In this paper, we wish to address a phenomenological question: "is the baryon asymmetry *sensitive* to the phases of the lepton mixing matrix (PMNS matrix)? ". Electroweak precision data was said to be sensitive to the top mass, meaning that a preferred range for m_t could be extracted from the data. Here, we wish to ask a similar question, assuming the baryon asymmetry is generated, via leptogenesis, from the decay of the lightest "right-handed" (RH) neutrino: given the measured value of the baryon asymmetry, can an allowed range for the PMNS phases be obtained?

It was shown in [3] that the BAU produced by thermal leptogenesis in the type 1 seesaw, without "flavour effects", is insensitive to PMNS phases. That is, the PMNS phases can be zero while leptogenesis works, and the CP asymmetry of leptogenesis can vanish for arbitrary values of the PMNS phases. In fact, the "unflavoured" asymmetry is controlled by phases from the RH sector only, and it would vanish were this sector CP conserving. However, it was recently realised that lepton flavour matters in leptogenesis[4, 5, 6]: in the relevant temperature range $10^9 \to 10^{12}$ GeV, the final baryon asymmetry depends separately on the lepton asymmetry in τs , and on the lepton asymmetry in muons and electrons. So in this paper, we revisit the question addressed in [3], but with the inclusion of flavour effects. Our analysis differs from recent discussions [7] (2RHN model), [8, 9] (CP as a symmetry of the N sector), [10] (sequential N dominance) in that we wish to do a bottom-up analysis of the three generation seesaw. Ideally, we wish to express the baryon asymmetry in terms of observables, such as the light neutrino masses and PMNS matrix, and free parameters. Then, by inspection, one could determine whether fixing the baryon asymmetry constrained the PMNS phases.

2.2 Notation and review

We consider a seesaw model [11], where three heavy ($M \gtrsim 10^9$ GeV) majorana neutrinos N_I are added to the Standard Model. The Lagrangian at the N_I mass scale is

$$\mathcal{L} = \overline{e_R}^j \mathbf{Y_e}_{ij} H_d \ell^i + \overline{N}^J \lambda_{iJ} H_u \ell^i + \overline{N}^J \frac{\mathbf{M}_{JK}}{2} N^{cK} + h.c. \tag{2.1}$$

where the flavour index order on the Yukawa matrices $\mathbf{Y_e}, \lambda$ is left-right, and $H_u = i\sigma_2 H_d^*$.

There are 6 phases among the 21 parameters of this Lagrangian. We can work in the mass eigenstate basis of the charged leptons and the N_I, and write the neutrino Yukawa matrix as

$$\lambda = V_L^\dagger D_\lambda V_R \quad , \tag{2.2}$$

where D_λ is real and diagonal, and V_L, V_R are unitary matrices, each containing three phases. So at the high scale, one can distinguish CP violation in the left-handed doublet sector (phases that appear in V_L) and in the right-handed singlet sector (phases in V_R). Leptogenesis can work when there are phases in either or both sectors.

At energies accessible to experiment, well below the N_I mass scale, the light (LH) neutrinos acquire an effective Majorana mass matrix [2]:

$$[m\,] = \lambda M^{-1} \lambda^T v^2 = U D_m U^T \tag{2.3}$$

where $v = 174$ GeV is the Higgs vev, D_m is diagonal with real eigenvalues, and U is the PMNS matrix. There are nine parameters in $[m\,]$, which is "in principle" experimentally accessible. Two mass differences and two angles of U are measured, leaving the mass scale, one angle and three phases of U unknown.

From the above we can write

$$D_m \;=\; U^\dagger V_L^\dagger D_\lambda V_R D_M^{-1} V_R^T D_\lambda V_L^* U^* v^2 \tag{2.4}$$

so we see that the PMNS matrix will generically have phases if V_L and/or V_R are complex. Like leptogenesis, it receives contributions from CP violation in the LH and RH sectors. Thus it seems "probable", or even "natural", that there is some relation between the CP violation of leptogenesis and of the PMNS matrix. However, the

[2] which appears in the Lagrangian as $\frac{1}{2}[m\,]_{\alpha\beta}\nu^\alpha\nu^\beta + h.c$

notion of relation or dependence is nebulous [12], so we address the more clear and simple question of whether the baryon asymmetry is *sensitive* to PMNS phases. By this we mean: if the total baryon asymmetry is fixed, and we assume to know all the neutrino masses and mixing angles, can we predict ranges for the PMNS phases?

We suppose that the baryon asymmetry is made via leptogenesis, in the decay of the lightest singlet N_1, with $M_1 \sim 10^{10}$ GeV. Flavour effects are relevant in this temperature range [4, 5, 6], [3]. N_1 decays to leptons ℓ_α, an amount $\epsilon_{\alpha\alpha}$ more than to anti-leptons $\overline{\ell}_\alpha$, and this lepton asymmetry is transformed to a baryon asymmetry by SM processes (sphalerons). We will further suppose that the partial decay rates of N_1 to each flavour are faster than the expansion rate of the Universe H. This implies that N_1 decays are close to equilibrium, and there is a significant washout of the lepton asymmetry due to N_1 interactions (strong washout regime); we discuss later why this assumption does not affect our conclusions.

Flavour effects are relevant in leptogenesis[4, 5, 6] because the final asymmetry cares which leptons ℓ are distinguishable. N_1 interacts only via its Yukawa coupling, which controls its production and destruction. The washout of the asymmetry, by decays, inverse decays and scatterings of N_1, is therefore crucial for leptogenesis to work, because otherwise the opposite sign asymmetry generated at early times during N_1 production would cancel the asymmetry produced as they disappear. To obtain the washout rates (for instance, for $\ell + H_u \to N_1$), one must know the initial state particles, that is, which leptons are distinguishable.

At $T \sim M_1$, when the asymmetry is generated, SM interactions can be categorised as much faster than H, of order H, or much slower. Interactions that are slower than H can be neglected. H^{-1} is the age of the Universe and the timescale of leptogenesis, so the faster interactions should be resummed— for instance into thermal masses. In the temperature range $10^9 \lesssim T \lesssim 10^{12}$ GeV, interactions of the τ Yukawa are faster than H, so the ℓ_τ doublet is distinguishable (has a different "thermal mass") from the other two lepton doublets. The decay of N_1 therefore produces asymmetries in $B/3 - L_\tau$, and in $B/3 - L_o$, where ℓ^o ("other") is the projection in ℓ^e and ℓ^μ space, of the direction into which N_1 decays[14]: $\hat{\ell}_o = (\lambda_{\mu 1}\hat{\mu} + \lambda_{e1}\hat{e})/\sqrt{|\lambda_{\mu 1}|^2 + |\lambda_{e1}|^2}$. Following [6], we approximate these asymmetries to evolve independently. In this case, the baryon

[3] provided the decay rate of N_1 is slower than the interactions of the τ Yukawa [13]

to entropy ratio can be written as the sum over flavour of the flavoured CP asymmetries $\epsilon_{\alpha\alpha}$ times a flavour-dependent washout parameter $\eta_\alpha < 1$ which is obtained by solving the relevant flavoured Boltzmann equations [4, 5, 6]:

$$Y_B \simeq \frac{12}{37}\frac{1}{3g_*}\left(\epsilon_{\tau\tau}\eta_\tau + \epsilon_{oo}\eta_o\right) \tag{2.5}$$

where $g_* = 106.75$ counts entropy, and the 12/37 is the fraction of a $B-L$ asymmetry which, in the presence of sphalerons, is stored in baryons.

In the limit of hierarchical RH neutrinos, the CP asymmetry in the decay $N_1 \to \ell_\alpha H$ can be written as

$$\epsilon_{\alpha\alpha} \simeq -\frac{3M_1}{16\pi v^2[\lambda^\dagger\lambda]_{11}}\mathrm{Im}\{[\lambda]_{\alpha 1}[m^\dagger\lambda]_{\alpha 1}\} \tag{2.6}$$

where m is defined in eqn (2.3).

In the case of " strong washout" for all flavours, which corresponds to $\Gamma(N_1 \to \ell_\alpha H_u) > H_{(T=M_1)}$ for $\alpha = \tau, o$, the washout factor is approximately [6, 15]

$$\eta_\alpha \simeq 1.3\left(\frac{m_*}{6A_{\alpha\alpha}\widetilde{m}_{\alpha\alpha}}\right)^{1.16} \to \frac{m_*}{5A_{\alpha\alpha}\widetilde{m}_{\alpha\alpha}} \tag{2.7}$$

where there is no sum on α, $m_* \simeq 10^{-3}$ eV, and $A_{\tau\tau} \simeq A_{oo} \sim 2/3$ [14, 6] [4]. The (rescaled) N_1 decay rate is

$$\widetilde{m} = \sum_\alpha \widetilde{m}_{\alpha\alpha} = \sum_\alpha \frac{|\lambda_{\alpha 1}|^2}{M_1}v^2 \tag{2.8}$$

2.3 An equation

Combining equations (3.20), (2.6), and (2.7), we obtain $Y_B \propto \epsilon_{\tau\tau}/\widetilde{m}_{\tau\tau} + \epsilon_{oo}/\widetilde{m}_{oo}$, where ($\alpha$ not summed)

$$\frac{\epsilon_{\alpha\alpha}}{\widetilde{m}_{\alpha\alpha}} = \frac{3M_1}{16\pi v^2\widetilde{m}}\sum_\beta \mathrm{Im}\{\hat{\lambda}_\alpha m_{\alpha\beta}\hat{\lambda}_\beta\}\frac{|\lambda_\beta|}{|\lambda_\alpha|} \tag{2.9}$$

[4] The A matrix parametrises the redistribution of asymmetries in chemical equilibrium.

and the Yukawa couplings of N_1 have been written as a phase factor times a magnitude : $\hat{\lambda}_\alpha|\lambda_\alpha| = \lambda^*_{\alpha 1}$. So the baryon asymmetry can be approximated as

$$Y_B \simeq Y_B^{bd}\left(\frac{\mathrm{Im}\{\hat{\lambda}_\tau \cdot m_\cdot \hat{\lambda}_\tau\}}{m_{atm}} + \frac{\mathrm{Im}\{\hat{\lambda}_o \cdot m_\cdot \hat{\lambda}_o\}}{m_{atm}} + \frac{\mathrm{Im}\{\hat{\lambda}_\tau \cdot m_\cdot \hat{\lambda}_o\}}{m_{atm}}\left[\frac{|\lambda_o|}{|\lambda_\tau|} + \frac{|\lambda_\tau|}{|\lambda_o|}\right]\right)\frac{1}{A_{\tau\tau}} \tag{2.10}$$

The prefactor of the parentheses $Y_B^{bd} = \frac{12}{37}\frac{M_1 m_{atm}}{16\pi v^2}\frac{m_*}{5g_*\widetilde{m}}$ is the upper bound on the baryon asymmetry, that would be obtained in the strong washout case by neglecting flavour effects. Recall that this equation is only valid in strong washout for all flavours.

This equation reproduces the observation [6], that: *(i)* for equal asymmetries and equal decay rates of all distinguishable flavours, flavour effects increase the upper bound on the baryon asymmetry by $\sum_a A^{-1}_{aa} \sim 3$. *(ii)* More interestingly, having stronger washout in one flavour, can increase the baryon asymmetry [via the term in brackets]. So models in which the Yukawa coupling $\lambda_{\tau 1}$ is significantly different from $\lambda_{\mu 1}, \lambda_{e1}$, can have an enhanced baryon asymmetry (with cooperation from the phases).

Finally, this equation is attractive step towards writing the baryon asymmetry as a real function of real parameters (Y_B^{bd}, depending on M_1 and $\tilde{m}_1$), times a phase factor [16]. In this case, the phase factor is a sum of three terms, depending on the phases of the N_1 Yukawa couplings, light neutrino mass matrix elements normalised by the heaviest mass, and a (real) ratio of Yukawas.

2.4 CP violation

In this section, we would like to use eqn (2.10) to show that the baryon asymmetry is insensitive to the PMNS phases. The parameters of the lepton sector can be divided into "measurables", which are the neutrino and charged lepton masses, and the three angles and three phases of the PMNS matrix U. The remaining 9 parameters are unmeasurable. We want to show that for any value of the PMNS phases, there is at least one point in the parameter space of the unmeasurables where a large enough baryon asymmetry is obtained. The approximations leading to eqn (2.10) are only valid in a subset of the unmeasurable parameter space, but if we can find points in

this subspace, we are done. We first show analytically that such points exist, then we do a parameter space scan to confirm that leptogenesis can work for any value of the PMNS phases.

If the phases of the $\lambda_{\alpha 1}$ were independent of the PMNS phases, and a big enough Y_B could be obtained for some value of the PMNS phases, then our claim is true by inspection: for any other values, the phases of the $\lambda_{\alpha 1}$ could be chosen to reproduce the same Y_B. However, there is in general some relation between the phases of m and those of $\lambda_{\alpha 1}$, so we proceed by looking for an area of parameter space where the phases of the $\lambda_{\alpha 1}$ can be freely varied without affecting the "measurables". Then we check that a large enough baryon asymmetry can be obtained.

Such an area of parameter space can be found using the R matrix parametrisation of Casas-Ibarra [17], where the complex orthogonal matrix R is defined such that $\lambda v \equiv U D_m^{1/2} R D_M^{1/2}$. Taking a simple R of the form

$$R = \begin{bmatrix} \cos\phi & 0 & -\sin\phi \\ 0 & 1 & 0 \\ \sin\phi & 0 & \cos\phi \end{bmatrix} \tag{2.11}$$

and parametrising $U = VP$, where V is a CKM-like unitary matrix with one "Dirac" phase $e^{-i\delta}$ appearing with $\sin\theta_{13}$, and $P = \mathrm{diag}\{e^{i\varphi_1/2}, e^{i\varphi_2/2}, 1\}$, gives

$$\frac{\lambda_{\tau 1} v}{\sqrt{M_1 m_3}} = U_{\tau 1}\sqrt{\frac{m_1}{m_3}}\cos\phi + U_{\tau 3}\sin\phi \simeq \frac{\sin\phi}{\sqrt{2}} \tag{2.12}$$

$$\frac{\lambda_{\mu 1} v}{\sqrt{M_1 m_3}} = U_{\mu 1}\sqrt{\frac{m_1}{m_3}}\cos\phi + U_{\mu 3}\sin\phi \simeq \frac{\sin\phi}{\sqrt{2}} \tag{2.13}$$

$$\frac{\lambda_{e 1} v}{\sqrt{M_1 m_3}} = U_{e 1}\sqrt{\frac{m_1}{m_3}}\cos\phi + U_{e 3}\sin\phi \tag{2.14}$$

where we took hierarchical neutrino masses. We neglect λ_{e1} because its absolute value is small. With this choice of the unknown R, the phases of the $\lambda_{\alpha 1}$ are effectively independent of the PMNS phases. So for any choice of PMNS phases that would appear on the m of eqn (2.10), the phases of the Yukawa couplings can be chosen independently, to ensure enough CP violation for leptogenesis.

We now check that a large enough baryon asymmetry can be obtained in this area of parameter space. The parentheses of eqn (2.10) can be written explicitly as

$$\mathrm{Im}\left\{\frac{\sin^2\phi^*}{|\sin\phi|^2}(m_{\tau\tau} + m_{\mu\mu} + 2m_{\mu\tau})\right\}\frac{1}{m_{atm}} \tag{2.15}$$

Writing $\phi^* = \rho - i\omega$, the final baryon asymmetry can be estimated from eqn (2.10) as

$$\frac{Y_B}{10^{-10}} \simeq -\left(\frac{M_1}{10^{11}\text{GeV}}\right) \frac{\sin\rho\cos\rho\sinh\omega\cosh\omega}{(\sin^2\rho\cosh^2\omega + \cos^2\rho\sinh^2\omega)^2} \tag{2.16}$$

which can equal the observed $8.7^{+0.3}_{-0.4}\times10^{-11}$ [18] for $M_1 \sim$ few $\times10^{10}$ GeV, and judicious choices of ρ and ω.

A similar argument can be made if the light neutrino mass spectrum is inverse hierarchical.

The scatter plots of figure 2.1 show that a large enough baryon asymmetry can be obtained for any value of the PMNS phases.

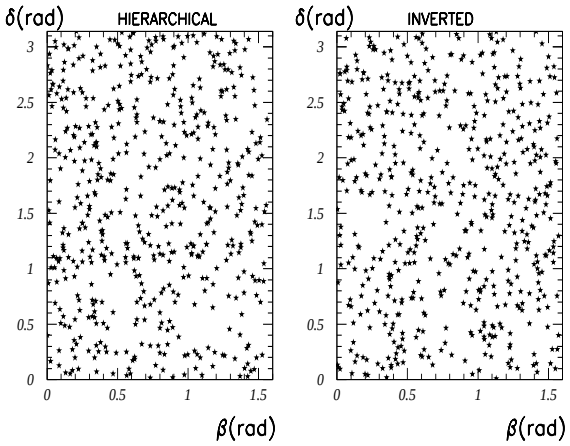

Figure 2.1: A random selection of points where the baryon asymmetry is large enough, for some choice of the unmeasurable parameters of the seesaw. The light neutrino masses are taken non-degenerate, and the Majorana phase of the smallest one can be neglected. The "Dirac" phase δ is defined such that $U_{e3} = \sin\theta_{13}e^{-i\delta}$, and β is the majorana phase of $m_2 = |m_2|e^{2i\beta}$. The baryon asymmetry arises in the decay of N_1 of mass $M_1 = 10^{10}$ GeV.

The plots are obtained by fixing $M_1 = 10^{10}$ GeV, and the measured neutrino parameters to their central values. To mimic the possibility that β and δ could be determined $\pm15^o$, β-δ space is divided into 50 squares. In each square, the programme randomly generates values for: β, δ, $.001 < \theta_{13} < .2$, the smallest neutrino mass $< \sqrt{\Delta m^2_{sol}}/10$, and the three complex angles of the R matrix. It estimates the baryon asymmetry from the analytic approximations of [6], and puts a cross if it is big enough. The programme

is a proto-Monte-Carlo-Markov-Chain, preferring to explore parameter space where the baryon asymmetry is large enough.

Parametrising with the R matrix imposes a particular measure (prior) on parameter space. This could mean we only explore a class of models. This is ok because the aim is only to show that, for any PMNS phases, a large enough asymmetry *can* be found.

2.5 Discussion

The relevant question, in discussing the "relation" between CP violation in the PMNS matrix and in leptogenesis, is whether the baryon asymmetry is *sensitive* to the PMNS phases. The answer was "no" for unflavoured leptogenesis in the Standard Model seesaw[3]. This was not surprising; the seesaw contains more phases than the PMNS matrix, and many unmeasurable real parameters which can be ajusted to obtain a big enough asymmetry. In this paper, we argue that the answer does not change with the inclusion of flavour effects in leptogenesis: for any value of the PMNS phases, it is possible to find a point in the space of unmeasurable seesaw parameters, such that leptogenesis works. This "flavoured" asymmetry can be written as a function of PMNS phases, and unmeasurables as entered the unflavoured calculation. These can still be ajusted to get a big enough asymmetry. In view of this discouraging conclusion, it is maybe worth to emphasize that CP violation from both the left-handed and right-handed neutrino sectors, contributes both to the PMNS matrix and the baryon asymmetry. Moreover, the answer to this question in an MSUGRA framework, with additional information from lepton flavour violating observables[19], is still work in progress.

In the demonstration that the baryon asymmetry (produced via thermal leptogenesis) is insensitive to PMNS phases, we found an interesting approximation for the "phase of leptogenesis" (see eqn (2.10)), when all lepton flavours are in strong washout.

Acknowledgments

J.G. is supported by a MEC-FPU Spanish grant. This project was partially supported by the Financement Projets Théorie de l'IN2P3, by Spanish grants FPA-2004-00996

and FPA2005-01269 and by the EC RTN network MRTN-CT-2004-503369.

References

[1] A. D. Sakharov, Pisma Zh. Eksp. Teor. Fiz. **5** (1967) 32 [JETP Lett. **5** (1967 SOPUA,34,392-393.1991 UFNAA,161,61-64.1991) 24].

[2] M. Fukugita and T. Yanagida, Phys. Lett. B **174** (1986) 45. G. F. Giudice *et al.*, Nucl. Phys. B **685** (2004) 89 [arXiv:hep-ph/0310123]. W. Buchmuller, P. Di Bari and M. Plumacher, Annals Phys. **315** (2005) 305 [arXiv:hep-ph/0401240]. A. Pilaftsis and T. E. J. Underwood, Phys. Rev. D **72** (2005) 113001 [arXiv:hep-ph/0506107].

[3] G. C. Branco *et al.*, Nucl. Phys. B **617** (2001) 475 [arXiv:hep-ph/0107164].

[4] A. Abada *et al.*, JCAP **0604** (2006) 004 [arXiv:hep-ph/0601083].

[5] E. Nardi *et al.*, JHEP **0601** (2006) 164 [arXiv:hep-ph/0601084].

[6] A. Abada *et al.*, JHEP **0609** (2006) 010 [arXiv:hep-ph/0605281].

[7] T. Fujihara *et al.*, Phys. Rev. D **72** (2005) 016006 [arXiv:hep-ph/0505076].

[8] S. Pascoli, S. T. Petcov and A. Riotto, Phys. Rev. D **75** (2007) 083511 [arXiv:hep-ph/0609125].

[9] G. C. Branco, R. Gonzalez Felipe and F. R. Joaquim, Phys. Lett. B **645** (2007) 432 [arXiv:hep-ph/0609297].

[10] S. Antusch, S. F. King and A. Riotto, JCAP **0611** (2006) 011 [arXiv:hep-ph/0609038].

[11] P. Minkowski, Phys. Lett. B **67** (1977) 421; M. Gell-Mann, P. Ramond and R. Slansky, *Proceedings of the Supergravity Stony Brook Workshop*, New York 1979, eds. P. Van Nieuwenhuizen and D. Freedman; T. Yanagida, *Proceedinds of the Workshop on Unified Theories and Baryon Number in the Universe*, Tsukuba, Japan 1979, ed.s A. Sawada and A. Sugamoto; R. N. Mohapatra, G. Senjanovic, *Phys.Rev.Lett.* **44** (1980)912.

[12] S. Davidson, arXiv:hep-ph/0409339.

[13] S. Blanchet, P. Di Bari and G. G. Raffelt, arXiv:hep-ph/0611337.

[14] R. Barbieri *et al.*, Nucl. Phys. B **575** (2000) 61 [arXiv:hep-ph/9911315].

[15] F. X. Josse-Michaux and A. Abada, arXiv:hep-ph/0703084.

[16] K. Hamaguchi, H. Murayama and T. Yanagida, Phys. Rev. D **65** (2002) 043512 [arXiv:hep-ph/0109030].

[17] J. A. Casas and A. Ibarra, Nucl. Phys. B **618** (2001) 171 [arXiv:hep-ph/0103065].

[18] D. N. Spergel *et al.* [WMAP Collaboration], arXiv:astro-ph/0603449.

[19] F. Borzumati and A. Masiero, Phys. Rev. Lett. **57** (1986) 961. J. Hisano *et al.*, Phys. Rev. D **53** (1996) 2442 [arXiv:hep-ph/9510309]. Y. Kuno and Y. Okada, Rev. Mod. Phys. **73** (2001) 151 [arXiv:hep-ph/9909265].

3

CP VIOLATION IN THE SUSY SEESAW: LEPTOGENESIS AND LOW ENERGY

AUTHORS: Sacha Davidson[1], Julia Garayoa[2], F.P.[1] and Nuria Rius[2]

(1) *IPN de Lyon, Université Lyon 1, CNRS, 4 rue Enrico Fermi, Villeurbanne, 69622 cedex France*

(2) *Depto. de Física Teórica and IFIC, Universidad de Valencia-CSIC, Valencia, Spain*

PUBLISHED IN: Journal of High Energy Physics 0809, 053 (2008) [1]

We suppose that the baryon asymmetry is produced by thermal leptogenesis (with flavour effects), at temperatures $\sim 10^9 - 10^{10}$ GeV, in the supersymmetric seesaw with universal and real soft terms. The parameter space is restricted by assuming that $\ell_\alpha \to \ell_\beta \gamma$ processes will be seen in upcoming experiments. We study the sensitivity of the baryon asymmetry to the phases of the lepton mixing matrix, and find that leptogenesis can work for any value of the phases. We also estimate the contribution to the electric dipole moment of the electron, arising from the seesaw, and find that it is (just) beyond the sensitivity of next generation experiments ($\lesssim 10^{-29} e$ cm). The fourteen dimensional parameter space is efficiently explored with a Monte Carlo Markov

[1] pre-print arXiv:0806.2832 [hep-ph]

Chain, which concentrates on the regions of interest.

3.1 Introduction

Neutrino masses are evidence for beyond the Standard Model (SM) physics. A simple extension of the standard model that accounts for neutrino masses is the seesaw mechanism [1], where heavy majorana right-handed neutrinos are added to the SM. Moreover, the seesaw scenario provides a very attractive framework to explain the baryon asymmetry of the universe (BAU) through the leptogenesis [2] mechanism, without inducing proton decay.

CP violation is a necessary ingredient to explain the BAU and, if this asymmetry is produced via leptogenesis, the required CP violation is encoded in the CP violating phases of the lepton sector. Three of them are the well known Dirac and Majorana phases of the PMNS mixing matrix, that are in principle measurable. Any observation of CP violation in the lepton sector, for instance CP violation in neutrino oscillations due to the PMNS phase δ, would then support leptogenesis by demonstrating that CP is not a symmetry of leptons. However, even in this very promising case, the question of whether the BAU is produced via leptogenesis is far from being answered, because it is not possible to reconstruct the high-energy CP odd observables from the low-energy ones [3] without assuming very constraining frameworks for the unmeasurable quantities. Therefore, the intent of this work is to clarify the relation between the CP violation accessible to low-energy experiments, and the CP violation necessary for leptogenesis, in a phenomenological *bottom-up* perspective, with minimal assumptions about the high scale theory. We just assume that the neutrino Yukawa couplings are hierarchical, which is the most natural assumption given the observed values of the charged lepton and quark Yukawas. Neutrino oscillation data then lead to hierarchical singlet masses.

In this paper, we aim to answer the phenomenological question of whether the BAU can be *sensitive* to low-energy phases, in the supersymmetric seesaw. We suppose the observed BAU is generated via thermal leptogenesis, and enquire whether this restricts the range of the phases. A similar issue was investigated by Branco *et.al* [4], where it was shown that for any value of the measurable CP violating phases, a large enough

BAU can be produced. This statement has been recently confirmed in a study [5] that includes flavour effects [6], in the Standard Model seesaw framework. In the present analysis, we want to address the question considering flavoured leptogenesis in a supersymmetric scenario, that has the interesting feature to potentially add new observables in the lepton sector, through the enhancement of flavour and CP violating processes (See *eg* [7] for a review and references on leptonic flavour and CP violation, induced by supersymmetry.).

The question we address, and the answer we find, differ from some other analyses [8, 9, 10, 11]. As written above, we aim to make few untestable assumptions, and to ask a precise phenomenological question: "Is the baryon asymmetry sensitive to PMNS phases?". We find the answer to be no. That is, there is "no correlation" between the BAU and PMNS phases, when all the unmeasurables in our scenario are allowed to vary over their whole range. To the best of our understanding, Refs. [8, 9, 10, 11] find a correlation between the BAU and the PMNS phases because they set unmeasurables (such as phases of the "right-handed" neutrinos) to fixed values.

We define "finding a correlation between Y_B and x" to mean "Y_B is sensitive to x". To show that the baryon asymmetry Y_B is insensitive to (or uncorrelated with) a parameter x, we must only show that, for any value of x, we can find a large enough Y_B. It would be numerically more challenging to show a correlation, because the point distribution in scatter plots may reflect the priors on the scanned parameters (see sections 3.6.4 and 3.7.2). Our definition of correlation differs from that used by [8, 9, 11], and also in [19] (who extract correlations from scatter plots). We use our narrow definition because it is parametrisation independent.

Since leptogenesis occurs at a very high-energy scale, a supersymmetric scenario is desirable in order to stabilize the hierarchy between the leptogenesis scale and the electroweak one. However, if supersymmetry exists at all, it must be broken and, in principle, the soft supersymmetry breaking Lagrangian can contain off-diagonal (in flavour space) soft terms, that would enhance lepton flavour violating (LFV) processes. These are strongly constrained by current experiments; this is the so-called supersymmetric flavour problem. In order to avoid it, we focus on the most conservative minimal Supergravity (MSUGRA) scenario with real boundary conditions, where the dynamics responsible for supersymmetry breaking are flavour blind and all the lepton flavour and

CP violation is controlled by the neutrino Yukawa couplings. Supersymmetric expectations for LFV [12, 13, 14] and possible relations to leptogenesis [7, 11, 15, 16, 17, 18] [2] and EDMs [19, 20] have been studied by many people.

We perform a scan over the seesaw parameters, looking for those points that give a large enough BAU, and where $\mu \to e\gamma$ and one of $\tau \to \ell\gamma$ would be seen in upcoming experiments. Our analysis is more restrictive than [19], in that we require these branching ratios to be "large". The aim is to verify if such experimental inputs imply a preferred range of values for the low-energy PMNS phases. We also estimate the contribution to the CP violating electron electric dipole moment. A detailed analysis of the MSUGRA scenario would require a scan also over the supersymmetric parameters, which is beyond the scope of our analysis.

Due to the large number of unknown parameters, instead of doing a usual grid scan in the seesaw parameter space we construct a Markov Chain using a Monte Carlo simulation (MCMC — see *e.g.* [21, 22]). This technique allows to efficiently explore a high-dimension parameter space, and we apply it for the first time to the supersymmetric seesaw model [3]. Our work is thus pioneering in the exhaustive scanning of the seesaw parameters, which would be otherwise prohibitive without the MCMC technique.

The paper is organized as follows. In section 3.2 we introduce the supersymmetric seesaw in the MSUGRA scenario and we review the low-energy interactions induced in the supersymmetric seesaw model. Section 3.3 is devoted to thermal leptogenesis with flavour effects, and section 3.4 describes our bottom-up reconstruction procedure. Section 3.5 gives analytic estimates, that complement our numerical analysis, using the MCMC technique, which is presented in section 3.6. We discuss our results in section 3.7 and conclude in section 3.8.

[2] See ref. [17] for a discussion about when the approximation used in [16] is not valid.

[3] See [23] for a detailed study of the Zee-Babu model of neutrino masses phenomenology using this technique.

3.2 Notation and review

We consider the superpotential for the leptonic sector in a supersymmetric seesaw model [1] with three hierarchical right-handed neutrinos ($M_1 < M_2 < M_3$):

$$W_{lep} = (L_L H_d) Y_e E^c + (L_L H_u) \lambda N^c + N^c \frac{M}{2} N^c. \tag{3.1}$$

In this expression, λ, Y_e and M are 3×3 matrices, and flavour indices are suppressed. The L_L are the supermultiplets containing left-handed lepton fields, E are those containing the right-handed charged leptons, while N are the supermultiplets of the right-handed singlets. The Majorana mass scale can be taken large 10^9 GeV $\lesssim M_i \lesssim 10^{15}$ GeV, since the corresponding operator is a singlet under the SM gauge group.

Without loss of generality one can work in the basis where Y_e and M are diagonal, so that the superpotential gives the following Lagrangian for leptons:

$$\mathcal{L} = Y_{e_\alpha} (\overline{\ell}_L^\alpha H_d^*) e_R^\alpha + (\overline{\ell}_L^\alpha H_u^*) \lambda^*{}_{\alpha i} N_i + \frac{M^i}{2} \overline{N^c}_i N_i + ... + h.c. \tag{3.2}$$

where the parentheses indicate SU(2) contractions and the flavour indices are written explicitly. Since supersymmetry is broken, to this Lagrangian we must add the soft SUSY breaking terms :

$$\mathcal{L}_{SSB} = \tilde{m}_0^2 \sum_f \tilde{f}^\dagger \tilde{f} + \left\{ \frac{B M^i}{2} \tilde{N}_i^c \tilde{N}_i^c + a_0 (y_{e_\alpha} \tilde{\ell}_L^\alpha \cdot H_d \tilde{e}_\alpha^c + \lambda_{\alpha i} \tilde{\ell}_L^\alpha \cdot H_u \tilde{N}_i^c) + h.c. \right\} \tag{3.3}$$

where $\tilde{f}$ collectively represents sfermions. This soft part is written at some high scale M_X where, in MSUGRA, the soft masses are universal and the trilinear couplings are proportional to the corresponding Yukawas. MSUGRA is then characterized by four parameters: the scalar (m_0) and gaugino ($m_{1/2}$) masses, shared by all of them at the GUT scale; the trilinear coupling involving scalars, a_0, at the GUT scale; and finally the Higgs vev ratio, $\tan\beta$.

In the chosen basis, the neutrino Yukawa matrix is in general not diagonal and complex, and can be written as:

$$\lambda = V_L^\dagger D_\lambda V_R \tag{3.4}$$

where D_λ is diagonal and real. Note that in this basis the neutrino Yukawa matrix is the only source of flavour violation in the lepton sector, through the unitary matrices V_L and

V_R that act respectively on the lepton doublet space and on the right-handed neutrino space. These matrices contribute also to CP violation, through six CP violating phases. In general, other sources of CP violation appear in the complex neutrino B-term, in the scalar mass $\tilde{m}_0$ and in the trilinear coupling a_0.

At energies well below the right-handed neutrino mass scale, the effective light neutrino majorana mass matrix can be written:

$$[m_\nu] = \lambda M^{-1} \lambda^T v_u^2 = U D_\nu U^T. \tag{3.5}$$

The first equality shows that the smallness of light neutrino masses is naturally explained once the right-handed neutrino mass is set at very high energy, $\sim 10^{14}$ GeV (in this expression $v_u = \langle H_u \rangle$). In the second equality, D_ν is a diagonal matrix with real positive eigenvalues and U is the $PMNS$ matrix containing the three low-energy CP violating phases, the Dirac phase δ and two Majorana phases α, β. Those phases are, in general, a combination of the 6 phases appearing in the complete theory. We use the standard parametrisation:

$$U = \begin{pmatrix} e^{i\alpha}\ c_{13}c_{12} & e^{i\beta}\ s_{12}c_{13} & s_{13}\ e^{-i\delta} \\ e^{i\alpha}\ (-s_{12}c_{23} - s_{23}s_{13}c_{12}\ e^{i\delta}) & e^{i\beta}\ (c_{23}c_{12} - s_{23}s_{13}s_{12}\ e^{i\delta}) & s_{23}c_{13} \\ e^{i\alpha}\ (s_{23}s_{12} - s_{13}c_{23}c_{12}\ e^{i\delta}) & e^{i\beta}\ (-s_{23}c_{12} - s_{13}s_{12}c_{23}\ e^{i\delta}) & c_{23}c_{13} \end{pmatrix}. \tag{3.6}$$

If we combine the equations (3.4) and (3.5), we can write:

$$D_\nu = U^\dagger V_L^\dagger D_\lambda V_R D_M^{-1} V_R^T D_\lambda V_L^* U^* v_u^2 \equiv W^\dagger D_\lambda V_R D_M^{-1} V_R^T D_\lambda W^* v_u^2, \tag{3.7}$$

with V_R diagonalizing the inverted right-handed neutrino mass matrix. This relation shows that non-zero angles and phases in the unmeasurable right-handed neutrino mixing matrix V_R imply non-zero angles and phases in $W = V_L U$, which being in the doublet sector, is potentially more accessible. We will use this relation to reconstruct the right-handed sector from low energy physics in sec. 3.4.

3.2.1 Low-energy footprints: LFV and EDMs in MSUGRA

Present bounds on LFV processes, shown in table 3.1, restrict the size of flavour off-diagonal soft terms. This suggests universal soft terms at some high scale M_X, see Eq. (3.3), like in the MSUGRA scenario. There are also stringent experimental bounds, as

	Present bounds	Future sensitivity
$\mathrm{BR}(\mu \to e\gamma)$	$< 1.2 \times 10^{-11}$	10^{-13} (MEG)[25]
$\mathrm{BR}(\tau \to \mu\gamma)$	$< 6.8 \times 10^{-8}$	10^{-9} (Belle)[26]
$\mathrm{BR}(\tau \to e\gamma)$	$< 1.1 \times 10^{-7}$	
$\mathrm{BR}(\mu \to e\bar{\nu}_e\nu_\mu)$	$\sim 100\%$	
$\mathrm{BR}(\tau \to \mu\bar{\nu}_\mu\nu_\tau)$	$17.36 \pm 0.05\%$	
$\mathrm{BR}(\tau \to e\bar{\nu}_e\nu_\mu)$	$17.84 \pm 0.05\%$	

Table 3.1: Present and predicted bounds on lepton flavour violating processes, and measured branching ratios for $\ell_\alpha \to \ell_\beta\nu_\alpha\bar{\nu}_\beta$ decays.

Present bounds (e cm)	Future sensitivity (e cm)
$d_e < 1.6 \times 10^{-27}$	10^{-29} (Yale group)[27]
$d_\mu < 2.8 \times 10^{-19}$	10^{-24} (Muon EDM Collaboration) [28]
$(-2.2 < d_\tau < 4.5) \times 10^{-17}$	

Table 3.2: Present and anticipated bounds on electric dipole moments. See [7] for a discussion of future experiments.

we can see in Table (3.2), on the CP violating electric dipole moments, which point towards very small CP phases. To address this "SUSY CP problem" [4], we suppose that all the soft breaking terms (namely a_0, m_0 and right-handed sneutrino B-term), as well as the μ term, are real. Even under this extremely conservative assumptions, it is well known that because of RGE running from high to low energy scales, the seesaw Yukawa couplings potentially induce lepton flavour and CP violating contributions to the soft terms [12, 13, 14].

We focus on these neutrino Yukawa coupling contributions to LFV and EDMs, assuming MSUGRA with real boundary conditions at M_X. Additional contributions, arising with less restrictive boundary conditions, are unlikely to cancel the ones we discuss, so the upper bounds that will be set if, for instance, no electron EDM is measured by the Yale group, will equally apply. Conversely, if an electron EDM is

[4]See *e.g.* [24] for an illuminating discussion.

measured above the range that we predict, it will prove the existence of a source of CP violation other than the neutrino Yukawa phases.

We are interested in analytic estimates for LFV rates and electric dipole moments. For this, we need the flavour-changing and CP violating contributions to the soft masses, that arise from the neutrino Yukawa. Following [29], we take the one-loop corrections to the flavour off-diagonal doublet slepton masses $\widetilde{m}^2_{L\alpha\beta} \to \widetilde{m}^2_{L\alpha\beta} + \Delta\widetilde{m}^2_{L\alpha\beta}$ and to the trilinear coupling $a_0\lambda \to a_0\lambda(1+\Delta a_0)$ to be:

$$\Delta\widetilde{m}^2_{L\alpha\beta} = -\frac{1}{16\pi^2}(3m_0^2+a_0^2)[C^{(1)}]_{\alpha\beta} - \frac{1}{16\pi^2}(m_0^2+a_0^2+2a_0B)[H]_{\alpha\beta}\ , \quad (3.8)$$

$$\Delta(a_0)_{\alpha\beta} = -\frac{1}{16\pi^2}[C^{(1)}]_{\alpha\beta} - \frac{1}{16\pi^2}[H]_{\alpha\beta}\ , \quad (3.9)$$

for $\alpha \neq \beta$ where the matrices H and $C^{(n)}$ are given by:

$$H \equiv \lambda\lambda^\dagger = V_L^\dagger D_\lambda^2 V_L\ , \quad (3.10)$$

$$C^{(n)} \equiv \lambda \log^n\left(\frac{MM^\dagger}{M_X^2}\right)\lambda^\dagger = V_L^\dagger D_\lambda V_R \log^n\left(\frac{MM^\dagger}{M_X^2}\right) V_R^\dagger D_\lambda V_L\ . \quad (3.11)$$

$C^{(1)}$ is the leading log contribution, and terms $\propto H$ arise in the finite part (they could be relevant for EDMs). The one loop corrections to the right handed charged slepton mass matrix, $\widetilde{m}^2_{R\alpha\beta}$ only contain the charged lepton Yukawa couplings and therefore cannot generate off-diagonal entries. These are generated at two loops and, as we will see later, they can be relevant for the lepton EDMs.

At one loop, sparticles generate the dipole operator (where e without subscript is the electro-magnetic coupling constant):

$$eX_{\alpha\beta}\overline{e_L}^\alpha \sigma^{\mu\nu} e_R^\beta F_{\mu\nu} + h.c. \quad (3.12)$$

which leads to LFV decays ($\ell_\alpha \to \ell_\beta\gamma$), and induces the flavour diagonal anomalous magnetic and electric dipole moments of charged leptons [7]. For $\alpha = \beta$, the anomalous magnetic moment is $a_\alpha = 4m_{e_\alpha}\mathrm{Re}\{X_{\alpha\alpha}\}$ and the electric dipole moment is $2\mathrm{Im}\{X_{\alpha\alpha}\}$.

In the mass insertion approximation the observable LFV rates are proportional to $|\widetilde{m}^2_{L\alpha\beta}|^2 \propto |C^{(1)}_{\alpha\beta}|^2$ and the corresponding branching ratios are of order [13]:

$$\begin{aligned}\frac{BR(\ell_\alpha \to \ell_\beta\ \gamma)}{BR(\ell_\alpha \to \ell_\beta \nu_\alpha \bar{\nu}_\beta)} &\sim \frac{\alpha^3}{G_F^2}\frac{\tan^2\beta}{m^8_{SUSY}}|\widetilde{m}^2_{\alpha\beta}|^2 \\ &\sim \frac{\alpha^3}{G_F^2}\frac{\tan^2\beta}{m^8_{SUSY}}\frac{(3m_0^2+a_0^2)^2}{(4\pi)^4}|[C]_{\alpha\beta}|^2,\end{aligned} \quad (3.13)$$

a_μ^{EXP}	$(116\ 592\ 080 \pm 63) \times 10^{-11}$ in BNK-E821
$\delta a_\mu = a_\mu^{EXP} - a_\mu^{SM}$	$(276 \pm 81) \times 10^{-11}$ [31] $(275 \pm 84) \times 10^{-11}$ [34] $(295 \pm 88) \times 10^{-11}$ [32]

Table 3.3: Experimental value and deviation from the SM predictions of the muon anomalous magnetic moment. The errors of δa_μ are the combination in quadrature of the experimental and theoretical ones.

where G_F is the Fermi constant, $\tan\beta = v_u/v_d$, and m_{SUSY} is a generic SUSY mass, which substitutes for the mixing angles and the function of the loop particle masses.

An estimate of m_{SUSY} can be obtained from the data on the anomalous magnetic moment of the muon, as suggested in [30]. A 3.3 or 3.4σ deviation from the Standard Model prediction is observed in the anomalous magnetic moment of the muon (in Table (3.3) is given the experimental value of a_μ and the deviation from the SM prediction [31, 32]). We assume it is due to new physics that can also contribute to flavour violation and EDMs. In the MSUGRA seesaw scenario that we are considering, the main contribution to a_μ comes from 1-loop diagrams with neutralino or chargino exchange and is given by [33]:

$$\delta a_\mu^{SUSY} \simeq \frac{\alpha m_\mu^2}{8\pi \sin^2\theta_{weak}} \frac{\tan\beta}{m_{SUSY}^2}. \tag{3.14}$$

Within this approximation, the observed deviation in the muon anomalous magnetic moment only fixes the ratio $\tan\beta/m_{SUSY}^2 \sim 5\ 10^{-5}\ GeV^{-2}$, so our SUSY masses scale with $\tan\beta$ as $m_{SUSY}^2 = \frac{\tan\beta}{2}(200\ \text{GeV})^2$.

Assuming [30] that the main contribution to the LFV branching ratio is given by analogous diagrams involving chargino and neutralino exchange, gives, from equations (3.13) and (3.14) with $m_0 \simeq a_0 \simeq m_{SUSY}$:

$$\frac{BR(\ell_\alpha \to \ell_\beta\ \gamma)}{BR(\ell_\alpha \to \ell_\beta \nu_\alpha \bar{\nu}_\beta)} \sim 10^{-8} |C_{\alpha\beta}|^2 \left(\frac{\delta a_\mu}{10^{-9}}\right)^2. \tag{3.15}$$

Since we aim to explore seesaw parameter space, we set the MSUGRA parameters $m_0 \simeq a_0 \simeq m_{SUSY}$.

In our analysis, we aim for values of $|C_{\alpha\beta}|^2$ that will give $\mu \to e\gamma$ and either of $\tau \to \ell\gamma$ in the next round of experiments. We require only one of the τ decays, because

the other must be small to suppress $\mu \to e\gamma$ (recall that we assume the neutrino Yukawas are hierarchical).

The neutrino Yukawa corrections to the soft terms can also enhance the predictions of the CP violating electric dipole moments. In our discussion we can neglect muon and tau EDMs, because the experimental sensitivity on d_μ is currently eight orders of magnitude weaker than on d_e and we expect $d_\mu/d_e \sim m_\mu/m_e$.

There are two potentially important contributions to the charged lepton EDMs induced by the neutrino Yukawa couplings. As discussed in [35, 29], the first non-zero contribution to the complex, flavour diagonal EDMs arises at two-loop order. The matrices Δa_0 and $\Delta\widetilde{m}_L^2$ in Eq.(3.8) are the available building blocks to make an EDM, which turns out to be proportional to the commutator $[H, C]$. This is the dominant contribution at low $\tan\beta$.

We follow [29] [5] to estimate:

$$d_e \sim \frac{4\alpha}{(4\pi)^5}\frac{m_e^2}{m_{SUSY}^2}\mathrm{Im}[H\,C]_{ee}(1.9\,10^{-11}\text{ e cm}) \sim 10^{-29}\,\left(\frac{2}{\tan\beta}\right)\mathrm{Im}[H\,C]\text{ e cm}\,, \quad (3.16)$$

where we have used $[H, C]/i = 2\mathrm{Im}[H\,C]$, and the $2/\tan\beta$ arises because we extracted m_{SUSY}^2 from the δa_μ.

In the large $\tan\beta$ region, it has been shown [36] that a different contribution to the EDMs can be the dominant one. This new contribution arises at three loops, and it involves the two loop correction to the right handed charged slepton mass matrix $\Delta\widetilde{m}_E^2$. It is proportional to the CP violating quantity:

$$D_\alpha = \mathrm{Im}\left[((\Delta\widetilde{m}_E^2)^T m \Delta\widetilde{m}_L^2\right]_{\alpha\alpha} \quad (3.17)$$

where m is the (diagonal) charged lepton mass matrix. Despite being a higher loop order, it is typically dominant for $\tan\beta \gtrsim 10$. The two loop expression for $\Delta\widetilde{m}_E^2$ can be found in [29]. We approximate this contribution as:

$$d_e \;\simeq\; \frac{-e}{2}\frac{8\alpha}{(4\pi)^7}\frac{10 m_e\tan\beta}{m_{SUSY}^2}\frac{\mathrm{Im}[\lambda^*_{ek}\lambda_{\alpha k}m^2_{\ell_\alpha}\lambda^*_{\alpha m}\lambda_{em}]}{v^2\cos^2\beta}F(M_k^2), \quad (3.18)$$

where

$$F(M_k^2) = \left(\log\frac{M_X^2}{M_N^2}\log\frac{M_X^2}{M_k^2}\log\frac{M_N^2}{M_k^2} + \log^2\frac{M_N^2}{M_k^2}\log\frac{M_N^2}{M_m^2}\right), \quad (3.19)$$

[5] [29] finds the same structure as [35, 36], but its result is smaller by one power of a large logarithm.

and $M_X = 3 \times 10^{16}$ GeV, $M_N = M_2$. It gives an electric dipole moment of order:

$$d_e \;\sim\; 10^{-29} \left(\frac{\tan\beta}{50}\right)^2 \frac{\mathrm{Im}[\lambda^*_{ek}\lambda_{\alpha k} m^2_{\ell_\alpha} \lambda^*_{\alpha m}\lambda_{em}]}{m^2_\tau}\; e\mathrm{cm}.$$

One comment is in order. Throughout this work, we use the approximated formulae (3.15), (3.16) (3.18), where we have set the supersymmetric parameters m_0 and a_0 at a common m_{SUSY} scale. Of course these are very rough approximations, but given that a detailed analysis of the MSUGRA scenario is beyond the scope of this study, which concentrates on the seesaw parameters, it is enough to illustrate our results.

Notice that, since we normalize the LFV branching ratios to the muon g-2 deviation from the SM, there is no enhancement of LFV for large $\tan\beta$. The three loop EDM contribution (3.18) is enhanced, because it has extra powers of $\tan\beta$.

3.3 Flavoured thermal leptogenesis

The observed Baryon Asymmetry of the Universe [37] is:

$$Y_{\Delta B} \;\equiv\; \left.\frac{n_B - n_{\bar{B}}}{s}\right|_0 = (8.75 \pm 0.23) \times 10^{-11} \tag{3.20}$$

where n_{B0}, $n_{\bar{B}0}$, and s_0 are the number densities of baryons, antibaryons, and entropy, in the Universe today. We assume this excess is produced via flavoured thermal leptogenesis[2, 6, 38], through the decays of the lightest singlet neutrino N_1 and sneutrino $\tilde{N}_1$, in the thermal plasma at $T \sim M_1$. The population of N_1 and $\tilde{N}_1$ is produced by inverse decays and scattering in the plasma. The decays are CP violating and controlled by the neutrino Yukawa coupling, thus for hierarchical right-handed (s)neutrinos the CP-asymmetry is given by [39]:

$$\begin{aligned}
\epsilon_{\alpha\alpha} &= \frac{\Gamma(N_1 \to \ell_\alpha H,\ \widetilde{\ell_\alpha} h) - \Gamma(N_1 \to \overline{\ell}_\alpha \overline{H},\ \overline{\widetilde{\ell_\alpha}}\,\overline{h})}{\Gamma(N_1 \to \ell H,\ \widetilde{\ell} h) + \Gamma(N_1 \to \overline{\ell H},\ \overline{\widetilde{\ell}}\,\overline{h})} \\
&\simeq \frac{3M_1}{8\pi v_u^2 \left[\lambda^\dagger\lambda\right]_{11}} \mathrm{Im}\left\{[\lambda]_{\alpha 1}[m_\nu^\dagger \lambda]_{\alpha 1}\right\},
\end{aligned} \tag{3.21}$$

where α specifies the flavour of the (s)lepton doublet in the final state. If the CP violating decays are out-of-equilibrium the lepton asymmetry produced can survive and be partially converted into a baryon asymmetry through non perturbative SM sphaleron processes[40].

In Eq.(3.21) we have intentionally not summed over the flavour index α, because flavours can have a role in the evolution of the lepton asymmetry [6]. That is, if a flavour in the thermal bath is distinguishable, then the corresponding lepton asymmetry follows an independent evolution. This occurs when the charged lepton Yukawa interaction rate $\Gamma_{\ell_\alpha} = 5 \times 10^{-3} T Y_\alpha^2$ is faster than the expansion rate H and the singlet inverse decay rate $\Gamma_{ID} \sim e^{-m/T}\Gamma_N$, where Γ_N is the right-handed neutrino decay rate. Since leptogenesis takes place at $T \sim M_1$ the mass of the lightest right-handed (s)neutrino tells us if flavour effects are important.

In the MSSM, the charged lepton Yukawas are larger than in the SM: $Y_\alpha = m_\alpha/(\cos\beta \times 174\text{GeV})$, so they come into equilibrium earlier. At very high temperatures $T > \tan^2\beta\ 10^{12}$ GeV [6], the charged lepton yukawa interactions are out of equilibrium ($\Gamma_{\ell_\alpha} \ll H$) and there are no flavour effects, so leptogenesis can be studied in one-flavour case. However, as the temperature drops, the τ interactions come into equilibrium. In the range $\tan^2\beta\ 10^9 \lesssim T \lesssim \tan^2\beta\ 10^{12}$ GeV, we have an intermediate two-flavour regime, so that the lepton asymmetry produced in the τ evolves separately from the lepton asymmetry created in the linear combination:

$$\hat{\ell}_o = \frac{\lambda_{\mu 1}\hat{\mu} + \lambda_{e1}\hat{e}}{\sqrt{|\lambda_{\mu 1}|^2 + |\lambda_{e1}|^2}}\ . \tag{3.22}$$

For $T \lesssim \tan^2\beta\ 10^9$ GeV, also the μ Yukawa interactions come into chemical equilibrium and all the three flavours become distinguishable.

In all the flavour regimes the baryon to entropy ratio can be written as:

$$Y_B \simeq \frac{10}{31}\frac{n_N + n_{\tilde{N}}}{s}\sum_\alpha \epsilon_{\alpha\alpha}\eta_\alpha\ \simeq \frac{10}{31}\frac{315\zeta(3)}{4\pi^4 g_*}\sum_\alpha \epsilon_{\alpha\alpha}\eta_\alpha\ . \tag{3.23}$$

The numerical prefactor indicates the fraction of $B-L$ asymmetry converted into a baryon asymmetry by sphalerons [41] in the MSSM. The second fraction is the equilibrium density of singlet neutrinos and sneutrinos, at $T \gg M_1$, divided by the entropy density s. Numerically, it is of order 4×10^{-3}, similar to the non-SUSY case [7]. The $\epsilon_{\alpha\alpha}$ are the CP asymmetries in each flavour (so that $\alpha = \tau, o$ or $\alpha = \tau, \mu, e$ in the two- or three-flavour regimes respectively) and the η_α are the efficiency factors which take

[6] We approximate $\tan\beta \simeq 1/\cos\beta$ because $\sin\beta \sim 1$ and $\tan\beta$ is a more familiar parameter.

[7] The addition of the $\tilde{N}$s is compensated by the approximate doubling of the degrees of freedom in the plasma : $g_* = 228.75$ for the MSSM.

into account that these CP asymmetries are partially erased by inverse decays and scattering processes. We assume the efficiency factors have the same functional form and numerical factors as for non-supersymmetric leptogenesis [6]:

$$\eta_\alpha \simeq \left[\left(\frac{m_*}{2|A_{\alpha\alpha}|\tilde{m}_{\alpha\alpha}}\right)^{-1.16} + \left(\frac{|A_{\alpha\alpha}|\tilde{m}_{\alpha\alpha}}{2m_*}\right)^{-1}\right]^{-1}, \tag{3.24}$$

where we neglect A-matrix [42] factors in our numerical analysis. The rescaled N_1 decay rate is defined as :

$$\widetilde{m} = \sum_\alpha \widetilde{m}_{\alpha\alpha} = \sum_\alpha \frac{|\lambda_{\alpha 1}|^2}{M_1} v_u^2, \tag{3.25}$$

and in supersymmetry $m_*^{MSSM} = m_*^{SM}/\sqrt{2} = 4\pi v_u^2 H_1/M_1^2 \simeq 0.78 \times 10^{-3}$ eV [8], where H_1 is the Hubble expansion rate at $T = M_1$.

Combining equations Eq.(3.23), Eq.(3.21), Eq.(3.24) and Eq.(3.25), we can write the BAU as:

$$Y_B = -\frac{10}{31}\frac{135 M_1}{4\pi^5 g_* v_u^2}\sum_\alpha \eta_\alpha \ \mathrm{Im}\{\hat{\lambda}_\alpha [m_\nu^\dagger \cdot \hat{\lambda}]_\alpha\}, \tag{3.26}$$

where $\hat{\lambda}_\alpha = [\lambda]_{\alpha 1}/\sqrt{[\lambda^\dagger\lambda]_{11}}$. Y_B is roughly a factor of $\sqrt{2}$ larger than in the SM, in the limit where $\tilde{m}_{\alpha\alpha} > m_*$ for all flavours.

Supersymmetric thermal leptogenesis suffers from the so called gravitino problem[43]: in a high temperature plasma gravitinos are copiously produced and their late decay can jeopardize successful nucleosynthesis (BBN). This gives an upper bound on the reheat temperature of the Universe T_{RH}, which constrains the temperature at which leptogenesis can take place, and gives an upper bound on the singlet neutrino mass $M_1 \lesssim 5T_{RH}$ [44, 45]. However, there is also a lower bound on $M_1 \gtrsim 10^9$ GeV [46] (for hierarchical Ns) to obtain a large enough lepton asymmetry. This can be seen from (3.26), where $Y_B \propto M_1$. It has recently been suggested [47] that this conflict can be avoided by generating the singlet masses after reheating. However, we here assume that $M_1 > 10^9$ GeV is fixed before reheating.

[8] There are factors of 2 for SUSY: defining Γ_D to be the total N decay rate, we have $\Gamma_D^{SUSY} = 2\Gamma_D^{SM}$. So with the definition of eq. (3.25) for $\tilde{m}$, we have $\tilde{m} = 4\pi v_u^2 \Gamma_D^{MSSM}/M_1^2$ as opposed to $\tilde{m} = 8\pi v_u^2 \Gamma_D^{SM}/M_1^2$. So $m_*^{SUSY} = m_*^{SM}/\sqrt{2}$, where m_* is the value of $\tilde{m}$ that would give $\Gamma_D = H_1$ at $T = M_1$, and the factor of $\sqrt{2}$ is because there are approximately twice as many degrees of freedom in the plasma.

There are various ways to obtain $T_{RH} \sim 10^9 - 10^{10}$ GeV. If the gravitino is unstable, the nucleosynthesis bound leads to very stringent upper bounds on the reheating temperature after inflation [48]: $T_{RH} \lesssim 10^4 - 10^5$ GeV for $m_{3/2} \lesssim 10$ TeV, or $T_{RH} \lesssim 10^9 - 10^{10}$ GeV for $m_{3/2} > 10$ TeV. A sufficiently high reheat temperature is obtained for very heavy gravitinos because they decay before BBN. Alternatively, if the gravitino is the stable LSP, a correct dark matter relic density can be obtained for $T_{RH} \sim 10^9 - 10^{10}$ GeV. In this scenario, one must ensure that the decay of the NLSP does not perturb BBN. This can be obtained, for instance by choosing the NLSP with care [49] or by having it decay before BBN via R-parity violating interactions[50].

We can summarise that a reheat temperature $\gtrsim 10^9$ GeV is difficult but not impossible in supersymmetry. So for the purposes of this paper, we will allow $M_1 < 10^{11}$ GeV.

3.4 Reconstructing leptogenesis from low energy observables

In order to search for a connection between the low-energy observables and leptogenesis, we need a parametrisation in which we can input the low energy observables, and then compute the BAU. Ideally we want to express the high-energy parameters in terms of observables [51]. Therefore, we write the seesaw parameters in terms of operators acting on the left-handed space, potentially more accessible: so we chose D_ν, D_λ and V_L (that appears in the combination $\lambda\lambda^\dagger$) and U_{PMNS}. Within this bottom-up approach, the CP violation is now encoded in the three, still unknown, low energy phases of the PMNS matrix U, and in the three unknown phases in V_L. We then reconstruct the right-handed neutrino parameters in terms of those inputs.

The matrices D_ν and U_{PMNS} can be determined in low-energy experiments. Through neutrino oscillation experiments we can extract the two neutrino mass differences, the PMNS matrix mixing angles and, in the future, the Dirac phase [52] (if Nature is kind with us). Furthermore, we have an upper bound on light neutrino masses that comes from cosmological evaluations[53], Tritium beta decay[54], and neutrinoless double beta decay[55]. Observing this last process could prove the Majorana nature of neutrinos and put some constraints on the combination of Majorana phases.

We have seen that in MSUGRA there is an enhancement of lepton flavour violating processes due to the neutrino Yukawa couplings. Assuming that these processes can be measured in the near future constrains the coefficients $[C]_{\alpha\beta}$, see Eq. (3.13), which depend on D_λ and V_L. We parametrise the V_L matrix as the product of three rotations along the three axes, with a phase associated to each rotation:

$$V_L^\dagger = \begin{pmatrix} c_{13}^L c_{12}^L & c_{13}^L s_{12}^L\ e^{-i\rho} & s_{13}^L\ e^{-i\sigma} \\ -c_{23}^L s_{12}^L\ e^{i\rho} - s_{23}^L\ e^{-i\omega} s_{13}^L c_{12}^L\ e^{i\sigma} & c_{23}^L c_{12}^L - s_{23}^L\ e^{-i\omega} s_{13}^L s_{12}^L\ e^{-i\rho}\ e^{i\sigma} & c_{13}^L s_{23}^L\ e^{-i\omega} \\ s_{23}^L\ e^{i\omega} s_{12}^L\ e^{i\rho} - s_{13}^L c_{23}^L c_{12}^L\ e^{i\sigma} & -s_{23}^L\ e^{i\omega} c_{12}^L - s_{13}^L s_{12}^L c_{23}^L\ e^{-i\rho}\ e^{i\sigma} & c_{23}^L c_{13}^L \end{pmatrix}, \tag{3.27}$$

¿From the bottom-up parameters defined above and using the equation (3.7), we are now able to reconstruct the right handed neutrino mass matrix and the V_R matrix appearing in the baryon asymmetry:

$$M^{-1} = V_R D_M^{-1} V_R^T = D_\lambda^{-1} V_L U D_\nu U^T V_L^T D_\lambda^{-1} v_u^{-2}\ . \tag{3.28}$$

In leptogenesis *without* flavour effects, the BAU is controlled only by the phases of V_R, which also contribute to the U_{PMNS} in the parametrisation we use. However, as demonstrated in the R matrix parametrisation [56], it is always possible to choose V_L such that the lepton asymmetry ϵ has any value for any value of PMNS phases [4]. So for Y_B in its observed range, the PMNS phases can be anything, and if we measure values of the PMNS phases, Y_B can still vanish. In flavoured leptogenesis, the BAU can be written as a function of PMNS phases and unmeasurables, but it was shown in [5] that for the Standard Model seesaw, Y_B is insensitive to the PMNS phases. Relations between low energy CP violation and leptogenesis can be obtained by imposing restrictions on the high-scale theory, for instance that there are no right-handed phases [8].

In the case of MSUGRA, we assume that we will have two more measurable quantities in the near future, $\mu \to e\gamma$ and either of $\tau \to \ell\gamma$. Naively, we do not expect LFV rates to add more information on the CP violating phases, because the rates can be used to fix two (real) parameters in D_λ and V_L. The question is whether the remaining phases and real parameters, can always be arranged to generate a large enough BAU. We find the answer to be yes. For instance, in the limit of taking only the largest neutrino Yukawa coupling in D_λ, the matrices $C^{(n)}$ become proportional to H, and

using the parametrisation of the V_L matrix given in Eq.(3.27) one can easily see that the CP violating phases of the V_L matrix disappear from the LFV branching ratios.

Besides the LFV processes, the neutrino Yukawa couplings can also contribute to the CP violating electric dipole moments. These contributions are expected to be below the sensitivity of current experiments [20, 57]. See [57] for a discussion of the impact of EDMs on seesaw reconstruction. In our framework with hierarchical Yukawas we expect some suppression on this contributions to the EDMs. As we have seen in Section 3.2.1, for low $\tan\beta$ the main contribution is proportional to the commutator of the matrices $C^{(1)}$ and H, see eq. (3.16). Thus in the limit of taking only the largest Yukawa, which implies $C^{(1)} \propto H$, the commutator is equal to zero. Regarding the large $\tan\beta$ regime, although the contribution to the EDMs has a different dependence, given in eq. (3.18), it can be shown that it also vanishes in this limit. This means that a non-zero contribution will be suppressed by mixing angles and a smaller eigenvalue of H.

3.5 Analytic Estimates

If a parametrisation existed, in which one could input the light neutrino mass matrix, the neutrino Yukawa couplings that control lepton flavour violation, *and* the baryon asymmetry, then it would be clear that the BAU, and other observables, are all insensitive to each other. In this section, we argue that at the minimum values of M_1 where leptogenesis works, such a parametrisation "approximately" exists.

We analytically construct a point in parameter space that satisfies our criteria (large enough BAU, LFV observable soon), and where the baryon asymmetry is insensitive to the PMNS phases. To find the point, we parametrise the seesaw with the parameters of the effective Lagrangian relevant to N_1 decay. Since the observed light neutrino mass matrix is not an input in this parametrisation, one must check that the correct low energy observables are obtained. This should occur, in the region of parameter space considered[9], because the contribution of N_1 to the light neutrino mass matrix can be neglected. We construct the point for the normal hierarchy and small $\tan\beta$; similar

[9]This area of parameter space was also found in [58] using a left-handed parametrisation inputting $W = V_L U$ instead of V_L. See also [59].

constructions are possible for the other cases.

The effective Lagrangian for N_1 and $\tilde{N}_1$, at scale $M_1 \lesssim \Lambda \ll M_2$, arises from the superpotential:

$$W_{N_1} = \lambda_{\alpha 1} L_L^\alpha H_u N_1^c + \frac{M_1}{2} N_1^c N_1^c + \kappa_{\alpha\beta}(L_L{}^\alpha H_u)(L_L{}^\beta H_u) \tag{3.29}$$

where $\kappa_{\alpha\beta}$ is obtained by integrating out N_2 and N_3. It is known [60] that the smallest M_1 for which leptogenesis (with hierarchical N_i) works, occurs at $m_* \lesssim \tilde{m} \lesssim m_{sol}$. So we assume that

$$\frac{\lambda_{\alpha 1}\lambda_{\beta 1}}{M_1} v_u^2 \ll m_{\alpha\beta}, \tag{3.30}$$

implying that N_1 makes negligible contribution to light neutrino observables. We are therefore free to tune the $\lambda_{\alpha 1}$s to maximise the baryon asymmetry.

To obtain a baryon asymmetry $Y_B \simeq 10^{-3} \sum_\alpha \epsilon_{\alpha\alpha}\eta_\alpha \simeq 8 \times 10^{-11}$, we require:

$$\sum_\alpha \epsilon_{\alpha\alpha}\eta_\alpha \simeq 8 \times 10^{-8} \ . \tag{3.31}$$

For $\tan\beta \simeq 2$, it is unclear whether the ℓ_μ is distinct for leptogenesis purposes. For simplicity we assume not, and use two flavours o and τ. The efficiency factors η_α are maximised to $\eta_\alpha \simeq 1/4$ for $\tilde{m}_{\alpha\alpha} = |\lambda_{\alpha 1}|^2 v_u^2/M_1 \simeq \sqrt{2} m_*$. Since $\tilde{m} \simeq 3m_*$, this is barely in the strong washout regime, and (3.24) should be an acceptable approximation.

We would therefore like to find a point in parameter space, such that $M_1 \sim 10^9$ GeV, $\epsilon_{oo} \simeq \epsilon_{\tau\tau} \simeq 1.6 \times 10^{-7}$. Defining $\hat{\lambda}_\alpha = \lambda_{\alpha 1}/\sqrt{\sum_\alpha |\lambda_{\alpha 1}|^2}$, equation (3.21) implies that we need, for $\alpha = o$ and $\alpha = \tau$:

$$\mathrm{Im}\Big\{\hat{\lambda}_{\alpha 1}\frac{[m^\dagger \hat{\lambda}]_{\alpha 1}}{m_3}\Big\} \gtrsim \frac{10^9 \mathrm{GeV}}{M_1} \ . \tag{3.32}$$

This means that $\hat{\lambda}_1$ needs a component along $\hat{u}_3$ (the eigenvector of m_3), and, since it should also generate m_1, it needs a component along $\hat{u}_1$. It can always be written as:

$$\vec{\lambda}_1 = \lambda_{11}\hat{u}_1 + \lambda_{21}\hat{u}_2 + \lambda_{31}\hat{u}_3 \quad , \tag{3.33}$$

where $\{1,2,3\}$ indices indicate the light neutrino mass basis. In the following we take $\lambda_{21} = 0$, $\lambda_{31} = |\lambda_{31}|e^{i\zeta}$, $|\lambda_{31}| \gg |\lambda_{11}|$. With equation (3.5),

$$\begin{aligned} \mathrm{Im}\Big\{\hat{\lambda}_{\alpha 1}\frac{[m^\dagger \hat{\lambda}]_{\alpha 1}}{m_3}\Big\} &= \frac{1}{|\lambda_{11}|^2 + |\lambda_{31}|^2}\mathrm{Im}\Big\{(\lambda_{11}\lambda_{31}U_{\alpha 1} + \lambda_{31}^2 U_{\alpha 3})U_{\alpha 3}^*\Big\} \\ &\to \frac{1}{|\lambda_{11}|^2 + |\lambda_{31}|^2}\mathrm{Im}\Big\{\frac{\lambda_{31}^2}{2}\Big\} \end{aligned}$$

(no sum on α). In the last formula, we drop the terms $\propto \lambda_{11}$, which may contain asymmetries that cancel in the sum $\epsilon_{oo} + \epsilon_{\tau\tau}$. These are not useful to us, because we aim for $\eta_o \simeq \eta_\tau \simeq 1/4$. For $\text{Im}\,\{\lambda_{31}^2\}/(|\lambda_{31}|^2 + |\lambda_{11}|^2) \gtrsim 1/2$, Eq.(3.32) implies that a large enough BAU could be produced for $M_1 \sim 3 \times 10^9$ GeV.

We now check that we obtain the observed light neutrino mass matrix, even with ζ, the phase of λ_{31}, of order $\pi/4$. The light neutrino mass matrix is:

$$[m]_{\alpha\beta} = \frac{\lambda_{\alpha 1}\lambda_{\beta 1}}{M_1} v_u^2 + \kappa_{\alpha\beta} v_u^2 = v_u^2 \Big[\frac{\lambda_{11}^2}{M_1} \hat{u}_1 \hat{u}_1^T + \kappa_2 \hat{u}_2 \hat{u}_2^T + (\frac{\lambda_{31}^2}{M_1} + \kappa_3) \hat{u}_3 \hat{u}_3^T \Big]_{\alpha\beta} \qquad (3.34)$$

where κ_2 and κ_3 are the eigenvalues of κ. By convention there is no phase on m_3, so in the 2 right-handed neutrino (2RHN) model that generates κ, we should put a phase on the larger eigenvalue κ_3. Since $\lambda_{31}^2 v_u^2/M_1 \simeq e^{i2\zeta} \times 10^{-3}$ eV, the phase on κ_3 is very small and we neglect it in the following discussion of lepton flavour violation.. It is well known [61] that the seesaw mechanism with 2 right-handed neutrinos can reproduce the observed light neutrino mass matrix, with $m_1 = 0$. In our case, we assume that N_2 and N_3 give the observed m_2, and m_3 up to (negligeable) corrections due to N_1 of order 10^{-3} eV. m_1 arises due to N_1.

In the 2RHN model, there is less freedom to tune the LFV branching ratios [62] than in the seesaw with three N_i. So as a last step, we check that we can obtain LFV branching ratios just below the current sensitivity. The 2RHN model can be conveniently parametrised with $\hat{D}_\kappa$, the 3×2 $\hat{U}_{PMNS}$ matrix, the 2×2 unitary matrix $\hat{W} = \hat{V}_L \hat{U}$, and the eigenvalues Λ_2 and Λ_3 of $\hat{\Lambda}$ (matrices in the 2RHN subspace are denoted by hats). $\hat{\Lambda}$ is a 2×2 sub-matrix of λ, obtained by expressing the 3×3 Yukawa matrix in the eigenbases of the heavy and light neutrinos, and dropping the first row and column, corresponding to ν_1 and N_1. It is straightforward to verify that $[\hat{V}_L]_{3e} \sim 10^{-3}$ can be obtained by taking $\tan\hat{\theta}_W \simeq s_{13}/(c_{13}s_{12})$, where $\hat{\theta}_W$ is the rotation angle in $\hat{W}$ and θ_{ij} are from U_{PMNS}. Choosing Λ_2, the smaller eigenvalue of Λ, to be $\sim .06$, ensures that $BR(\mu \to e\gamma)$ is small enough. We can simultaneously take $\Lambda_3 \sim 1$ and obtain $[V_L]_{3\tau} \sim [V_L]_{3\mu} \sim 1$, which allows $BR(\tau \to \mu\gamma) \sim 10^{-8}$. The resulting masses of N_2, N_3 are $\sim 10^{12}, 10^{15}$ GeV.

Our MCMC has some difficulties in finding the analytic points. We imagine this to be because they are "fine-tuned" in the parametrisation used by the MCMC. The amount of tuning required in the angles of V_L, to obtain the desired $\{\lambda_{j1}\}$, can be

Light neutrino best fit values
$\Delta m^2_{sol} = (7.60 \pm 0.20) \times 10^{-5}$ eV^2
$\lvert\Delta m^2_{atm}\rvert = (2.40 \pm 0.15) \times 10^{-3}$ eV^2
$\sin\theta^2_{sol} = 0.320 \pm 0.023$
$\sin\theta^2_{atm} = 0.500 \pm 0.063$

Table 3.4: The best fit values of the light neutrino parameters and their 1σ errors [63].

estimated by taking logarithmic derivatives. In Appendix .1, we find a fine-tuning of order:

$$\frac{\tilde{m}^2}{m_3^2\theta_{13}} \sim .01 \tag{3.35}$$

where θ_{ij} are the U_{PMNS} phases, and we optimistically assumed $\theta_{13} \simeq .1$. These points at $M_1 \lesssim 10^{10}$ GeV with $\tilde{m} \gtrsim 10^{-3}$ eV, were also not found in the analysis of [19].

3.6 MCMC

In this section we describe our numerical analysis. In order to verify if the baryon asymmetry of the universe is sensitive to the low energy PMNS phases, we perform a scan over the neutrino sector parameters aiming for those points compatible with the measured baryon asymmetry and the bound on the reheating temperature, that have large enough LFV branching ratios to be seen in the next experiments.

Using the bottom-up parametrisation of the seesaw defined by the V_L, D_λ, D_ν and U matrices, our parameter space consists of the 14 variables displayed in Table 3.5. We take as an experimental input the best fit values of the light neutrino mass differences and of the solar and atmospheric mixing angles, Table 3.4. With respect to the SUSY parameters, we choose two different regimes for $\tan\beta$, equal to 2 or 50, while the m_{SUSY} scale is deduced from the data on the anomalous magnetic moment, see section 3.2.1.

Due to the large number of parameters it would prohibitive to consider a usual grid scan. Thus, we choose to explore our parameter space by a Markov Chain Monte Carlo that behaves much more efficiently, and has been already successfully employed in other analyses [64].

3.6.1 Bayesian inference

Given a model with free parameters $X = \{x_1, \ldots, x_n\}$ and a set of derived parameters $\xi(X)$, for an experimental data set d, the central quantity to be estimated is the *posterior distribution* $P(X|d)$, which defines the probability associated to a specific model, given the data set d. Following the Bayes theorem, it can be written as:

$$P(X|d) = \frac{\mathcal{L}(d|\xi(X))\pi(X)}{P(d)} \ , \tag{3.36}$$

where $\mathcal{L}(d|X)$ is the well known likelihood, that is the probability of reproducing the data set d from a given model X, $\pi(X)$ is the prior density function, which encodes our knowledge about the model, and $P(d) = \int \mathcal{L}(d|\xi(X))\pi(X)dX$ is an overall normalization neglected in the following. In the case of flat priors:

$$\pi(X) = \begin{cases} \frac{1}{X_{max}-X_{min}} & \text{if } \ X \in [X_{min}, X_{max}] \\ 0 & \text{otherwise} \end{cases} \tag{3.37}$$

the posterior distribution reduces to the likelihood distribution in the allowed parameter space.

The main feature of the Markov chains is that they are able to reproduce a specific target distribution we are interested in, in our case the posterior distribution, through a fast random walk over the parameter space. The Markov chain is an ordered sequence of points X_i with a *transition probability* $W(X_{i+1}|X_i)$ from the $i-th$ point to the next one. The first point X_0 is randomly chosen with prior probability $\pi(X)$. Then a new point is proposed by a *proposal distribution* $Q(X_{i+1}|X_i)$ and accepted with probability $\mathcal{A}(X_{i+1}|X_i)$. The transition probability assigned to each point is then given by $W(X_{i+1}|X_i) = Q(X_{i+1}|X_i)\mathcal{A}(X_{i+1}|X_i)$. Given a *target distribution* $P(X)$, if the following *detailed balance condition*:

$$W(X_k|X_j)P(X_j) = W(X_j|X_k)P(X_k) \tag{3.38}$$

is satisfied for any j, k, then the points X_i are distributed according to the target distribution. For a more detailed discussion see [21, 22].

3.6.2 The Metropolis-Hastings algorithm

In order to generate the MCMC with a final posterior distribution (3.36), we use the Metropolis-Hastings algorithm. In the following, we briefly recall how the algorithm

behaves, but the discussion is done in terms of the likelihood, instead of the posterior distribution, since we assume flat priors on our parameter space, see eq. (3.37).

Let X be the parameter set we want to scan, and $\mathcal{L}(X)$ our likelihood function, the target distribution. ¿From a given point in the chain X_i with likelihood $\mathcal{L}(X_i)$, a new point X_{new} with likelihood $\mathcal{L}(X_{new})$ is randomly selected by a gaussian proposal distribution $Q(X_{new}, X_i)$ centered in X_i and having width ϵ. This last quantity ϵ controls the *step size* of the random walk. The new point is surely added to the chain if it has a bigger likelihood, otherwise the chain adds the new point with probability $\mathcal{L}(X_{new})/\mathcal{L}(X_i)$. So the value of the next point X_{i+1} in the chain is determined by:

$$X_{i+1} = \begin{cases} X_{new} & \text{with probability } \min[\mathcal{A}(X_{new}, X_i), 1] \\ X_i & \text{with probability } 1 - \min[\mathcal{A}(X_{new}, X_i), 1] \end{cases} , \tag{3.39}$$

where $\mathcal{A}(X_{new}, X_i)$ is the acceptance probability:

$$\mathcal{A}(X_{new}, X_i) = \frac{\mathcal{L}(X_{new})}{\mathcal{L}(X_i)} . \tag{3.40}$$

Given this acceptance distribution and using the symmetry of our proposal distribution $Q(X_l, X_i)$ under the exchange $l \leftrightarrow i$, it is straightforward to see that the detailed balance condition 3.38 is satisfied for the likelihood $\mathcal{L}(X)$ as target distribution. This implies that when the chain has reached the equilibrium, after a sufficiently long run, our sample is independent of the initial point and distributed according to $\mathcal{L}(X)$.

In order to arrive at the equilibrium in a reasonable amount of time, the step scale ϵ of our random walk must be accurately chosen. Indeed, if we define the acceptance rate as the number of points accepted over the number of points proposed, a too big step ϵ implies a too low acceptance rate, so that our Markov Chain never advances, while a too small ϵ and, so, a very large acceptance ratio, implies that our chain needs a very large time to scan all the space. It has been suggested that ϵ must be chosen according to an optimal acceptance rate between 20% and 50%. However, in order to ensure the detailed balance condition, ϵ cannot change during the run of the chain, thus, it is set by our program in a burn-in period.

A valid statistical inference from the numerical sample relies on the assumption that the points are distributed according to the target distribution. The first points of the chain are arbitrarily chosen and the chain needs a burn-in period to converge to the

Free parameters	**Allowed range** $[X_{min}, X_{max}]$	
	$\lambda_2/\lambda_1 \simeq \lambda_3/\lambda_2 \simeq 30$	$\lambda_2/\lambda_1 \simeq 100,\ \lambda_3/\lambda_2 \simeq 50$
$\log_{10}\lambda_3$	$[-0.3, 0.3]$	$[-0.5, 0.5]$
$\log_{10}\lambda_2$	$[-1.77, -1.17]$	$[-2.2, -1.2]$
$\log_{10}\lambda_1$	$[-3.25, -2.65]$	$[-4.2, -3.2]$
$\log_{10}(m_1/\text{eV})$	$[-6, -3]$	
$\log_{10}\theta_{ij}^{V_L}$	$[-4, \log_{10}\pi]$	
ρ, ω, σ	$[0, \pi]$	
θ_{13}	$[0., 0.2]$	
δ	$[0, \pi]$	
α, β	$[0, \pi/2]$	

Table 3.5: Allowed parameter space, so that the uniform prior on each parameter is defined as in eq.(3.37).

target distribution. The length of the burn-in strongly depends on the intrinsic properties of the chain and cannot be set *a priori*. It changes according to the complexity of the model, to the target distribution, and the efficiency of the proposal distribution employed. Once the chain has reached the equilibrium the first burn-in points must be discarded to ensure the independence of the chain from the initial conditions. Nevertheless, as we will see in section 3.6.4, even following the procedure above, it can be a delicate issue to determine if a chain has really converged.

3.6.3 The seesaw sample

In our work the free variables X are given by the 14 seesaw parameters, with uniform priors, Eq. 3.37, on the allowed range of parameter space (see Table 3.5). The choice of a logarithmic scale on some unknown parameters allows us to scan with the same probability different orders of magnitude. We analyze models with two different hierarchies in the neutrino Yukawas, so that, for a $\lambda_3 \sim 1$ we impose $\lambda_2/\lambda_1 \sim \lambda_3/\lambda_2 \sim 30$ or $\lambda_2/\lambda_1 \sim 100$ and $\lambda_3/\lambda_2 \sim 50$. The lightest neutrino mass is allowed to vary between three orders of magnitude $10^{-6} < m_1 < 10^{-3}\ eV$ and the θ_{13} mixing angle within its 3σ range, $0 < \theta_{13} < 0.2$ rad. The V_L mixing angles can vary over 4 orders of magnitude,

with maximum value π. All the CP violating phases, those of the V_L matrix indicated by ρ, ω and σ and the Dirac and Majorana phases δ, α and β, are allowed to vary on all their definition range: $[0, \pi/2]$ for the Majorana phases and $[0, \pi]$ for the others (this avoids degeneracies).

The idea is, now, to generate a sample of points in our parameter space that provide enough BAU, give LFV rates big enough to be seen in the next generation of experiments, and also have an M_1 light enough to avoid the gravitino problem. We then define our set of derived parameters $\xi(X)$ as in Table 3.6 and we associate to them a multivariate gaussian likelihood with uncorrelated errors:

$$\mathcal{L}(\xi_{exp}|\xi) = \frac{1}{(2\pi)^{1/2}\mathcal{R}^{m/2}} \exp\{-\frac{1}{2}(\xi - \xi_{exp})^t \mathcal{R}^{-1}(\xi - \xi_{exp})\} \ . \tag{3.41}$$

Where $m = 4$ is the dimension of the derived parameter set. The centre values ξ_{exp} are the best fit values and $\mathcal{R}$ is an $m \times m$ error matrix, in this case diagonal, since we assume no correlation between the errors. As we can see in Table 3.6, the BAU is set to its experimental value, while the LFV rates are set to be one order of magnitude below the present bounds, and the expected value of lightest heavy neutrino mass $M_1 \sim 10^9$ GeV is set to escape the gravitino problem. The branching ratio of LFV τ decays is given in terms of the combination $BR(\tau \to e\gamma) + BR(\tau \to \mu\gamma) \equiv BR_{\tau\alpha}$, since one of them is suppressed to respect the stringent bound from $BR(\mu \to e\gamma)$ (we assume hierarchical yukawas).

For each point X_i of the chain, the lepton flavour violating branching ratios are estimated with equation Eq.(3.15), while Y_B is computed after the reconstruction of the right neutrino mass, see Eq.(3.28), using Eq.(3.23) in the flavour regime is in act at the temperatures we consider. We recall that the temperature at which leptogenesis takes place is of the same order of the reconstructed right-handed neutrino mass. Depending on the value of $\tan\beta$, the range of temperatures at which the flavour regimes have a role changes. As we already mentioned in Section 3.3: for small $\tan\beta$, in the temperature range 10^9 GeV $< T < 10^{12}$ GeV the τ flavour is in equilibrium and the two flavour regime is in order; while for $T < 10^9$ GeV μ are also in equilibrium and the three flavours are distinguishable. Since we aim for values of $M_1 \sim 10^9$ GeV if we consider a small value of $\tan\beta$ our program takes into account that the BAU can be produced in both two or three flavour regimes. For very large $\tan\beta$, instead, already for $T <$ 10^{12} GeV τ and μ are in equilibrium, thus the three flavour regime always takes place.

Derived parameters $\xi(X)$	$\xi_{exp} \pm \sigma$
Y_B	$(8.75 \pm 0.23)\ 10^{-11}$
$\log_{10} BR(\mu- > e\gamma)$	-13 ± 0.1
$\log_{10} BR(\tau- > l\gamma)$	-9 ± 0.1
$\log_{10}(M_1/GeV)$	-9 ± 0.1

Table 3.6: Best values and errors for the derived parameters $\xi(X)$ we want to maximize.

In the case of steeper yukawa hierarchy, in agreement with our analytical estimate, we enlarge our set of derived parameters and maximise the rescaled N_1 decay rate to $\tilde{m} \sim 10^{-3}$ eV and the heaviest right-handed neutrino masses to $M_2 \sim 10^{12}$ GeV and $M_3 \sim 3\ 10^{14}$ GeV.

All the points that do not respect the present bounds on LFV, do not have large enough baryon asymmetry or have $M_1 > 10^{11}$ GeV, have a null likelihood. We assume that the largest uncertainty on the baryon asymmetry comes from our calculation, so we allow Y_B to be as small as $4\ 10^{-11}$. Those points having one of the RH neutrino masses above the $M_{GUT} \sim 3\ 10^{16}$ GeV scale have a null likelihood too, since in that case the equations we use for the evaluation of LFV processes do not apply.

3.6.4 Convergence

Convergence of the chain ensures the sample is distributed according to the target distribution and thus allows to be confident of its statistical information. The question we want to answer in this paper, however, does not require a statistical interpretation of the sample. Here we only aim to show that, for any value of the low energy phases, the unmeasurable high energy parameters can be rearranged to obtain the right baryon asymmetry. Therefore a careful diagnostic of the convergence is not a priority. Nevertheless, we briefly discuss it in this section since it is an important issue that can help the reader to have a better overview on our results. Our sample, indeed, has some typical features that can make difficult to check if the chain has reached the target distribution.

As a rudimentary attempt, in our analysis we use the simplest and straightforward approach. We run different chains starting from different values and compare the

behaviour of the free parameters, once the chains have converged they should move around the same limiting values. However, this method can be inadequate in case of *poor mixing*, i.e. when the chains are trapped in a region of low probability relative to the maximum of the target distribution. This happens in models with strongly correlated variables, when the proposal distribution does not efficiently escape this region. Therefore, it can be an issue for our numerical analysis, when, as mentioned in section 3.5, we look for a fine-tuned region with a large baryon asymmetry and low M_1. We can understand the poor mixing situation if we imagine a landscape on the parameter space corresponding to the target distribution, with some broad hills and a tall but very thin peak at the maximum of the target distribution. In that case, the step of the chain can be optimized to efficiently scan all the space but, if its size is larger than the width of the peak, it can easily miss it.

In case of strongly correlated variables it can also happen that the region to be scanned is mainly a plane, that is with almost null likelihoods. This is the case of our sample, where we expect a large region with null or almost null likelihood, for all those points that do not have large enough baryon asymmetry, low M_1 or do not respect the bounds on LFV. In this context, if a gaussian-like proposal distribution, as in our sample, is employed, the choice of the starting point becomes important to allow the chain to advance. Indeed, if the initial value is surrounded by points with null likelihood (and so null acceptance rate) and its distance from the interesting region is much larger than the step of the random walk, the chain cannot move from this point, since it always finds points with null likelihood. On the other side, if the chain starts in a region which is a reasonable fit to the data, it advances. Discarding the first points of the chain can ensure independence of the chain of the initial conditions inside the interesting region however, if this region is well separated from another interesting region, the chain has almost null probability to find the second one.

In order to perform a valid statistical analysis, more sophisticated methods should be employed to decide if the chain has converged. In literature many studies exist on convergence criterion that help to check the mixing of the sample and are based on the similarity of the resulting sampling densities of input parameters from different chains. An example can be found in [65] and [66].

3.6.5 Run details

In this subsection we explain the details of our MCMC run. The parameter space we scan is very large if compared to the derived variables and, in addition, we expect a strong correlation between the evaluated baryon asymmetry and the lightest right-handed neutrino mass, see eq. 3.26. Thus, since we expect a sample with poor mixing, as discussed in section 3.6.4, we first look for an initial point which is a reasonable fit to our observables. This procedure is done running previous shorter chains without imposing null likelihoods to the not interesting points. Once a wide enough set of interesting starting points is found, we start running the chains.

All the simulations we present are performed by running 5 chains with 10^6 points each. As explained before, during the first burn-in iterations, the scale of the random walk ϵ is varied until the acceptance rate of points is between the optimal range 20% and 50%. This usually takes much less than 3 10^3 iterations. When the optimal acceptance rate is reached, the scale ϵ is fixed during the rest of the run. The chains are then added together after having discarded the first 10^5 points, corresponding to the burn-in period, in order to give enough time to the chain to converge. As discussed above, this procedure should eliminate the dependence on the initial point inside the interesting region, but is only a first attempt to ensure the sample has reached equilibrium. We run simulations for both normal and inverted hierarchy, in the two cases of small and large $\tan\beta$.

3.7 Discussion

3.7.1 Assumptions

We assume a three generation type I seesaw with a hierarchical neutrino Yukawa matrix. We require that this model produces the baryon asymmetry via flavoured thermal leptogenesis, and induces the observed light neutrino mass matrix. This model has a hierarchy problem, so we include supersymmetry.

We make a number of approximations and assumptions in supersymmetrising the seesaw. First, we use real and universal soft terms at some high scale, above the masses M_i of the singlet neutrinos. In this restrictive model, the only contributions

to flavour off-diagonal elements of the slepton mass^2 matrix $\equiv [\tilde{m}^2]_{\alpha\beta}$, arise due to Renormalisation Group running. Second, we use simple leading log estimates for the off-diagonals $[\tilde{m}^2]_{\alpha\beta}$. Third, we estimate the SUSY contributions to the dimension five dipole operator (see Eq.3.12) using simple formulae of dimensional analysis (see equations (3.15),(3.16), (3.18)). This operator induces flavour diagonal electric and magnetic dipole moments, and the flavour changing decays $\ell_\alpha \to \ell_\beta\gamma$. We assume the $(g-2)_\mu$ anomaly is due to supersymmetry, and use it to "normalise" the dipole operator. This implies that our SUSY masses scale with $\tan\beta$: $m^2_{SUSY} = \frac{\tan\beta}{2}(200$ GeV$)^2$. We imagine that there is an uncertainty ~ 10 in our estimates of electric dipole moments and $\ell_\alpha \to \ell_\beta\gamma$ decays rates, due to mixing angles and sparticle mass differences.

Our first approximation, of universal soft terms, seems contrary to our phenomenological perspective: the RG-induced contributions to $[\tilde{m}^2]_{\alpha\beta}$ can be interpreted as lower bounds on the mass^2 matrix elements. However, we neglect other contributions, and require that the RG induced flavour-violating mass terms are $\propto C^{(1)}_{e\mu}$ (see eq. (3.11)), give detectable rates for $\mu \to e\gamma$ and $\tau \to \ell\gamma$ in upcoming experiments. Realistically, measuring $\mu \to e\gamma$ mediated by sleptons might allow to determine $\tilde{m}^2_{e\mu}$, but does not determine the seesaw model parameters $C^{(1)}_{e\mu}$. This model dependence is compatible with our phenomenological approach, because our result is negative: we say that *even if* we could determine $C^{(1)}_{e\mu}$, the baryon asymmetry is insensitive to the PMNS phases.

In our numerical analysis we sample the lightest neutrino mass m_1 and the PMNS mixing angle θ_{13}, but these two low energy parameters could be eventually measured. In this case our simulations should be reconsidered. However, from the analytical estimates, we do not expect that fixing these parameters will change our conclusions.

3.7.2 Method

We explore the seesaw parameter space with a Monte Carlo Markov Chain, for two reasons. First, an MCMC is more efficient than a grid scan for multi-dimensional parameter space. It is essentially a programme for exploring hilltops in the dark. Since the programme likes to step up and is reluctant to step down, it takes most of its steps in the most probable areas of parameter space.

The second potential advantage of a MCMC, is that it could make the results less

dependent on the priors, that is, the choice of seesaw parametrisation, and of the distribution of points. The results of parameter space scans are often presented as scatter plots, and it is difficult to not interpret the point distribution as probability. However, the density of points in the scatter plots depends not only on what the model predicts, but also on the distribution of input points. For this reason, seesaw scans using different parametrisations can distribute points differently in scatter plots. For example, if a model parameter such as a Yukawa can vary between 0 and 1, the results will be different depending on whether the Yukawa is $\mathcal{O}(1)$ (take points uniformly distributed between 0 and 1) or can vary by orders of magnitude (take the exponential of a variable uniformly distributed between $-n$ and 0). We had hoped that an MCMC could improve this, because a converged MCMC distributes points in parameter space according to a likelihood function. However, in practise there are various difficulties.

The prior on the seesaw model parameter space matters, because the MCMC takes steps of some size in each parameter: broad hilltops are easier to find than sharp peaks. As discussed in [66], this can be addressed by describing the model with parameters that match closely to physical observables. For this reason we parametrise the seesaw in terms of the diagonal singlet mass matrix D_M, the light neutrino mass matrix $m = UD_\nu U^T$, and the neutrino Yukawa matrix $\lambda\lambda^\dagger = V_L^\dagger D_\lambda^2 V_L$. These are related to low energy observables, because $\lambda\lambda^\dagger$ controls the RG contributions to the slepton mass matrix. We take the priors for our inputs as given in Table 3.5. However, the baryon asymmetry and the mass M_1 belong to the "right-handed" sector, so are complicated functions of the "left-handed" input parameters. The bridge between the LH and RH sector is the Yukawa matrix, whose hierarchies may strongly distort the MCMC step size. To obtain a large enough baryon asymmetry for $M_1 \sim 10^9$ GeV requires careful tuning in the "right-handed" space, and our MCMC has difficulty to find these points. This is related to a second, practical problem, that there are many more parameters than observables, so the space to explore is big, but the peaks with enough baryon asymmetry and small enough M_1 are rare. It is difficult to ensure that the MCMC has found all the peaks, as is discussed in section 3.6.4.

In section 3.5, we find analytically an area of parameter space that satisfies our constraints, but where the baryon asymmetry is insensitive to PMNS phases. This area corresponds to the limit where N_1 makes a negligible contribution to the light neutrino

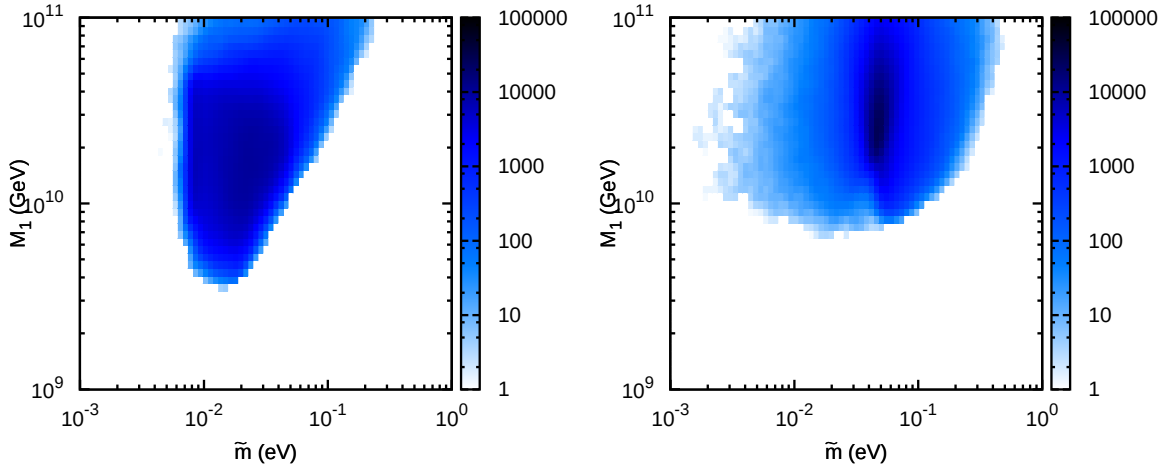

Figure 3.1: Density of "successful" points, as a function of the lightest right-handed neutrino mass M_1 and rescaled decay rate $\tilde{m}$, assuming $\lambda_3 \sim 1$ and $\lambda_2/\lambda_1 \sim \lambda_3/\lambda_2 \sim 30$, for two different simulations: NH and $\tan\beta = 50$ (left), and IH and $\tan\beta = 2$ (right). "Successful" points have $Y_B > 4\ 10^{-11}$, and $BR(\mu \to e\gamma)$ and $BR(\tau \to \ell\gamma)$ an order of magnitude below the current bounds. See section 3.6.3.

mass matrix. In this area, the seesaw model can be conveniently parametrised with the interactions of the effective theory at M_1, and it is straightforward to tune the coupling constants to fit the light neutrino mass matrix, LFV rates, and the baryon asymmetry.

3.7.3 Results

The aim of our analysis was to verify if a preferred range of values for PMNS phases δ, α and β can be predicted, once low energy neutrino oscillation data, a large enough BAU, and LFV processes within the sensitivity of future experiments are requirements of the model.

In Fig. 3.1, we show the distribution, as a function of the singlet mass M_1 and the (rescaled) decay rate $\tilde{m}_1$, of the successful points for a yukawa hierarchy $\lambda_2/\lambda_1 \sim \lambda_3/\lambda_2 \sim 30$, with $\lambda_3 \sim 1$.

With the parametrisation described in section 3.6.3, the MCMC easily finds larger values of M_1 and $\tilde{m}$, than the "tuned" points found analytically in Section 3.5. This preference for larger M_1 is expected, because the baryon asymmetry and right-handed

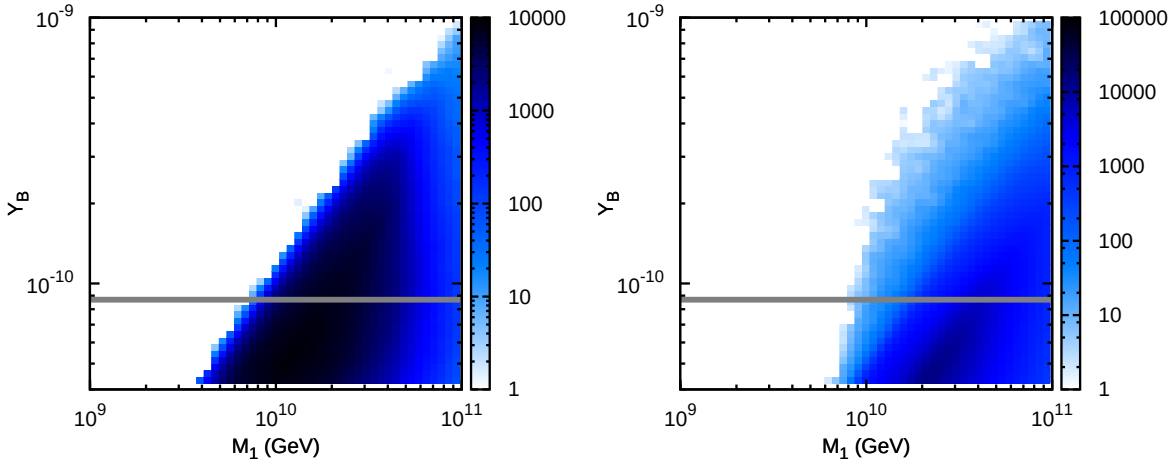

Figure 3.2: Density of "successful" points, as a function of the baryon asymmetry and the lightest right-handed neutrino mass, assuming $\lambda_3 \sim 1$ and $\lambda_2/\lambda_1 \sim \lambda_3/\lambda_2 \sim 30$, for two different simulations: NH and $\tan\beta = 50$ (left), and IH and $\tan\beta = 2$ (right). "Successful" points are defined as for Figure 3.1.

neutrino masses are strongly correlated, see Fig. 3.2 and eqn (3.21).

Nonetheless, as illustrated in Fig.3.3, the MCMC succeeded in finding points at lower M_1, with a steeper [10] hierarchy in the yukawas $\lambda_3 \sim 1$, $\lambda_2/\lambda_1 \sim 100$ and $\lambda_3/\lambda_2 \sim 50$. The difficulties of finding these tuned points are discussed in section 3.6.4.

The importance of the ~ 2 decrease in M_1 and $\tilde{m}$, at the tuned points, is unclear to us: the cosmological bound is on T_{RH}, rather than M_1. Since in strong washout, an equilibrium population of N_1 can be generated for $T_{RH} \gtrsim M_1/5$, the points found by the MCMC at $M_1 \sim 10^{10}$ GeV, could perhaps generate the BAU at the same T_{RH} as the analytic points. In any case, we see in Fig.3.2 that the fraction of points with big enough Y_B is very sensitive to M_1, and therefore to details of the complicated reheating/preheating process.

In Fig. 3.4, we show density plots of the points resulting from our Markov Chains, corresponding to the the yukawa hierarchy $\lambda_2/\lambda_1 \sim \lambda_3/\lambda_2 \sim 30$, with $\lambda_3 \sim 1$, for normal hierarchy (NH) of the light neutrino masses and $\tan\beta = 2$, and for inverse hierarchy (IH) and $\tan\beta = 50$. In Fig. 3.7 (plot on the left) we show a density

[10] The smallest yukawa must be small enough to ensure $\tilde{m} \sim m_*$.

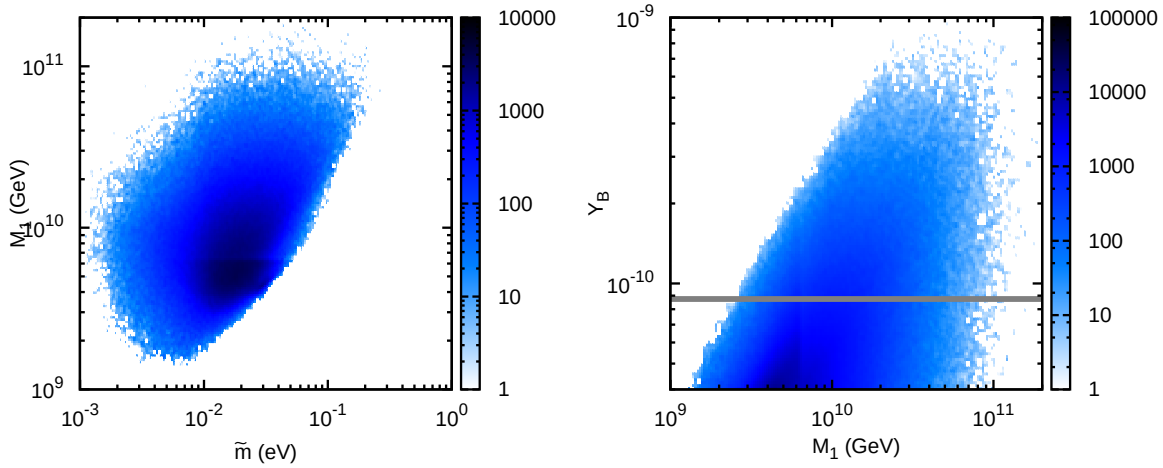

Figure 3.3: Density of "successful" points, as a function of the lightest right-handed neutrino mass M_1 and rescaled decay rate $\tilde{m}$, on the left-side, and between the baryon asymmetry and the lightest right-handed neutrino mass, on the right-side. We assume here $\lambda_3 \sim 1$ and $\lambda_2/\lambda_1 \sim 100$ and $\lambda_3/\lambda_2 \sim 50$, for a NH in the light neutrinos and $\tan\beta = 2$. "Successful" points are defined as for Figure 3.1.

plot in the $\delta - \beta$ plane for $\tan\beta = 2$, NH and the steeper hierarchy $\lambda_2/\lambda_1 \sim 100$, $\lambda_3/\lambda_2 \sim 50$ and $\lambda_3 \sim 1$. From those plots we see that, for any value of the phases δ, α and β our conditions are satisfied. The analytic results of Section 3.5 agree with this. Thus, we can conclude that the baryon asymmetry of the universe is *insensitive* to the low energy PMNS phases, even in the "best case" where we see MSUGRA-mediated lepton flavour violating processes. For completeness we also show correlation plots between the generated BAU and the three low energy phases in Fig.3.5. The low energy observables do not depend on $\tan\beta$, because we assume the $(g-2)_\mu$ discrepancy is due to slepton loops, and we use it to normalise the LFV rates (see Eqn. 3.15). On the contrary, the value of $\tan\beta$ is relevant in leptogenesis because it changes the number of distinguishable flavours. However, as we can see comparing plots for small/large $\tan\beta$, the value of $\tan\beta$ does not change our conclusions.

In Figs.3.6 and 3.7 (plot on the right), we plot the contribution to the electric dipole moment of the electron, arising in the MSUGRA seesaw with real soft parameters at the high scale. For both low and large $\tan\beta$, points from our MCMC generate an

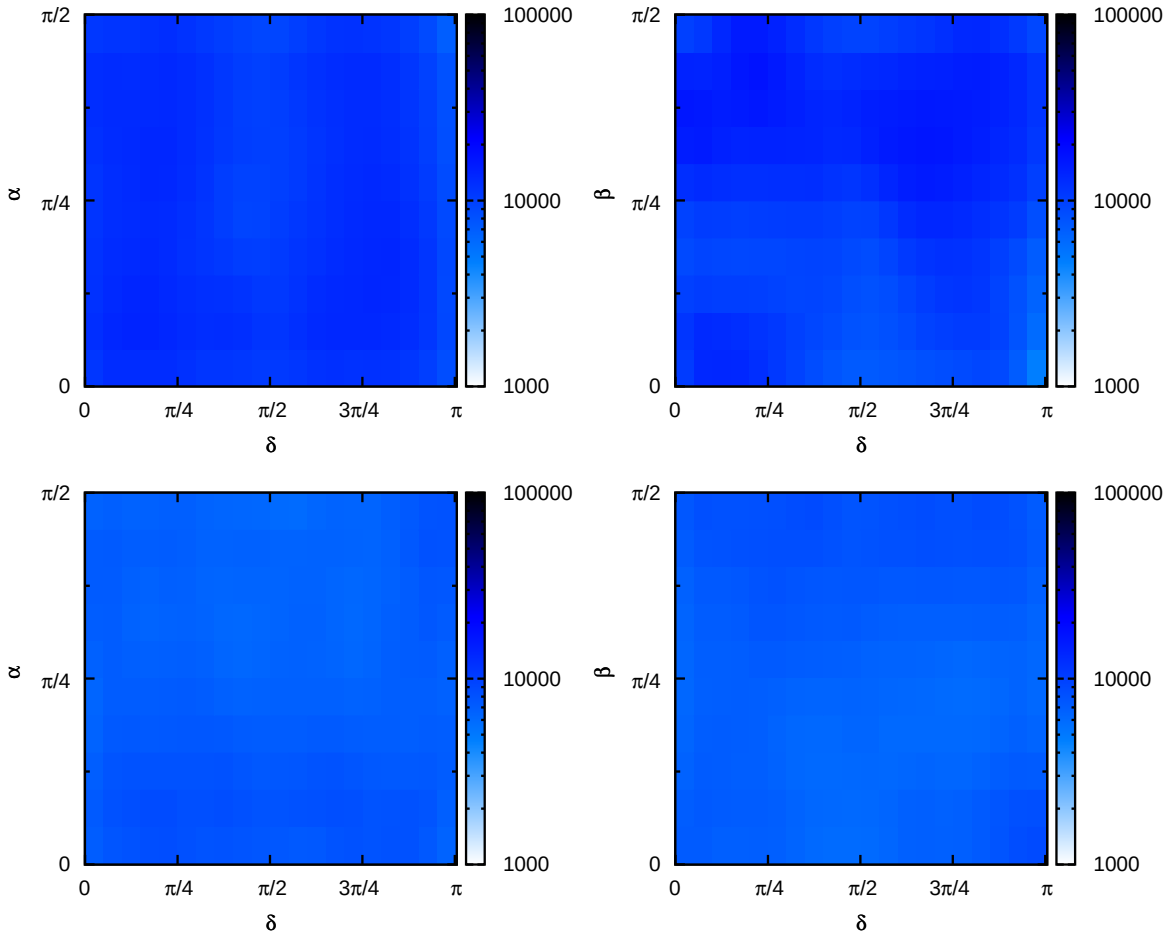

Figure 3.4: Density plots in the plane of the low energy phases $\delta - \alpha$ and $\delta - \beta$ in models with $\lambda_3 \sim 1$ and $\lambda_2/\lambda_1 \sim \lambda_3/\lambda_2 \sim 30$. Upper plots correspond to a simulation with NH and $\tan\beta = 50$, and lower plots to IH and $\tan\beta = 2$. "Successful" points are defined as for Figure 3.1.

electron EDM $\lesssim 10^{-30} e$cm. This agrees with the results of [29, 35, 20].

3.8 Summary

The aim of this work was to study whether the baryon asymmetry produced by thermal leptogenesis was sensitive to the "low energy" phases present in the leptonic mixing matrix U_{PMNS}. We considered the three generation type-I supersymmetric seesaw

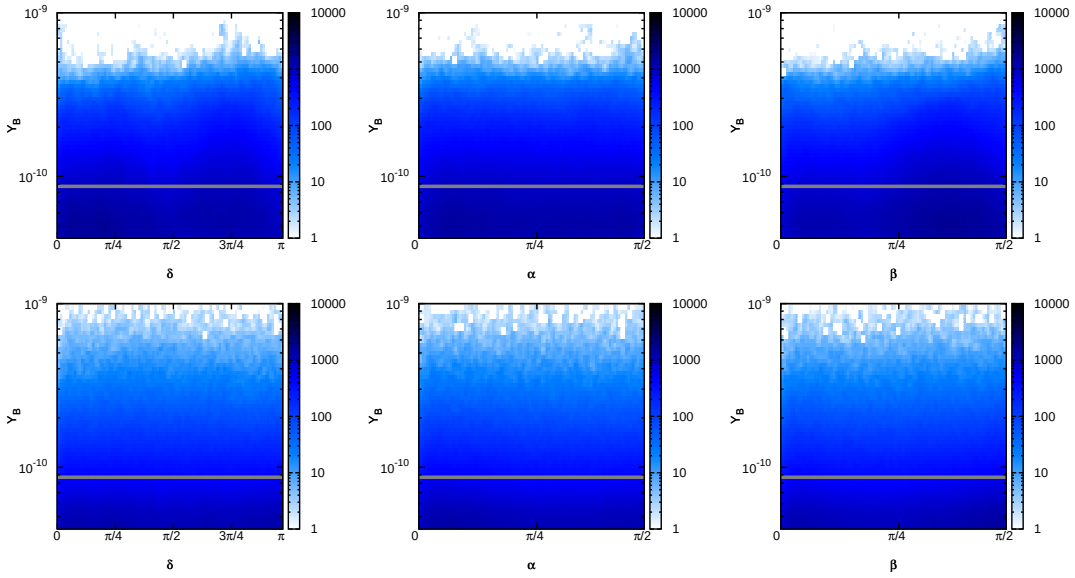

Figure 3.5: Density of "successful" points, as a function of the BAU and the low energy phases in models with $\lambda_3 \sim 1$ and $\lambda_2/\lambda_1 \sim \lambda_3/\lambda_2 \sim 30$. Upper plots correspond to a simulation with NH and $\tan\beta = 50$, and the lower plots to IH and $\tan\beta = 2$. "Successful" points are defined as for Figure 3.1.

model, in the framework of MSUGRA with real soft parameters at the GUT scale, and required that it reproduces low energy neutrino oscillation data, generates a large enough baryon asymmetry of the Universe via flavoured leptogenesis and induces lepton flavour violating rates within a few orders of magnitude of current bounds. We then enquired whether a preferred range for the low energy PMNS phases δ and β can be predicted.

We used a "left-handed" bottom-up parametrisation of the seesaw. Our parameter space scan was performed by a Monte Carlo Markov Chain (MCMC), which allows to efficiently explore high-dimensional spaces. It prefers to find the right-handed neutrino mass $M_1 \gtrsim 10^{10}$ GeV, but can also find successful points with a smaller M_1 if it takes small steps in the relevant area of parameter space. In this area, we can also show analytically that the baryon asymmetry is insensitive to the PMNS phases.

We have checked that there is no correlation between successful leptogenesis and the low energy CP phases. That is: for any value of the low energy phases, the

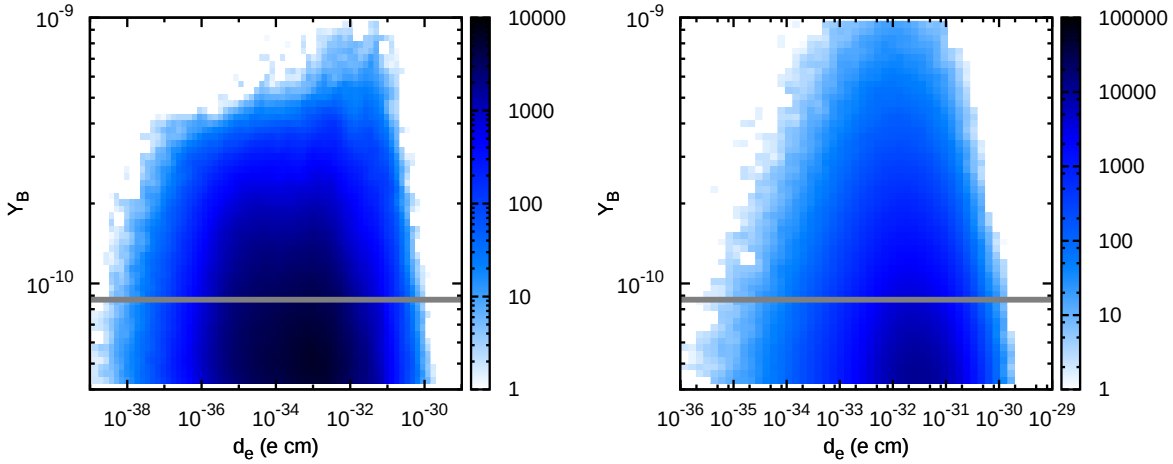

Figure 3.6: Density of "successful" points, as a function of the baryon asymmetry and the electron EDM generated by neutrino yukawas in models with $\lambda_3 \sim 1$ and $\lambda_2/\lambda_1 \sim \lambda_3/\lambda_2 \sim 30$. The left panel corresponds to a simulation with NH and $\tan\beta = 50$, and the right panel to IH and $\tan\beta = 2$. "Successful" points are defined as for Figure 3.1.

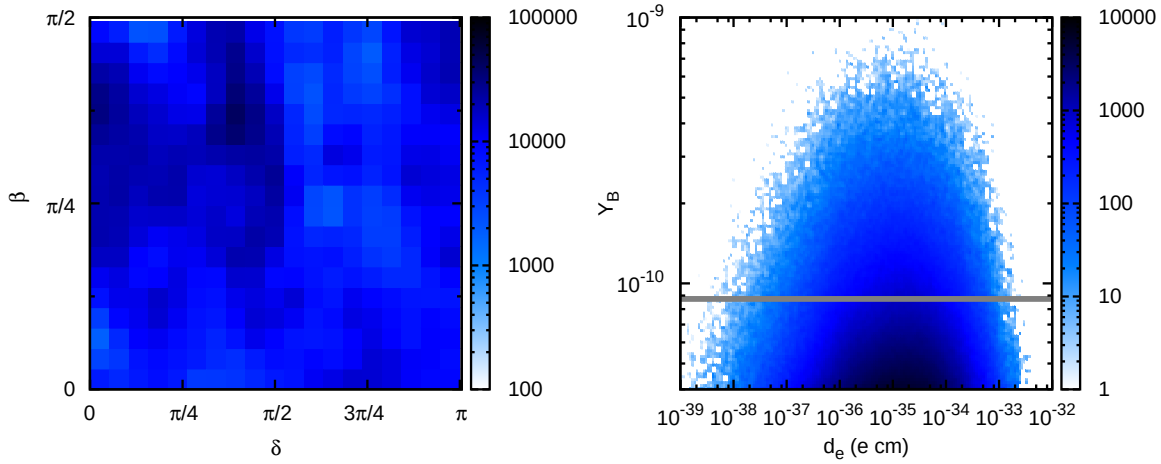

Figure 3.7: Density plot in $\delta - \beta$ plane and correlation between the baryon asymmetry and the electron EDM generated by neutrino yukawas. We assume here $\lambda_3 \sim 1$, $\lambda_2/\lambda_1 \sim 100$ and $\lambda_3/\lambda_2 \sim 50$, for a NH in the light neutrinos and $\tan\beta = 2$. "Successful" points are defined as for Figure 3.1.

unmeasurable high energy parameters and the still unmeasured m_1 and θ_{13} can be arranged in order to have successful leptogenesis and LFV rates in the next round of experiments. The analytic estimates indicate that this result will still be true even if m_1 and θ_{13} are measured and fixed to their experimental values. Finally, we have estimated, for each point in our chains, the contribution of the complex neutrino Yukawa couplings to the electric dipole moment of the electron. As expected, we find it to be $\lesssim 10^{-30} e$cm, just beyond the reach of next generation experiments.

Acknowledgments

We would like to thank Yasaman Farzan, Filipe Joaquim, Martin Kunz, Isabella Masina, Miguel Nebot and Oscar Vives for useful discussions. J.G. is supported by a MEC-FPU Spanish grant. This work is supported in part by the Spanish grants FPA-2007-60323 and FPA2005-01269, by the MEC-IN2P3 grant IN2P3-08-05 and by the EC RTN network MRTN-CT-2004-503369.

.1 Fine tuning of the analytic points

In this Appendix, we estimate the fine-tuning of the points discussed in section 3.5, with respect to the parametrisation of section 3.4, which is used by the MCMC.

We do this in two steps. First, in the parametrisation of section 3.5, we estimate the 3×3 matrix $W^\dagger = U^\dagger V_L^\dagger$ which diagonalises m in the basis where $\lambda\lambda^\dagger$ is diagonal. Approximating this diagonal Yukawa basis to be the one where $\hat{\Lambda}\hat{\Lambda}^\dagger$ is diagonal, we obtain:

$$W^\dagger = [\delta W]^\dagger \begin{bmatrix} 1 & 0 & 0 \\ 0 & & \\ 0 & & \hat{W} \end{bmatrix} \tag{42}$$

where $[\delta W]^\dagger$ is the small rotations that rediagonalise $m = (\Delta_{ij} + \hat{D}_\kappa) v_u^2$, and $\Delta_{ij} = \lambda_{i1}\lambda_{j1}/M_1$. If $W^\dagger$ is parametrised as in eqn (3.27) (but neglecting phases for simplicity),

we find

$$\theta_{13}^W \simeq \frac{\Delta_{13}}{\kappa_3}\cos\hat{\theta}_W + \frac{\Delta_{12}}{\kappa_2}\sin\hat{\theta}_W \quad (43)$$

$$\theta_{12}^W \simeq -\frac{\Delta_{13}}{\kappa_3}\sin\hat{\theta}_W + \frac{\Delta_{12}}{\kappa_2}\cos\hat{\theta}_W \quad (44)$$

$$\sin\theta_{23}^W \simeq \sin\hat{\theta}_W + \frac{\Delta_{23}}{\kappa_3}\cos\hat{\theta}_W \quad . \quad (45)$$

To obtain λ_{21} negligeable compared to λ_{31} in eqn (3.33), requires no particular tuning of θ_{12}^W and θ_{13}^W with respect to λ_{21} andλ_{31}.

The second step is to estimate the tuning required to obtain small angles θ_{12}^W and θ_{13}^W in $W^\dagger = U^\dagger V_L^\dagger$. With $V_L^\dagger$ parametrised as in eqn (3.27), this happens if the angles of V_L satisfy $\theta_{ij}^L \simeq \theta_{ij}$ (for $i,j = 12, 13$). So the "tuning" required in θ_{12}^L and θ_{13}^L to obtain small $\theta_{ij}^W = \theta_{ij}^L - \theta_{ij}$ is

$$\frac{\theta_{12}^W}{\theta_{12}^L}\frac{\theta_{13}^W}{\theta_{13}^L} \simeq \frac{\tilde{m}^2}{m_3^2\theta_{13}} \quad (46)$$

This implies that θ_{13}^L must be tuned against θ_{13} to obtain $\theta_{13}^W \sim .01$. If instead $\theta_{13} \lesssim .01$, there is no particular tuning of θ_{13}^W, and the tuning of θ_{12}^W with respect to θ_{12}^L is or order $\tilde{m}/m_3$.

References

[1] P. Minkowski, Phys. Lett. B **67**, 421 (1977); M. Gell-Mann, P. Ramond and R. Slansky, Proceedings of the Supergravity Stony Brook Workshop, New York, 1979, eds. P. Van Nieuwenhuizen and D. Freedman (North-Holland, Amsterdam); T. Yanagida, Proceedings of the Workshop on Unified Theories and Baryon Number in the Universe, Tsukuba, Japan 1979 (eds. A. Sawada and A. Sugamoto, KEK Report No. 79-18, Tsukuba); R. Mohapatra and G. Senjanovic, Phys. Rev. Lett. **44**, 912 (1980).

[2] M. Fukugita and T. Yanagida, Phys. Lett. **B174** (1986) 45.

[3] S. Davidson and A. Ibarra, JHEP 0109, (2001), 013. hep-ph/0104076.

[4] G. C. Branco, T. Morozumi, B. M. Nobre and M. N. Rebelo, Nucl. Phys. B **617** (2001) 475 [arXiv:hep-ph/0107164].

[5] S. Davidson, J. Garayoa, F. Palorini and N. Rius, arXiv:0705.1503 [hep-ph].

[6] A. Abada, S. Davidson, F. X. Josse-Michaux, M. Losada and A. Riotto, JCAP **0604** (2006) 004 [arXiv:hep-ph/0601083]; E. Nardi, Y. Nir, E. Roulet and J. Racker, JHEP **0601**, 164 (2006) [arXiv:hep-ph/0601084]; A. Abada, S. Davidson, A. Ibarra, F. X. Josse-Michaux, M. Losada and A. Riotto, arXiv:hep-ph/0605281.

[7] M. Raidal *et al.*, arXiv:0801.1826 [hep-ph].

[8] S. Pascoli, S. T. Petcov and A. Riotto, Phys. Rev. D **75** (2007) 083511 [arXiv:hep-ph/0609125]. G. C. Branco, R. Gonzalez Felipe and F. R. Joaquim, Phys. Lett. B **645** (2007) 432 [arXiv:hep-ph/0609297], notice that the analysis of this paper includes only the decay of the lightest right handed neutrino, N_1, so the excluded regions found may be allowed if the baryon asymmetry is generated by N_2 decays.

[9] S. Pascoli, S. T. Petcov and A. Riotto, Nucl. Phys. B **774** (2007) 1 [arXiv:hep-ph/0611338].

[10] A. Anisimov, S. Blanchet and P. Di Bari, JCAP **0804** (2008) 033 [arXiv:0707.3024 [hep-ph]].

[11] E. Molinaro and S. T. Petcov, arXiv:0803.4120 [hep-ph].

[12] Borzumati, Francesca and Masiero, Antonio, Phys. Rev. Lett. **57** , (1986) 961.

[13] J. Hisano, T. Moroi, K. Tobe and M. Yamaguchi, Phys. Rev. D **53** (1996) 2442 [arXiv:hep-ph/9510309].

J. Hisano and D. Nomura, Phys. Rev. D **59** (1999) 116005 [arXiv:hep-ph/9810479].

[14] S Lavignac, I Masina and C Savoy, *Phys. Lett.* **B520** (2001), 269-278 . hep-ph/0106245.
Petcov, S. T. and Rodejohann, W. and Shindou, T. and Takanishi, Y.", *Nucl. Phys.* **B739** (2006) 208-233. hep-ph/0510404. T. Blazek and S. F. King, Nucl. Phys. B **662** (2003) 359 [arXiv:hep-ph/0211368].

[15] S. Antusch and A. M. Teixeira, JCAP **0702** (2007) 024 [arXiv:hep-ph/0611232].

[16] G. C. Branco, R. Gonzalez Felipe, F. R. Joaquim and M. N. Rebelo, Nucl. Phys. B **640** (2002) 202 [arXiv:hep-ph/0202030].

[17] E. K. Akhmedov, M. Frigerio and A. Y. Smirnov, JHEP **0309** (2003) 021 [arXiv:hep-ph/0305322].

[18] S. T. Petcov and T. Shindou, Phys. Rev. D **74** (2006) 073006 [arXiv:hep-ph/0605151].

[19] J. R. Ellis and M. Raidal, Nucl. Phys. B **643** (2002) 229 [arXiv:hep-ph/0206174].

[20] F. R. Joaquim, I. Masina and A. Riotto, Int. J. Mod. Phys. A **22**, 6253 (2007) [arXiv:hep-ph/0701270].

[21] D. J. C. MacKay, "Information Theory, Inference, and Learning Algorithms", Cambridge University Press.

[22] W. R. Gilks, S. Richardson and D. J. Spiegelhalter, "Markov Chain Monte Carlo in Practice", Chapman and Hall.

[23] M. Nebot, J. F. Oliver, D. Palao and A. Santamaria, Phys. Rev. D **77** (2008) 093013 [arXiv:0711.0483 [hep-ph]].

[24] L. Calibbi, J. J. Perez and O. Vives, arXiv:0804.4620 [hep-ph].

[25] S. Ritta and the MEG Collaboration, *Nucl. Phys. Proc. Suppl.* 162 (2006) 279.

[26] A. G. Akeroyd *et al.* [SuperKEKB Physics Working Group], arXiv:hep-ex/0406071.

[27] D.DeMille et al, *Phys. Rev.* A 61, (2000)05250; L.R. Hunter et al,*Phys. Rev.* A 65, (2002) 030501(R); D. Kawall, F. Bay, S. Bickman, Y. Jiang, and D. DeMille, *Phys. Rev. Lett.* 92 (2004) 133007.

[28] J. P. Miller *et al.* [EDM Collaboration], AIP Conf. Proc. **698** (2004) 196.

[29] Y. Farzan and M. E. Peskin, Phys. Rev. D **70**, 095001 (2004) [arXiv:hep-ph/0405214].

[30] J. Hisano and K. Tobe, Phys. Lett. B **510** (2001) 197 [arXiv:hep-ph/0102315].

[31] K. Hagiwara, A. D. Martin, D. Nomura and T. Teubner, Phys. Lett. B **649** (2007) 173 [arXiv:hep-ph/0611102].

[32] D. W. Hertzog, J. P. Miller, E. de Rafael, B. Lee Roberts and D. Stockinger, arXiv:0705.4617 [hep-ph].

[33] T. Moroi, Phys. Rev. D **53** (1996) 6565 [Erratum-ibid. D **56** (1997) 4424] [arXiv:hep-ph/9512396].

[34] M. Davier, Nucl. Phys. Proc. Suppl. **169** (2007) 288 [arXiv:hep-ph/0701163].

[35] J. R. Ellis, J. Hisano, M. Raidal and Y. Shimizu, Phys. Lett. B **528** (2002) 86 [arXiv:hep-ph/0111324].

[36] I. Masina, Nucl. Phys. B **671** (2003) 432 [arXiv:hep-ph/0304299].

[37] E. Komatsu *et al.* [WMAP Collaboration], arXiv:0803.0547 [astro-ph].

[38] S. Davidson, E. Nardi and Y. Nir, arXiv:0802.2962 [hep-ph].

[39] L. Covi, E. Roulet and F. Vissani, Phys. Lett. B **384** (1996) 169 [arXiv:hep-ph/9605319].

[40] V. A. Kuzmin, V. A. Rubakov and M. E. Shaposhnikov, Phys. Lett. B **155** (1985) 36.

[41] Khlebnikov, S. Yu. and Shaposhnikov, M. E., *Nucl. Phys.*, **B308**, (1988) 885-912. Harvey, Jeffrey A. and Turner, Michael S., *Phys. Rev.*, **D42**, (1990) 3344-3349.

[42] R. Barbieri, P. Creminelli, A. Strumia and N. Tetradis, Nucl. Phys. B **575** (2000) 61 [arXiv:hep-ph/9911315].

[43] M. Y. Khlopov and A. D. Linde, Phys. Lett. B **138** (1984) 265; J. R. Ellis, J. E. Kim and D. V. Nanopoulos, Phys. Lett. B **145** (1984) 181; J. R. Ellis, D. V. Nanopoulos and S. Sarkar, Nucl. Phys. B **259** (1985) 175; T. Moroi, H. Murayama and M. Yamaguchi, Phys. Lett. B **303** (1993) 289; M. Kawasaki, K. Kohri and T. Moroi, Phys. Lett. B **625** (2005) 7; For a recent discussion, see: K. Kohri,

T. Moroi and A. Yotsuyanagi, Phys. Rev. D **73** (2006) 123511. C. Bird, K. Koopmans and M. Pospelov, arXiv:hep-ph/0703096. F. D. Steffen, arXiv:0806.3266 [hep-ph].

[44] Buchmuller, W. and Di Bari, P. and Plumacher, M., *Ann. Phys.* 315 (2005) 305-351. hep-ph/0401240.

[45] G. F. Giudice, A. Notari, M. Raidal, A. Riotto and A. Strumia, Nucl. Phys. B **685** (2004) 89 [arXiv:hep-ph/0310123].

[46] S. Davidson and A. Ibarra, Phys. Lett. B **535** (2002) 25 [arXiv:hep-ph/0202239].

[47] G. F. Giudice, L. Mether, A. Riotto and F. Riva, arXiv:0804.0166 [hep-ph].

[48] M. Kawasaki, K. Kohri, T. Moroi and A. Yotsuyanagi, arXiv:0804.3745 [hep-ph].

[49] T. Kanzaki, M. Kawasaki, K. Kohri and T. Moroi, Phys. Rev. D **75** (2007) 025011 [arXiv:hep-ph/0609246]. J. L. Diaz-Cruz, J. R. Ellis, K. A. Olive and Y. Santoso, JHEP **0705** (2007) 003 [arXiv:hep-ph/0701229].

[50] W. Buchmuller, L. Covi, K. Hamaguchi, A. Ibarra and T. Yanagida, JHEP **0703** (2007) 037 [arXiv:hep-ph/0702184]. A. Ibarra and D. Tran, arXiv:0804.4596 [astro-ph]. K. Ishiwata, S. Matsumoto and T. Moroi, arXiv:0805.1133 [hep-ph].

[51] S. Davidson, arXiv:hep-ph/0409339.

[52] A. Bandyopadhyay *et al.* [ISS Physics Working Group], arXiv:0710.4947 [hep-ph].

[53] M. Cirelli and A. Strumia, JCAP **0612** (2006) 013 [arXiv:astro-ph/0607086].

S. Hannestad and G. G. Raffelt, JCAP **0611** (2006) 016 [arXiv:astro-ph/0607101].

U. Seljak, A. Slosar and P. McDonald, JCAP **0610** (2006) 014.

[54] C. Kraus *et al.*, Eur. Phys. J. C **40** (2005) 447 [arXiv:hep-ex/0412056].

[55] H. V. Klapdor-Kleingrothaus *et al.*, Eur. Phys. J. A **12** (2001) 147 [arXiv:hep-ph/0103062].

[56] J. A. Casas and A. Ibarra, Nucl. Phys. B **618** (2001) 171 [arXiv:hep-ph/0103065].

[57] D. A. Demir and Y. Farzan, JHEP **0510** (2005) 068 [arXiv:hep-ph/0508236].

[58] S. Davidson, JHEP **0303** (2003) 037 [arXiv:hep-ph/0302075].

[59] O. Vives, Phys. Rev. D **73** (2006) 073006 [arXiv:hep-ph/0512160].

[60] F. X. Josse-Michaux and A. Abada, JCAP **0710** (2007) 009 [arXiv:hep-ph/0703084].

[61] P. H. Frampton, S. L. Glashow and T. Yanagida, Phys. Lett. B **548**, 119 (2002) [arXiv:hep-ph/0208157]. W. l. Guo, Z. z. Xing and S. Zhou, Int. J. Mod. Phys. E **16**, 1 (2007) [arXiv:hep-ph/0612033].

[62] A. Ibarra and G. G. Ross, Phys. Lett. B **591** (2004) 285 [arXiv:hep-ph/0312138]. A. Ibarra, JHEP **0601** (2006) 064 [arXiv:hep-ph/0511136].

[63] M. Maltoni, T. Schwetz, M. A. Tortola and J. W. F. Valle, New J. Phys. **6** (2004) 122 [arXiv:hep-ph/0405172], W.-M. Yao et al. (Particle Data Group), J. Phys. G 33, 1 (2006).

[64] E. A. Baltz and P. Gondolo, JHEP **0410** (2004) 052 [arXiv:hep-ph/0407039]; M. Kunz, R. Trotta and D. Parkinson, Phys. Rev. D **74** (2006) 023503 [arXiv:astro-ph/0602378].

[65] B. C. Allanach, C. G. Lester and A. M. Weber, JHEP **0612** (2006) 065 [arXiv:hep-ph/0609295].

[66] L. Verde *et al.* [WMAP Collaboration], Astrophys. J. Suppl. **148** (2003) 195 [arXiv:astro-ph/0302218].

A

THE NUMBER DENSITY OF A CHARGED RELIC

AUTHORS: Carola F. Berger[1,2], Laura Covi[3], Sabine Kraml[4] and F. P.[5]

(1) *Center for Theoretical Physics, Massachusetts Institute of Technology, Cambridge, MA 02139, USA*

(2) *Kavli Institute for Theoretical Physics, University of California, Santa Barbara, CA 93106-4030, USA*

(3) *DESY Theory Group, Notkestrasse 85, D-22603 Hamburg, Germany*

(4) *Laboratoire de Physique Subatomique et de Cosmologie, UJF Grenoble 1, CNRS/IN2P3, 53 Avenue des Martyrs, F-38026 Grenoble, France*

(5) *IPN de Lyon, Université Lyon 1, CNRS, 4 Rue Enrico Fermi, Villeurbanne, 69622 Cedex France*

PUBLISHED IN: JCAP 0810 (2008) 005 [1]

We investigate scenarios in which a charged, long-lived scalar particle decouples from the primordial plasma in the Early Universe. We compute the number density at time of freeze-out considering both the cases of abelian and non-abelian interactions and including the effect of Sommerfeld enhancement at low initial velocity. We also discuss as extreme case the maximal cross section that fulfils the unitarity bound. We then compare these number densities to the exotic nuclei searches for stable relics and to

[1] pre-print arXiv:0807.0211 [hep-ph]

the BBN bounds on unstable relics and draw conclusions for the cases of a stau or stop NLSP in supersymmetric models with a gravitino or axino LSP.

A.1 Introduction

The early Universe may have been populated by many exotic particles that, especially if charged, should have easily been in thermal equilibrium. No charged relic seems to have survived to the present day. In fact there are very strong upper bounds on the density of electromagnetically and/or colour charged particles with masses below 10–100 TeV from extensive searches for exotic nuclei [1]. The standard lore is therefore that only neutral relics may have survived until today.

However, it is possible that some unstable but very long-lived charged particle froze-out from thermal equilibrium and decayed much later to a neutral one. A typical example of this kind in supersymmetric models with R-parity conservation is the next-to-lightest supersymmetric particle (NLSP) if the LSP and Cold Dark Matter is very weakly interacting like the axino [2, 3, 4] or the gravitino [5, 6]. Recently, such candidates have attracted a lot of attention, and indeed the signal of a charged metastable NLSP at colliders would be spectacular [7, 8].

In general, strong bounds on the number density of any metastable relic with lifetime of about 1 s or longer are provided by Big Bang Nucleosynthesis (BBN) [9]. They come from two classes of processes: on one hand injection of very energetic photons or hadrons from decays during or after BBN adds an additional non-thermal component to the plasma and can modify the abundances of the light elements [10]; on the other hand, if the relic particle is electromagnetically charged, bound states with nuclei may arise that strongly enhance some of the nuclear rates and allow for catalysed production of e.g. ^6Li [11]. The bounds of the first type are very tight for lifetimes of the order of 10^4 s and exclude, for instance, a neutralino NLSP with a gravitino LSP in the CMSSM [6]. An electrically charged NLSP like the $\tilde{\tau}$ can instead escape the first class of constraints in part of the parameter space, but it is excluded for long lifetimes by bound state effects [12]. In the axino LSP case, the NLSP has a shorter lifetime; the BBN bounds are hence much weaker and both, neutralino and stau, NLSP are still allowed [2].

In this paper, we investigate the most general case of a scalar charged thermal relic. We compute the number density and compare it to the bounds on exotic nuclei for stable particles and the BBN constraints for unstable ones. Similar studies have been carried out model-independently many years ago [13, 14, 15] for stable relics and we will update and improve these computations.[2] We mostly consider the role of the gauge interaction for two main reasons: i) the annihilation into gauge bosons is often the dominant channel for a charged particle and ii) it depends only on very few parameters, just the mass of the particle and its charge or representation. It is also enhanced by the Sommerfeld effect [17], analogous to heavy quark production at threshold, which has previously been considered for dark matter annihilations in [18, 19, 16, 20, 21] and recently also in the context of leptogenesis in [22]. We discuss this Sommerfeld enhancement for the general abelian and non-abelian cases. Moreover, we compare the cross sections with the unitarity bound and update the unitarity limit on the mass of a stable relic.

Our main goal is to determine if it is at all possible to evade *completely* either the exotic nuclei bounds or the BBN ones and how strongly the particle has to interact in this case. We then apply our findings to the Minimal Supersymmetric Standard Model and discuss in more detail the cases of the stau and stop NLSP.

The paper is organised as follows. In Section 2, we briefly review the computation of the number density from thermal freeze-out. The formulae for the annihilation cross section of a charged particle into gauge bosons are given in Section 3. Here we discuss abelian and non-abelian cases, the Sommerfeld enhancement and the unitarity cross section. Moreover, we compare the thermal averages with the first order in velocity expansion. The resulting relic density is discussed in Section 4. In Section 5, we review the constraints on stable and unstable relics. These are then applied in Section 6 to the concrete examples of relic staus and stops. Section 7 finally contains our conclusions. Details on the computation of the annihilation cross section and the case of massive gauge bosons are given in the Appendices A and B.

[2]Recently the case of general EW charged relics as DM was also considered in full detail [16].

A.2 Number density of a thermal relic

The number density of a stable or quasi-stable thermal relic is determined by its annihilation cross section. In fact the number density of a particle in a thermal bath and an expanding Universe is described by the Boltzmann equation [23, 24]:

$$\dot{n}_X + 3Hn_X = \int \frac{dp_X^3}{(2\pi)^3 2E_X}\, \mathcal{C}[f_X] \tag{A.1}$$

where the dot indicates the time derivative, $\mathcal{C}$ denotes the collision integral of all processes that change the particle number and f_X is the phase-space density for the particle X. For a particle with a conserved parity, like R-parity, the lowest order processes to be considered in the collision integral are just two particle scatterings, i.e. annihilations and coannihilations. If there is a lighter particle carrying the conserved parity number, $\mathcal{C}$ includes also the decay into this lighter state, but we will assume that such a decay rate is so small it can be neglected at the time of freeze-out and becomes effective only much later. Then we have effectively a two step process and we can treat freeze-out and decay separately. This is a general feature if the decay takes place via a non-renormalisable interaction and is suppressed by an intermediate or even the Planck scale (see e.g. the axino [2, 4] and gravitino cases [5, 6]).

Taking into account only the annihilation of particle and antiparticle, we can write the collision integral as [24]

$$\mathcal{C}[f_X] = -\int \frac{dp_{\bar{X}}^3}{(2\pi)^3 2E_{\bar{X}}} \left(f_X f_{\bar{X}} - f_X^{eq} f_{\bar{X}}^{eq}\right) 4\sqrt{(p_X \cdot p_{\bar{X}}) - m_X^4}\, \sigma_{ann} \tag{A.2}$$

where σ_{ann} denotes the unpolarised annihilation cross section of an $X\bar{X}$ pair summed over initial and final states. We are here assuming that CP is conserved and no asymmetry exists between n_X and $n_{\bar{X}}$. Note that the production cross section is taken into account by the term proportional to $f_X^{eq} f_{\bar{X}}^{eq}$ since we are assuming that the products of the annihilation are much lighter than X and are still in thermal equilibrium.

In this paper we will consider charged relics and concentrate therefore on the annihilation into gauge bosons, which is the dominant channel in most of parameter space and does depend only on the mass and charge of the relic. Note that adding more channels only increases the cross section and reduces the relic particle number density further. Instead, the inclusion of coannihilations for a charged particle does not always reduce the number density as discussed in [25].

We can rewrite eq. (A.1) by changing variable to $Y_X = n_X/s$, where $s(T) = g_S \frac{2\pi^2}{45} T^3$ is the entropy density, so that the dilution due to the expansion of the universe cancels out in the ratio as long as entropy is conserved. It is also convenient to replace the time variable with $x = \frac{m_X}{T}$, thanks to the relation $dt = \frac{dx}{(xH)}$. We thus obtain

$$\frac{dY_X}{dx} = -\frac{xs(x)}{H(x)m_X^2}\langle\sigma v\rangle_x \left(Y_X^2 - Y_{eq}^2\right) \tag{A.3}$$

$$= -\frac{2\pi g_S}{15}\left(\frac{10}{g_\rho}\right)^{1/2}\frac{M_P}{m_X}\langle\sigma v\rangle_x \left(Y_X^2 - Y_{eq}^2\right) \ . \tag{A.4}$$

Here we have used $H^2 = \frac{\pi^2}{90} g_\rho \frac{T^4}{M_P^2}$, for $M_P = 2.43 \times 10^{18}$ GeV, valid during the radiation dominated era. Moreover, we define the thermally averaged cross section as[3]

$$\langle\sigma v\rangle_x = \frac{1}{4x^4 K_2^2(x)} \int_{2x}^{\infty} dz z^2 \tilde{\sigma}\left(\frac{x}{z}\right) K_1(z) \tag{A.5}$$

where $K_i(z)$ are the modified Bessel functions of order i, characteristic of Maxwell-Boltzmann statistics (we are assuming that we can approximate Bose-Einstein statistics with Maxwell-Boltzmann statistics). In this expression the rescaled cross section $\tilde{\sigma}$ is given by the annihilation cross section *averaged* over initial and *summed* over final states and multiplied by a factor proportional to the squared Møller velocity,

$$\tilde{\sigma}\left(\frac{m_X}{\sqrt{s}}\right) = (s - 4m_X^2)\sigma(m_X, s) \ . \tag{A.6}$$

Note that in the centre-of-mass system the Møller velocity is equal to the relative velocity between the annihilating particles and given by

$$v_{\text{Møl}} = 2\beta = 2\sqrt{1 - \frac{4m_X^2}{s}} \ . \tag{A.7}$$

The rescaled cross section $\tilde{\sigma}$ defined above is dimensionless and function only of $x/z = m_X/\sqrt{s}$ (or β) for the case of annihilation into massless gauge bosons and it always vanishes at threshold. Then it is easy to see that since we integrate in both x, z, the main dependence on the charged relic mass is contained in the prefactor in eq. (A.4) and can be reabsorbed in a rescaling of $Y_X \to Y_X/m_X$. For this reason we obtain nearly exactly $Y_X \propto m_X$ if there is no other mass scale involved. Note that in principle

[3]Note that our definition differs from the one in [24] by a factor m_X^2/x^2 since we prefer to work with a dimensionless quantity and to absorb here all the dependence on x.

a much weaker logarithmic dependence on m_X is present in the value of the freeze-out temperature, when Y begins to deviate from Y_{eq}.

We are here computing the yield of the particle X and to obtain the yield of particle and antiparticle we multiply by a factor of 2 or divide the cross section by 1/2, since we are assuming $n_X = n_{\bar{X}}$. Also note that, contrary to intuition, for a particle with internal degrees of freedom like a coloured state, the total yield is the solution of the Boltzmann equation (A.4) with the cross section averaged over the initial states. Instead the yield per degree of freedom is obtained from the cross section averaged over X, but summed over $\bar{X}$ [4]. The presence of many degrees of freedom in the initial state has then the effect of partially compensating the large cross section coming from the multiplicity of the final states.

A.3 Annihilation cross section for a charged particle into gauge bosons

A.3.1 Abelian case

For an abelian gauge symmetry, there are only three Feynman diagrams contributing to the annihilation cross section, analogous to those shown in Fig. A.1: the t- and u-channel exchange of the scalar particle itself, and the 4-boson vertex. The amplitude is symmetric in the exchange of the gauge bosons and for a particle of charge $e_X g_1$ it is given by

$$\mathcal{A}^{\mu\nu} = i g_1^2 e_X^2 \left[\frac{(2p_1 - p_3)^\mu (2p_2 - p_4)^\nu}{t - m_X^2} + \frac{(2p_1 - p_4)^\nu (2p_2 - p_3)^\mu}{u - m_X^2} + 2g^{\mu\nu} \right] . \qquad \text{(A.8)}$$

The cross section is a function of the mass and charge of the relic:

$$\begin{aligned} \sigma_{ab}(m_X, s) \;=\; & \frac{4\pi\alpha_1^2 e_X^4}{s - 4m_X^2} \left[\sqrt{1 - \frac{4m_X^2}{s}} \left(1 + \frac{4m_X^2}{s} \right) \right. \\ & \left. + \frac{4m_X^2}{s} \left(1 - \frac{2m_X^2}{s} \right) \log \left(\frac{1 - \sqrt{1 - \frac{4m_X^2}{s}}}{1 + \sqrt{1 - \frac{4m_X^2}{s}}} \right) \right] \end{aligned} \qquad \text{(A.9)}$$

[4] In fact any rescaling of the cross section by a factor p due to a different counting of the degrees of freedom can be absorbed into a rescaling $1/p$ of the yield(s).

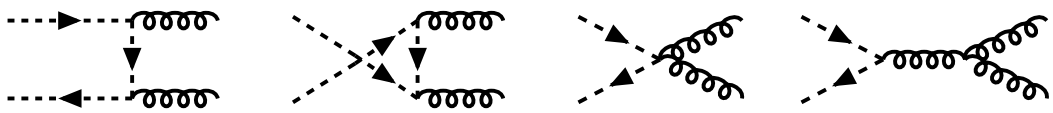

Figure A.1: Feynman diagrams for the annihilation into gauge bosons, here for the case of gluons. In the abelian case, there is no 3-gauge-boson vertex, so the last diagram is absent.

where $\alpha_1 = g_1^2/(4\pi)$ is the gauge coupling; note that a symmetry factor 1/2 has to be added due to the symmetric final state of identical particles. For the rescaled cross section this gives

$$\tilde{\sigma}_{ab}(\beta) = 8\pi\alpha_1^2 e_X^4 \beta \left[1 - \frac{1}{2}\beta^2 + \frac{1-\beta^4}{4\beta}\log\left(\frac{1-\beta}{1+\beta}\right)\right], \tag{A.10}$$

which is a function only of $\beta = \sqrt{1-4m_X^2/s}$ and the charge of the particle.

A.3.2 Non-abelian case

The computation for the annihilation into non-abelian gauge bosons is slightly more involved, since there is an additional contribution from the Feynman diagram with a gauge boson in the s-channel and the 3-gauge-boson vertex. The amplitude can be divided into a symmetric and an antisymmetric piece in the group indices. The symmetric one is analogous to the abelian case:

$$\begin{aligned}\mathcal{A}^{\mu\nu}_{sym} &= i\frac{g_N^2}{2}\left\{T^a, T^b\right\}_{ji}\left[\frac{(2p_1-p_3)^\mu(2p_2-p_4)^\nu}{t-m_X^2}\right. \\ &\quad \left. + \frac{(2p_1-p_4)^\nu(2p_2-p_3)^\mu}{u-m_X^2} + 2g^{\mu\nu}\right],\end{aligned} \tag{A.11}$$

while the antisymmetric part is given by

$$\begin{aligned}\mathcal{A}^{\mu\nu}_{asym} &= -i\frac{g_N^2}{2}\left[T^a, T^b\right]_{ji}\left[\frac{(2p_1-p_3)^\mu(2p_2-p_4)^\nu}{t-m_X^2} - \frac{(2p_1-p_4)^\nu(2p_2-p_3)^\mu}{u-m_X^2}\right. \\ &\quad \left. + 2\frac{g^{\mu\nu}(t-u) - (2p_4+p_3)^\mu(p_1-p_2)^\nu + (p_1-p_2)^\mu(2p_3+p_4)^\nu}{s}\right]\end{aligned} \tag{A.12}$$

The two contributions do not interfere due to the different symmetry, so we have for the amplitude squared, summing only over physical polarisations of the final gauge

bosons:

$$\begin{aligned}|\mathcal{M}|^2 &= 4g_N^4 \left\{ \left| \left\{T^a, T^b\right\}_{ji} \right|^2 \left[\frac{1}{2} + \frac{2m_X^4}{(t-m_X^2)^2} + \frac{2m_X^2}{t-m_X^2}\left(1 - \frac{2m_X^2}{s}\right)\right] \right. \\ &\quad + \left| \left[T^a, T^b\right]_{ji} \right|^2 \left[\frac{1}{2}\frac{(s+2(t-m_X^2))^2}{s^2} + \frac{4m_X^2}{s} + \frac{2m_X^4}{(t-m_X^2)^2} \right. \\ &\quad \left. \left. + \frac{2m_X^2}{t-m_X^2}\left(1 + \frac{2m_X^2}{s}\right)\right]\right\} . \end{aligned} \tag{A.13}$$

Then the sum over all final and initial states for a scalar in the fundamental representation T^a of the gauge group $SU(N)$, normalised such that $\mathrm{Tr}(T^aT^b) = \delta^{ab}/2$, can be obtained from the usual group invariants:

$$\begin{aligned}\sum_{j,i,a,b} \frac{1}{2}\left| \left\{T^a, T^b\right\}_{ji} \right|^2 &= \sum_{a,b} \frac{1}{2}\left(\frac{1}{N}\delta^{ab} + \frac{1}{2}\sum_c |d_{abc}|^2\right) \\ &= C_F(N)\left(1 + \frac{1}{2}(C_A^2(N) - 4)\right) = \frac{(N^2-1)(N^2-2)}{4N} \end{aligned} \tag{A.14}$$

where we have separated the singlet and adjoint contributions to the symmetric part for later convenience, included a factor $1/2$ for identical particles in the final states and used the Casimir invariants for the fundamental and adjoint representations, $C_F(N) = \frac{N^2-1}{2N}, C_A(N) = N$. Note that the ratio of the singlet to adjoint contributions is given simply by $\frac{2}{N^2-4}$. The antisymmetric channel instead gives

$$\sum_{j,i,a,b} \frac{1}{2}\left| \left[T^a, T^b\right]_{ji} \right|^2 = \frac{N^2-1}{4} C_A(N) = \frac{N(N^2-1)}{4} . \tag{A.15}$$

Finally we obtain for the cross section averaged over initial states:

$$\begin{aligned}\sigma_{nab}(m_X, s) &= \frac{\pi\alpha_N^2}{s-4m_X^2}\frac{(N^2-1)^2}{N^3} \times \\ &\quad \left[\sqrt{1-\frac{4m_X^2}{s}}\left(1 + \frac{4m_X^2}{s} - \frac{N^2}{3(N^2-1)}\left(1 - \frac{10m_X^2}{s}\right)\right)\right. \\ &\quad \left. + 4\frac{m_X^2}{s}\left(1 + \frac{2}{N^2-1}\frac{m_X^2}{s}\right)\log\left(\frac{1-\sqrt{1-\frac{4m_X^2}{s}}}{1+\sqrt{1-\frac{4m_X^2}{s}}}\right)\right] . \end{aligned} \tag{A.16}$$

This result coincides for $N = 3$ with that reported in [26] for the Born cross section of a pair of gluons into squarks, allowing for the exchange of the initial and final state.

Then the rescaled cross section for $SU(N)$ is

$$\tilde{\sigma}_{nab}(\beta) = 2\pi\alpha_N^2 \frac{(N^2-1)^2}{N^3}\beta\left[1+\frac{N^2}{4(N^2-1)}-\frac{\beta^2}{2}\left(1+\frac{5N^2}{6(N^2-1)}\right)+\frac{1-\beta^2}{2\beta}\left(1+\frac{1}{2(N^2-1)}-\frac{\beta^2}{2(N^2-1)}\right)\log\left(\frac{1-\beta}{1+\beta}\right)\right]. \quad \text{(A.17)}$$

Note that the contribution of order β in the expression above in the limit $\beta \to 0$ is due to the symmetric part of the matrix element and that the antisymmetric piece instead vanishes at that order. Therefore the symmetric part of the cross section dominates at threshold.

So we see that for a non-abelian interaction the cross section is larger than for the abelian case, not only due to the possibly larger coupling α_N, but also due to the opening of an antisymmetric channel and of course to the multiplicity of the final states. In fact for large N the averaged cross section increases as N and therefore the yield decreases as $1/N$.

A.3.3 Annihilation into $SU(N)$ gauge boson and photon

The annihilation cross section into gluon and photon is just the same as the abelian one, but with a different vertex for the gluon. Then considering a particle of electromagnetic charge $e_X g_1$, in the representation T^a of the gauge group $SU(N)$ with coupling g_N, annihilating with its own antiparticle, the amplitude is given by [5]

$$\mathcal{A}^{\mu\nu} = i g_1 e_X g_N T^a_{ji}\left[\frac{(2p_1-p_3)^\mu(2p_2-p_4)^\nu}{t-m_X^2}+\frac{(2p_1-p_4)^\nu(2p_2-p_3)^\mu}{u-m_X^2}+2g^{\mu\nu}\right]. \quad \text{(A.18)}$$

From this we easily obtain the cross section as:

$$\sigma_{1N}(m_X,s) = \frac{8\pi\alpha_1\alpha_N e_X^2}{s-4m_X^2}|T^a_{ji}|^2\left[\sqrt{1-\frac{4m_X^2}{s}}\left(1+\frac{4m_X^2}{s}\right)+\frac{4m_X^2}{s}\left(1-\frac{2m_X^2}{s}\right)\log\left(\frac{1-\sqrt{1-\frac{4m_X^2}{s}}}{1+\sqrt{1-\frac{4m_X^2}{s}}}\right)\right], \quad \text{(A.19)}$$

[5] Strictly speaking, in this case the final state particles are different and therefore there are no independent t- and u-channels, but we can still write the amplitude to be symmetric in t and u in order to make direct contact with the previous results.

where $\alpha_{1,N}$ are the gauge couplings and the symmetry factor 1/2 in this case is absent since the final particles are not identical.
Averaging over the initial and summing over the final state, we have

$$\frac{1}{N}\sum_{j,i,a} T^a_{ji}T^a_{ij} = \frac{1}{N}\sum_{j,i} C_F(N)\delta_{ij} = \frac{N^2-1}{2N} \tag{A.20}$$

for the fundamental representation. This gives for the rescaled cross section

$$\tilde{\sigma}_{1N}(\beta) = 8\pi\alpha_1\alpha_N e_X^2 \frac{N^2-1}{N}\beta\left[1-\frac{1}{2}\beta^2+\frac{1-\beta^4}{4\beta}\log\left(\frac{1-\beta}{1+\beta}\right)\right] \tag{A.21}$$

which is a factor $(N^2-1)\alpha_N/(N\alpha_1 e_X^2)$ larger than the pure $U(1)$ contribution. Again the cross section increases as N for large N.

A.3.4 Annihilation into physical Z and $SU(N)$ gauge boson/photon

The annihilation cross section into massive Z and photon/SU(N) gauge boson has the same form as the abelian one. We consider here a particle with Z-coupling $g_1 e_Z$, in the representation T^a of the gauge group $SU(N)$ with coupling g_N, annihilating with its own antiparticle and we obtain

$$\mathcal{A}^{\mu\nu} = ig_1 e_Z g_N T^a_{ji}\left[\frac{(2p_1-p_3)^\mu(2p_2-p_4)^\nu}{t-m_X^2}+\frac{(2p_1-p_4)^\nu(2p_2-p_3)^\mu}{u-m_X^2}+2g^{\mu\nu}\right], \tag{A.22}$$

where p_4 is the Z boson momentum obeying $p_4^2 = M_Z^2$; the annihilation into photon and Z is easily read off by taking just $g_N T^a_{ji} \to g_1' e_X$. Then we easily obtain the cross section as:

$$\begin{aligned}\sigma_{\mathrm{ZN}}(m_X, M_Z, s) &= \frac{8\pi\alpha_1\alpha_N e_Z^2}{s-4m_X^2}|T^a_{ji}|^2\left[\sqrt{1-\frac{4m_X^2}{s}}\left(1-\frac{M_Z^2}{s}+\frac{4(m_X^2-M_Z^2)}{s-M_Z^2}\right)\right.\\ &\left.+\frac{4m_X^2}{s}\left(1-\frac{5M_Z^2}{8m_X^2}-\frac{4m_X^2-3M_Z^2}{2(s-M_Z^2)}\right)\log\left(\frac{1-\sqrt{1-\frac{4m_X^2}{s}}}{1+\sqrt{1-\frac{4m_X^2}{s}}}\right)\right]\end{aligned} \tag{A.23}$$

where $\alpha_{1,N}$ are the gauge couplings.
Averaging over the initial and summing over the final state as in eq. (A.20), we have for the rescaled cross section

$$\begin{aligned}\tilde{\sigma}_{1N}(\beta, a_Z) &= 8\pi\alpha_1\alpha_N e_Z^2\frac{N^2-1}{2N}\beta\left[1-a_Z(1-\beta^2)+\frac{(1-4a_Z)(1-\beta^2)}{1-a_Z(1-\beta^2)}\right.\\ &\left.+\frac{1-\beta^2}{\beta}\left(1-\frac{5}{2}a_Z-(1-\beta^2)\frac{1-3a_Z}{2-2a_Z(1-\beta^2)}\right)\log\left(\frac{1-\beta}{1+\beta}\right)\right]\end{aligned} \tag{A.24}$$

where $a_Z = M_Z^2/m_X^2$. Note that the cross section for annihilation into photon and Z, is given by the substitution $\alpha_N \frac{N^2-1}{2N} \to \alpha_1' e_X^2$. For the specific case of the right-handed stau (stop), the coupling with the Z boson and photon are respectively given by $e_Z^2\alpha_1 = \alpha_{em}\tan^2\theta_W$ ($e_Z^2\alpha_1 = 4/9\,\alpha_{em}\tan^2\theta_W$) and $e_X^2\alpha_1' = \alpha_{em}$ ($e_X^2\alpha_1' = 4/9\,\alpha_{em}$), where θ_W is the Weinberg angle.

A.3.5 Annihilation into massless EW gauge bosons

The cross section for annihilation into massless $SU(2)_L$ gauge bosons can be obtained directly from the general formula for the non-abelian case. One has to take into account, however, that in this case the scalar $SU(2)_L$ doublet is not degenerate in mass and that the initial particles can be a mixture of left- and right-chiral states. We neglect here the effects of EW symmetry breaking; the results are hence applicable for the case of a heavy relic that decouples before EW symmetry breaking takes place.

Considering the scalar relic to be $X = X_L\cos\theta + X_R\sin\theta$ and denoting with $m_{X'}$ the mass of its left-handed doublet partner, which is sufficiently larger than m_X to neglect coannihilations, we obtain for the annihilation cross section into $W^{1,2}$ gauge bosons:

$$\begin{aligned}
&\sigma_{W2}(s, m_X, m_{X'}) = \\
&\frac{2\pi\alpha_2^2\cos^4\theta}{s-4m_X^2}\left[\sqrt{1-\frac{4m_X^2}{s}}\left(\frac{2}{3}+\frac{13}{3}\frac{m_X^2}{s}-\frac{m_{X'}^2}{s}+\frac{(m_X^2+m_{X'}^2)^2}{s m_{X'}^2+(m_{X'}^2-m_X^2)^2}\right)\right. \\
&\left.+\,2\left(\frac{m_{X'}^2+m_X^2}{s}-\frac{(m_{X'}^2-m_X^2)^2}{2s^2}\right)\log\left(\frac{s+2(m_{X'}^2-m_X^2)-\sqrt{s(s-4m_X^2)}}{s+2(m_{X'}^2-m_X^2)+\sqrt{s(s-4m_X^2)}}\right)\right],
\end{aligned} \tag{A.25}$$

while the annihilation into W^3 is similar to the abelian one in eq. (A.9) for $e_X = \cos\theta/2$. Note that the cross section is suppressed by the mixing angle as $\cos^4\theta$ and by the fact that the group indices are not summed for the initial state. Also in this case the rescaled cross section is not just a simple function of β, but also of the mass difference in the doublet. We have in fact

$$\begin{aligned}
\tilde{\sigma}_{W2}(\beta,\delta^2) = 2\pi\alpha_2^2\cos^4\theta\,\beta\left[\frac{5}{2}+\frac{11}{6}\beta^2-\delta^2+\frac{4\beta^2\delta^4}{(1+2\delta^2)^2-\beta^2}\right. \\
\left.+\,\frac{1-\beta^2+2\delta^2-\delta^4}{\beta}\,\log\left(\frac{1+2\delta^2-\beta}{1+2\delta^2+\beta}\right)\right],
\end{aligned} \tag{A.26}$$

where $\delta^2 = (m_{X'}^2 - m_X^2)/s$. The cross section still vanishes for $\beta = 0$ and is finite for $\delta^2 \to \infty$. The detailed expressions for the case of broken EW symmetry are much more involved and include also the contribution of the Higgs s-channel allowing for resonance enhancement. They are given in Appendix B.

A.3.6 Sommerfeld enhancement

In the previous sections we have computed the annihilation cross sections to lowest order in the gauge coupling. However, it was shown long ago [17] that an expansion in terms of the coupling is inadequate close to threshold, where the velocities of the annihilating particles go to zero,

$$\beta \equiv \sqrt{1 - \frac{4m_X^2}{s}} \to 0\,. \tag{A.27}$$

The enhancement at low velocities becomes apparent when one computes the one-loop corrections, which are enhanced by a factor $\frac{C\alpha\pi}{2\beta}$. Here, C is a process-dependent constant, α is the gauge coupling of the annihilating scalars, α_1 in the case of $U(1)$ boson exchanges, or α_N for $SU(N)$ gauge boson exchanges, respectively. To account for this long-distance effect, one therefore has to resum a whole class of diagrams, which consist of t-channel ladder-type exchanges of *massless* soft Coulomb $SU(N)$ or $U(1)$ gauge bosons between the annihilating charged particles.

This resummation of terms $\sim \alpha^n/\beta^n$ leads to the so-called Sommerfeld factor which multiplies the lowest-order annihilation cross section. The Sommerfeld enhancement is given by the modulus squared of the particle wave function at the origin,

$$E \equiv |\Psi(0)|^2 = \frac{z}{1 - \exp(-z)}, \quad z = \frac{C\alpha\pi}{\beta}\,. \tag{A.28}$$

Because this effect is a long-distance one, taking place at a scale $\sim \beta m_X$, it factorises from the annihilation cross section which is a short-distance effect at the hard-scattering scale of order of the mass m_X. Schematically,

$$\sigma^{\rm SF}(\beta, m_X) = E(\alpha(\beta m_X)) \times \sigma^0(\beta)\,. \tag{A.29}$$

Here, σ^0 is the leading-order annihilation cross section, which has been presented in the preceding subsections. Eq. (A.29) is in principle only valid if the annihilating partons

are in a single $SU(N)$ channel, i.e. for particle in the fundamental representation either in the singlet or adjoint configurations. If multiple channels c contribute, eq. (A.29) has to be modified to

$$\sigma^{\rm SF}(\beta, m_X) = \sum_c E_c(\alpha(\beta m_X)) \times \sigma_c^0(\beta)\,. \tag{A.30}$$

Here, $\sigma_c^0(\beta)$ is the projection of the leading-order annihilation cross section in the relevant channel. For a scalar in the fundamental representation of the $SU(N)$ gauge group annihilating into massless $SU(N)$ gauge bosons, we have seen that only the contribution proportional to the group-symmetric part survives in the limit of vanishing β and is enhanced at low velocities. Therefore at leading order the cross sections σ_c^0 can be taken to be the same for the singlet and adjoint part up to colour factors and proportional to the total cross section given in eq. (A.17) [6]. We note also that due to the presence of more than one channel, the Sommerfeld factor for an $SU(N)$ gauge theory becomes dependent also on the final states, since not all channels may contribute to the annihilation into a given final state.

However, the presence of the thermal bath complicates things, as the interactions with the background gauge bosons may prevent the annihilating partons to be initially in a definite $SU(N)$ channel. The time scales for the Sommerfeld effect and the interactions with the thermal bath are of competing order, so it is not clear how strong such effect can be. In this paper we will consider both extreme situations, i.e. the case when the thermal bath has no effect and the case when there is no definite initial channel. In the latter case, it was argued in the literature that due to the mixing of states one should just take an average C^{av} extracted from the averaged one-loop correction, leading again to a single Sommerfeld factor as in eq. (A.29) (see, for example, ref. [27]). While the two approaches give identical results by construction at first order, they correspond to two quite distinct resummations of the higher orders and they are numerically substantially different.

We obtained the coefficients C by computing the $1/\beta$-enhanced contributions for t-channel $SU(N)$ gauge boson exchange at one loop in the threshold expansion (see for example [28] and references therein). For the generation of the relevant one-loop

[6] Taking the true $\sigma_{\mathbf{1}}^0$ and $\sigma_{\mathbf{A}}^0$ instead, differs from the total σ^0 only in the terms suppressed by β^2 and amounts to a correction smaller than 1% at threshold where the Sommerfeld factor is effective.

graphs and the Lorentz algebra we used the *Mathematica* packages `FeynArts` and `FeynCalc` [29]. We simplified the resulting expressions to only keep terms that are leading in β, that is, we only kept terms that are enhanced in the soft region of the one-loop integrals, which were then simple enough to perform by hand. Alternatively, as mentioned above, one obtains the form (A.28) directly by computing the normalised wave function at the origin from the Schrödinger equation, describing the annihilating parton pair, with a Coulomb interaction potential for positive energies $\sim \beta^2 m_X$ [17].

The Sommerfeld enhancement due to exchanges of massless Coulomb $SU(N)$ gauge bosons is the same for the singlet channel of annihilation into $SU(N)$ gauge bosons B_N and the annihilation into $U(1)$ gauge bosons B_1,

$$C^{\mathbf{1}}_{S\bar{S}\to B_N B_N} = C_{S\bar{S}\to B_1 B_1} = C_F(N) = \frac{N^2-1}{2N}\,. \tag{A.31}$$

The factor for the adjoint channel is instead found to be negative and thus suppressing,

$$C^{\mathbf{A}}_{S\bar{S}\to B_N B_N} = C_F(N) - \frac{C_A(N)}{2} = -\frac{1}{2N}\,. \tag{A.32}$$

The same factors $C^{\mathbf{1}}$ or $C^{\mathbf{A}}$ apply also for other final states of the singlet or adjoint channels. For example, the Sommerfeld factor for $\tilde{t}\tilde{t}^* \to hh$ is $C^{\mathbf{1}}_{SU(3)} = 4/3$, while that for $\tilde{t}\tilde{t}^* \to gh, g\gamma, gZ$ is $C^{\mathbf{A}}_{SU(3)} = -1/6$.

Even if the adjoint channel leads to a suppression, upon summing over both contributions in eq. (A.30), the net effect is still quite enhancing for small N. We have then in fact

$$\sigma^{\mathrm{SF}sum}(\beta, m_X) = \sigma^0(\beta)\left[E_{\mathbf{1}}(\alpha(\beta m_X)) \times \frac{2}{N^2-2} + E_{\mathbf{A}}(\alpha(\beta m_X)) \times \frac{N^2-4}{N^2-2}\right], \tag{A.33}$$

where, as described above, we have taken $(N^2-2)/2\ \sigma^0_{\mathbf{1}} = (N^2-2)/(N^2-4)\ \sigma^0_{\mathbf{A}} = \sigma^0(\beta)$, and $\sigma^0(\beta)$ is given in eq. (A.17). For $SU(3)$ this gives

$$\sigma^{\mathrm{SF}sum}_{SU(3)}(\beta, m_X) = \sigma^0_{SU(3)}(\beta)\ \frac{\pi\alpha_3}{42\beta}\ \left[\frac{16}{1-e^{-\frac{4}{3}\frac{\pi\alpha_3}{\beta}}} - \frac{5}{1-e^{\frac{1}{6}\frac{\pi\alpha_3}{\beta}}}\right], \tag{A.34}$$

so that the enhancement in the singlet dominates over the suppression in the adjoint channel.

On the other hand, averaging the one loop contribution over initial channels [7] results

[7] Averaging over initial channels is not to be confused with averaging over initial states which is to be done in addition when solving the Boltzmann equation.

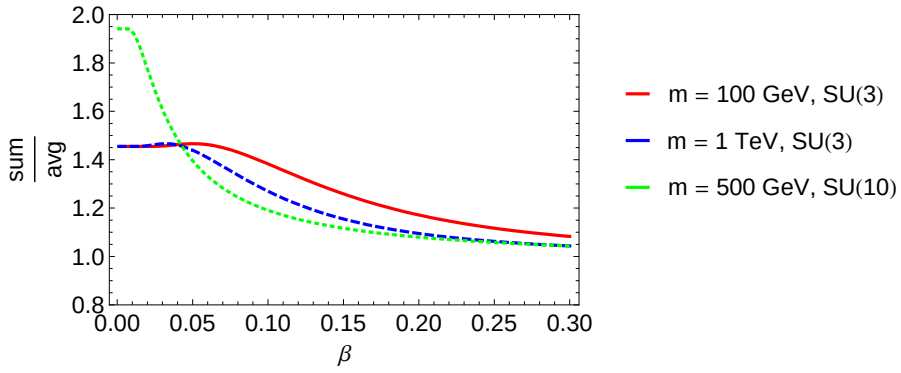

Figure A.2: Ratio of summed over averaged Sommerfeld enhancement, $\sigma^{\mathrm{SF}sum}_{SU(3)}/\sigma^{\mathrm{SFav}}_{SU(3)}$, as a function of β. The full red line shows the $SU(3)$ case for a mass $m = 100$ GeV and the dashed blue line for a mass $m = 1$ TeV; the dotted green line is for the hypothetical case of $SU(10)$ with $m = 500$ GeV.

in a factor

$$C_{S\bar{S}\to B_N B_N} = \frac{N^2+2}{2N(N^2-2)} =: C^{\mathrm{av}}_{SU(N)}\,, \tag{A.35}$$

which is although enhancing, much less so than the net effect of the summation over singlet and adjoint channels. For $SU(3)$, this factor is $C^{\mathrm{av}}_{SU(3)} = 11/42$, leading to

$$\sigma^{\mathrm{SFav}}_{SU(3)}(\beta, m_X) = \sigma^{0}_{SU(3)}(\beta)\,\frac{\pi\alpha_3}{42\beta}\,\frac{11}{1-e^{-\frac{11\pi\alpha_3}{42\beta}}}. \tag{A.36}$$

Note that the first term of the expansion of eq. (A.36) coincides with the 1-loop result of [26] for $gg \to \tilde{q}\tilde{q}^*$ near threshold.

If the difference in the exponents in the denominators of eqs. (A.34) and (A.36) could be neglected the two expression would be equal. However, in the small β region where the Sommerfeld enhancement is relevant, the difference amounts to up to 50 % for $SU(3)$, and is even larger for hypothetical larger N, see Figure A.2.

For scalars charged under a $U(1)$ group, there is of course a corresponding enhancement due to $U(1)$ boson exchanges. However, the enhancement factor is now governed by the $U(1)$ coupling, and thus weaker than an enhancement under a strong $SU(N)$ gauge group. The Sommerfeld factor for the dominant annihilation channel into $U(1)$ gauge boson pairs can very simply be determined from the abelian part of

the calculation that led to the factor quoted above. We find,

$$C_{S\bar{S}\to B_1 B_1} = 1\,, \tag{A.37}$$

for t-channel $U(1)$ exchange, and the coupling in eq. (A.28) is the $U(1)$ coupling α_1.

Another issue regarding the thermal bath is the fact that gauge bosons acquire a mass through interactions with the plasma. This Debye screening effect happens at a scale of order $\sim gT$, whereas the Sommerfeld effect is of order $\sim \alpha m_X \beta \sim \alpha\sqrt{m_X T} \gg gT$. Thus the thermal masses of initially massless gauge bosons do not affect the Sommerfeld enhancement.

Finally, there are also massive gauge bosons such as Ws and Zs to consider. The Sommerfeld factor arises from instantaneous Coulomb exchanges of massless gauge bosons between the slow moving annihilating pair close to threshold, thus resulting in an $1/\beta$ enhancement, signalling the inadequacy of trying to describe this exchange in an expansion in terms of loop corrections. Naturally, massive gauge bosons have a finite width, and thus cannot be exchanged instantaneously. In terms of Feynman graphs, the momentum flowing through a massive gauge boson that is exchanged between the annihilating pair is naturally cut off by the mass of the exchanged boson and can never become too soft. The Sommerfeld effect is exponentially suppressed with the mass of the gauge boson, as an analysis of the wavefunction picture reveals. It can nevertheless become important for relics with masses much larger than the electroweak scale, as a very heavy Wino discussed in [19]. In the following we will consider only the case of massless gauge bosons, which is the dominant effect for coloured relics and for purely right-handed sleptons. For a more detailed discussion in case of massive EW gauge bosons we refer the reader to [19, 16].

A.3.7 Unitarity bound

We next compare the above cross sections with the unitarity bound. Using unitarity and partial wave expansion, the non-elastic cross section for a particle with spin s_p is given by [15]

$$\sigma_{non-el,J} = \frac{4\pi(2J+1)(1-\eta_J^2)}{(2s_p+1)^2\,\vec{p}_i^{\,2}} \tag{A.38}$$

where J is the angular momentum of the process, $\vec{p}_i$ is the initial particle momentum, $4\vec{p}_i^{\,2} = s\beta^2$ in the centre of mass frame in our case, and η_J^2 is the contribution of the

elastic part. This gives an upper bound for the annihilation cross section with angular momentum J as

$$\sigma_{ann,J} \leq \frac{16\pi(2J+1)}{(2s_p+1)^2 s\beta^2} \,. \tag{A.39}$$

The lowest value is obtained taking $J = 0$ and since the s-wave annihilation is usually the dominant contribution for a scalar non-relativistic particle with $s_p = 0$, we will take it as a reference value. We therefore have for the maximal rescaled cross section:

$$\tilde{\sigma}_{max} = 16\pi \tag{A.40}$$

independent of the particle mass or energy. In this case the thermal averaging is simple and we obtain

$$\langle \sigma_{max} v \rangle_x = \frac{16\pi}{x^2} \frac{K_2(2x)}{K_2(x)^2} \,, \tag{A.41}$$

which we will consider in the following to be the maximal cross section per degree of freedom[8]. We see clearly that the cross sections discussed above satisfy this bound and are suppressed at the very least by α^2. Figure A.3 shows the rescaled cross sections for the abelian and non-abelian cases, eqs. (A.10) and (A.17), together with the unitarity bound eq. (A.40) as a function of the relative velocity of the annihilating particles.

The unitarity cross section $\tilde{\sigma}_{max}$ can be used to obtain a lower bound of the yield. Moreover, it can be taken as the maximal annihilation cross section possible even after the QCD phase transition, when the coloured states are confined into the equivalent of scalar hadrons and fermionic mesons [30]. Constraints from cosmology on such kind of hadronic states have been mostly studied for the case of a stable exotic quark [14], a gluino LSP [27] or for very long-lived gluino in the split SUSY scenarios [18]. It has been argued in [31] that the annihilation cross section for such states could become much stronger, if bound states between two scalar hadrons/fermionic mesons are formed with rate $\sim \pi/\Lambda_{QCD}^2$ and in that case the coloured relic abundance after the QCD phase transition is further reduced below $Y \sim 10^{-16} - 10^{-17}$. We will not consider this possibility in the following, but note however that, while most of the cosmological bounds for a decaying relicare then satisfied, one still needs to consider the bounds for a stable relic.

[8]Note that here we are computing explicitly in the centre of mass frame, while the Boltzmann equation requires to use the covariant or lab frame. The difference between the two frames has been discussed in [24] and gives only a small correction for non-relativistic particles, which we neglect here.

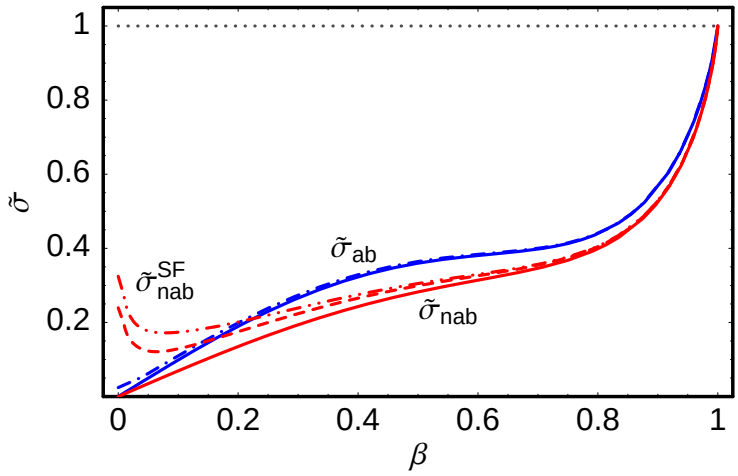

Figure A.3: Dependence of the rescaled cross sections on the relative velocity β, normalised to 1 at large s, i.e. $\beta = 1$. The solid lines show the leading order section, the dashed/dashed dotted lines the effect of the Sommerfeld enhancement, that makes the cross sections non-vanishing at the threshold $\beta = 0$. The $SU(3)$ cross sections are the upper (red) lines, including the averaged Sommerfeld factor in the dashed line and the summed one in the dash-dotted. For the abelian case (blue lines) the Sommerfeld effect is much milder and shown in the dash-dotted line. Note that the region for $\beta \sim 0$ contributes more strongly to the thermally averaged cross section due to the Boltzmann-suppression for large β.

A.3.8 Thermally averaged cross sections and velocity expansion

We integrate eq. (A.5) numerically to obtain the thermally averaged cross section. Very often such a quantity is instead approximated with the first terms of its velocity expansion, since the relevant regime takes place when the annihilating particles are already non-relativistic. To obtain such an expansion, one can use the approximation

$$s - 4m_X^2 \simeq 4m_X^2\beta^2 \tag{A.42}$$

and expand in β the expression

$$\sigma v_{\text{Møl}} \simeq \frac{1}{2m_X^2\beta}\tilde{\sigma}\left(\beta\right) \ . \tag{A.43}$$

We see that if $\tilde{\sigma}$ is constant at zero velocity, the cross section is enhanced like $1/\beta$ in that limit. This is indeed the case both for the Sommerfeld-enhanced cross section and the unitarity one.

The first term in the expansion, which is independent of the velocity and coincides therefore with the first term in the expansion of the thermally averaged cross section [24], is given by

$$\sigma_{ab}v \rightarrow \frac{2\pi\alpha_1^2 e_X^4}{m_X^2} + \mathcal{O}(\beta^2) \,, \tag{A.44}$$

$$\sigma_{nab}v \rightarrow \frac{\pi\alpha_N^2}{m_X^2}\frac{(N^2-1)(N^2-2)}{4N^3} + \mathcal{O}(\beta^2) \,, \tag{A.45}$$

for the abelian and non-abelian cases respectively.

We plot in Figure A.4 the thermally averaged cross sections as a function of x normalised with respect to the first term in their velocity expansion including also the Sommerfeld enhancement factor, both for the abelian case and for the QCD case with $N = 3$. We see that keeping only the lowest order overestimates the thermally averaged cross section, i.e. underestimates the yield, in the abelian case by at most 20% in the region of freeze-out ($x \sim 30$). The non-abelian case for $N = 3$ is approximated better also because the freeze-out takes place at a larger $x \sim 40$, i.e. smaller β. On the other hand, once we include the Sommerfeld enhancement, the thermally averaged cross section does no more converge to the first constant term in the velocity expansion due to the threshold singularity at $\beta = 0$. Nevertheless the first order term *without* the enhancement can still give a reasonably good approximation for the abelian case, since the Sommerfeld enhancement partially compensate the 20% underestimation of the Born result. For the non-abelian case the Sommerfeld enhancement is so strong that the low energy expansion can give only an order of magnitude estimate.

A.4 Results for the relic density

We solve the Boltzmann equation (A.4) numerically for the exact thermally averaged cross sections given above. This improves the old results [13] that were obtained with the velocity expansion.

For the case of an abelian charged relic, we consider $e_X = \pm 1$ and we set the coupling to be $\alpha_{em} = 1/128$. For the non-abelian case we take $N = 3$ and α_N to be

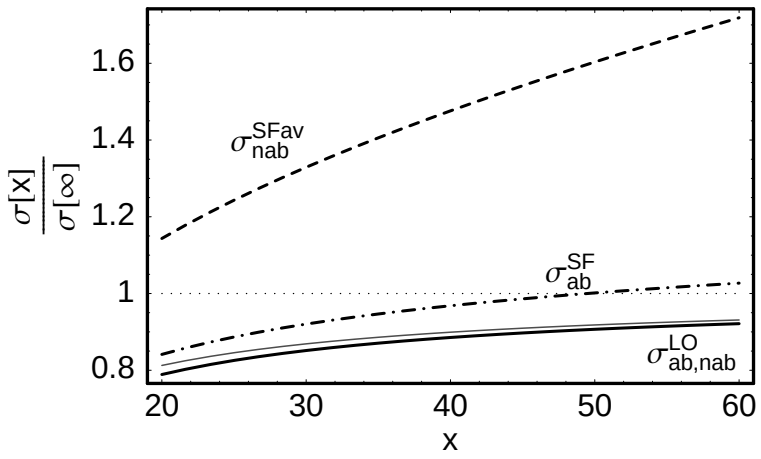

Figure A.4: Ratio of the thermally-averaged cross section and the first term in the velocity expansion around $\beta = 0$, for $m_X = 350$ GeV. The thick solid line is for the abelian, the thin line for the non-abelian ($SU(3)$) case. Dash-dotted and dashed respectively are the same ratios including the Sommerfeld enhancement, only the averaged one for the non-abelian case: we see that in this case the thermally averaged cross sections do not converge to the first order term in velocity, but that the latter can still give a good estimate within 15% of the full result in the abelian case; for the non-abelian case the Sommerfeld enhancement changes the result considerably and the velocity expansion fails. Note that the case of the summed Sommerfeld factor is outside the range of the plot.

the QCD coupling $\alpha_3(Q)$ with $Q = 2m_X$ in the hard process and $Q = \beta m_X$ in the Sommerfeld correction, c.f. Sect. A.3.6. In order to avoid the non-perturbative regime, we cut off the running of α_3 at $Q = 2$ GeV, i.e. $\alpha_3(Q < 2 \text{ GeV}) \equiv \alpha_3(2 \text{ GeV})$.

For the entropy and energy density parameters we take $g_S^{1/2} = g_\rho^{1/2} = 10$, since we expect the freeze-out to take place between 10–100 GeV, when only the light Standard Model particles are still in equilibrium in the thermal bath.

Our results are plotted in Figure A.5. We see that the yield Y follows relatively closely the equilibrium density until the time of freeze-out, which happens at different values of x for the different cross sections. As expected the non-abelian interactions being stronger gives a considerably lower relic density. The ratio between the two cases

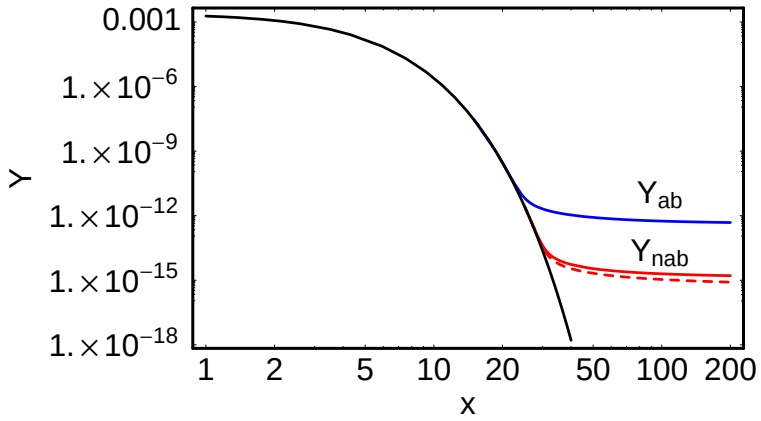

Figure A.5: Time evolution of the particle yield for the cases of abelian and non-abelian cross section, for $m_X = 200$ GeV. The upper (blue) curve is for an electromagnetically charged scalar particle with unit charge, while the lower (red) curves correspond to a single coloured scalar in the fundamental representation without the Sommerfeld factor (solid) and with the Sommerfeld factor averaged (dashed). We see that the treatment of the Sommerfeld factor has an impact of about 30% on the final number density.

is well approximated by the ratio of cross sections, $\sigma_{nab}v/\sigma_{ab}v$, at zero velocity :

$$\frac{Y_{ab}}{Y_{nab}} = \frac{7}{27}\,\frac{\alpha_3^2}{\alpha_{em}^2} \approx 40\,. \tag{A.46}$$

We next consider the dependence on the only dimensional parameter, the mass of the charged relic. We have seen that the thermal average can be written only as a function of x and since we are integrating the Boltzmann equation to $x \to \infty$ we get rid of the dependence on m_X that is contained there. A subleading dependence would survive by integrating to a finite value of x, but this effect is negligible for the present universe with a temperature $T_{now} \sim 10^{-4}$eV $\ll m_X$. On the other hand, the mass directly enters in the coefficient of eq. (A.4) and that is the stronger dependence on m_X. Note that this dependence is present even in the unitarity case, where the reduced cross section is explicitly independent of the mass and velocity. In general therefore the yield is proportional to the mass and can be rescaled as

$$Y(m_X) = Y(1\,\text{TeV})\left(\frac{m_X}{1\,\text{TeV}}\right)\,. \tag{A.47}$$

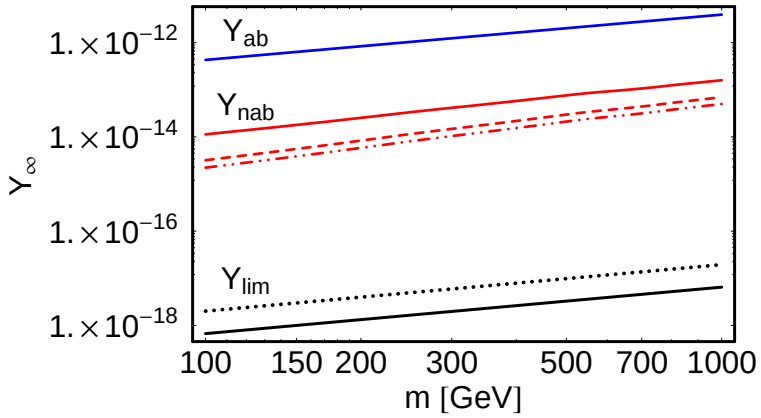

Figure A.6: Dependence of the yield on the mass of the charged relic. From top to bottom, the first (blue) line is for the case of an electromagnetically charged relic, while the second (red) line is for a coloured relic, the dashed and dash-dotted lines include the Sommerfeld factor, averaged and summed respectively. The lower two (black) lines correspond to the maximal annihilation cross section given by unitarity – the solid one for a single d.o.f., the dotted one for 3 d.o.f. for the fundamental representation of QCD. Note that the non-abelian case is still three orders of magnitudes away from the unitarity cross section.

with $Y_{ab}(1\,\mathrm{TeV}) = 3.9 \times 10^{-12}$ and $Y_{nab}(1\,\mathrm{TeV}) = 1.6 \times 10^{-13}$ for the abelian and non-abelian cases, respectively, for the total degrees of freedom, including antiparticles. For the case of the unitarity cross section, the total yield becomes instead $Y_{lim}(1\,\mathrm{TeV}) = 6.6 \times 10^{-18}$ (or 2×10^{-17} for three degrees of freedom).

Since the energy density also increases for larger masses, this can be used to give a constraint on the mass of any stable thermal relic from the maximal cross section allowed by unitarity [15]. Using the WMAP 5-year results [32] for the most conservative upper bound for the matter density, we can update such bound. In fact imposing

$$\Omega_X h^2 = m_X Y_{X+\bar{X}}(T_{now}) s(T_{now})/\rho_c \leq 0.13 \tag{A.48}$$

gives us for a single degree of freedom the constraint

$$\frac{m_X Y_{X+\bar{X}}(T_{now})}{\mathrm{GeV}} \leq 4.6 \times 10^{-10} \tag{A.49}$$

resulting for a scalar particle in

$$m_X \leq 280 \text{ TeV} . \tag{A.50}$$

Note that for a fermionic spin 1/2 relic the unitarity cross section is reduced by a factor four and therefore the bound on the mass is stronger by a factor two.

A.5 Constraints on cosmological relics

We review here the constraints on the abundance of cosmological relics that we will compare with the number density of a charged scalar relic in the next section. First we will consider the case of stable relics (i.e. with lifetimes longer than 10^{27} s) and next relics with lifetimes in the window $0.1 - 10^{12}$s. Note that for shorter lifetimes the constraints are non-existent, as long as the particle did not dominate the universe dynamics before decaying or produce a large amount of entropy, while for lifetimes between $10^{10} - 10^{27}$s bounds from CMB distortion [33] and from the measured photon diffuse flux [34] apply, but will not be discussed here.

A.5.1 Stable relics

The possibility of existence of some more exotic cosmological relics than the known light elements stimulated many years ago the search for exotic nuclei in water and other materials on the earth. Those searches were unsuccessful and provide a very strong limit on the number density of any relic that would bind electromagnetically with an electron or in nuclei, under the assumption that such particles are equally distributed in the Universe compared to baryons. If such relics were present long before structure formation, it is highly probable that they were trapped together with baryons when the universe's density was still nearly homogeneous, so that we can expect their number density not to be too strongly dependent on the local environment. Note that in any case these bounds are so strong that the possibility of such a relic to be Dark Matter is completely excluded.

The most recent constraints are those obtained by [35] looking for anomalously heavy hydrogen in deep sea water, which apply to an electrically positively charged

relic, and give for masses 5 GeV $\leq m_X \leq$ 1.6 TeV:

$$Y_{X^+} \leq 4 \times 10^{-17}\, Y_B = 3.5 \times 10^{-27} \left(\frac{\Omega_B h^2}{0.0223}\right) \tag{A.51}$$

Taking into account the gravitational effect in deep sea, this corresponds to a concentration of the order of 10^{-28} at sea level or equivalently

$$Y_{X^+} \leq 0.9 \times 10^{-38} \left(\frac{\Omega_B h^2}{0.0223}\right) \ , \tag{A.52}$$

which is comparable to other limits in the same mass range, [36]. For larger masses up to a TeV, a slightly looser bound $Y_{X^+}/Y_B < 3 \times 10^{-20}$ was found by [37], while for even larger masses 10 TeV $\leq m_X \leq 6 \times 10^4$ TeV it weakens even further to $Y_{X^+}/Y_B < 7 \times 10^{-15}$, as given by [38], i.e.

$$Y_{X^+} \leq 6 \times 10^{-25} \left(\frac{\Omega_B h^2}{0.0223}\right) \ . \tag{A.53}$$

For electromagnetically neutral, but coloured relics, the bounds are obtained from considering heavier elements and are considerably weaker; using the results of [37] for Carbon, the limits are of the order $Y_{X^+}/Y_B \leq 4 - 8 \times 10^{-20}$ for $m_X = 0.1 - 1$ TeV, reaching 2×10^{-16} at the largest mass considered 10 TeV. For larger masses $m_X \leq$ 100 TeV only the constraint by [39] for lead is present, giving

$$Y_X \leq 1.5 \times 10^{-13}\, Y_B = 1.3 \times 10^{-25} \left(\frac{\Omega_B h^2}{0.0223}\right) \ . \tag{A.54}$$

We see that these constraints are very strong. In order to reach even the weakest bound of $Y_X \leq 10^{-25}$, the unitarity cross section is way too weak and needs to be increased at least by nine orders of magnitude, i.e.

$$\sum_J (2J+1) > 10^9 \ . \tag{A.55}$$

Therefore stable relics are allowed only if their interaction does not belong to the Standard Model and they cannot form exotic atoms/nuclei or if their annihilation rate becomes much larger than the unitarity one as it can happen if they interact strongly and can form intermediate bound states. But in any case, note that cross sections of the order π/Λ^2_{QCD} that can arise after the QCD phase transition are not sufficient to evade these constraints [31], so their interaction would have to be stronger than QCD.

A.5.2 Unstable relics

Different cosmological constraints exist on the density of an unstable relic, depending on its lifetime. For lifetimes between 0.1 s and 10^{10} s, the strongest constraints come from Big Bang Nucleosynthesis. In fact, if the relic decay injects very energetic particles into the thermal bath during BBN, it can change the abundances of the light elements. Since standard BBN agrees quite well with the primordial abundances of Helium-4, Deuterium and (within a factor of two) Lithium-7 inferred from present astronomical observations [9], the relic density has to be low enough not to change those predictions too strongly. These effects are present for any decaying particle and have been studied in various papers (see [10, 40, 41, 42] and references therein). For lifetimes above 3000 s, corresponding to the time of production of Lithium, additional constraints are present if the relic is electromagnetically charged and can form a bound state with positively charged nuclei increasing the rates for Lithium-6 production [11]. The Standard BBN prediction for the ^6Li abundance is actually way too small compared to the observed one, so that the presence of a charged relic with appropriate lifetime can help reconciling BBN with the measured abundances of ^6Li, ^7Li [43], but we will disregard this possibility and only concentrate on the exclusion region.

We summarise here the main results from various BBN analyses and give conservative bounds on the energy density of the decaying relic and compare them with our computation of the relic density. Since we are interested in escaping the BBN constraints, we focus mainly on the strongest bounds, but we keep conservative values for the light element abundances. Note that in many of the analysis slightly different ranges for these abundances are considered, corresponding to slightly different constraints on the decaying relic.

In general, the decay can produce very energetic SM particles that can initiate either hadronic or electromagnetic showers in the plasma. The most stringent bounds are obtained for a relic that produces mostly hadronic showers, since electromagnetic particles like photons or electrons can thermalise very quickly by interacting with the tail of the CMB distribution until times of about 10^6 s. So we will consider in the following the constraints for relics producing hadronic showers with a branching ratio $B_H = 1$. We will comment later on the case where this branching ratio is smaller. There are then practically three regions of the lifetimes as discussed in [40]:

- $10^{-1}\,\mathrm{s} \leq \tau \leq 10^{2}\,\mathrm{s}$: the dominant effect is the interconversion between protons and neutrons, that changes the Helium abundance, overproducing it;
- $10^{2}\,\mathrm{s} \leq \tau \leq 10^{7}\,\mathrm{s}$: hadrodissociation is the most efficient process and the bound come from the non-thermal production of Li and D;
- $10^{7}\,\mathrm{s} \leq \tau \leq 10^{12}\,\mathrm{s}$: photodissociation caused both by direct electromagnetic showers and by those generated by the daughter hadrons starts to dominate and the overproduction of ^{3}He is the main result.

It is clear that these limits depend on the decay branching ratio B_H into hadrons for lifetimes $\tau \leq 10^{7}$ s, while they are independent of B_H for longer lifetimes. In Table A.1, we give conservative bounds taken from the general analysis of [40] for the three regions, assuming $B_H = 1$. Similar constraints were obtained independently also by [41]. Note that the bound for short lifetimes becomes approximately one order of magnitude weaker if one takes a more recent value of the ^{4}He abundance as discussed in [42]. Unfortunately this new publication does not provide constraints for a general relic, but discusses only the explicit cases of a bino neutralino or a right-handed stau.

The limits we use can be parameterised as

$$Y_{X+\bar{X}} \leq 1.0 \times 10^{-13} \left(\frac{m_X}{1\mathrm{TeV}}\right)^{-0.3} \quad \text{for } \tau_X \sim 0.1 - 10^{2}\,\mathrm{s}\,, \tag{A.56}$$

$$Y_{X+\bar{X}} \leq 1.1 \times 10^{-16} \left(\frac{m_X}{1\mathrm{TeV}}\right)^{-0.57} \quad \text{for } \tau_X \sim 10^{2} - 10^{7}\,\mathrm{s}\,. \tag{A.57}$$

The assumption $B_H = 1$ is surely valid if the decaying relic is coloured, while B_H can be different if it is only electromagnetically charged, as in the case of the stau. If the branching ratio into hadronic modes for the relic is less than one, the hadronic BBN bounds are relaxed accordingly by a factor $1/B_H$. For intermediate lifetimes, then electromagnetic showers can become a more important effect, but only if $B_H < 0.01$.

For electromagnetically charged relics with lifetimes longer than about 3000 s and low $B_H < 0.1 - 0.01$, strong bounds also come from considering the catalysed over-production of ^{6}Li [11]. In fact when bound states between nuclei and the relic can form such as $^{4}HeX^{-}$, many nuclear rate are modified and change the final abundance especially of ^{6}Li and ^{7}Li. For particles decaying after 5×10^{5}s it has been argued that uncertainties in the nuclear rates make such constraints weaker than the general ones

Maximal values of $m_X Y_{X+\bar{X}}$ (GeV) allowed by BBN

m_X (TeV)	$10^{-1} - 10^{2}$ s	$10^{2} - 10^{7}$ s	$10^{7} - 10^{12}$ s
0.1	2×10^{-11}	5×10^{-14}	10^{-14}
1	1×10^{-10}	10^{-13}	10^{-14}
10	5×10^{-10}	3×10^{-13}	10^{-14}

Table A.1: Maximal allowed values of $m_X Y_{X+\bar{X}}$ in the different region of lifetimes taken from Figures 38–40 of [40]. We are assuming here that the energy released in Standard Model particles is one half of m_X as happens in a two body decay of the NLSP into LSP and the NLSP non-supersymmetric partner and that all the energy is released in hadrons. In general the strongest bound is for longer lifetimes and it is independent of m_X and the hadronic branching ratio. The bounds in the second column come from D, but the ^6Li ones, that are sometimes considered too strong [43], are not very far away.

discussed above [44], so we will consider here catalysed BBN constraints only for the intermediate lifetime range.

Unfortunately, different values for these bounds are given in the literature; in [45, 46] they are found to be maximally at the level of $Y_{X^-} < 1.4 - 2 \times 10^{-16}$, while the latest value in [44] is maximally $Y_{X^-} < 10^{-14}$, taking a larger window for the ratio $^6Li/^7Li$.

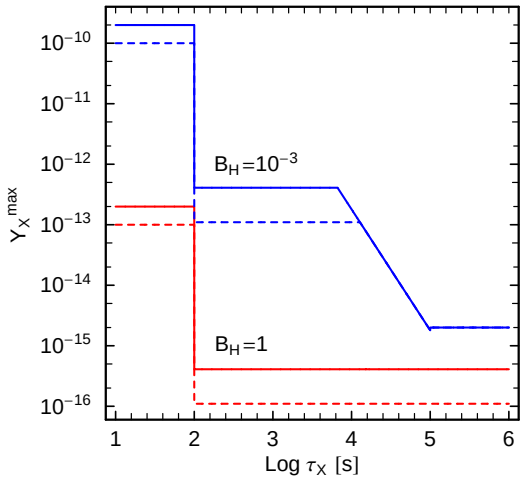

Figure A.7: Maximal total yield $Y^{\max}_{X+\bar{X}}$ allowed by BBN as a function of the relic's lifetime τ_X for the two cases $B_H = 1$ (red) and $B_H = 10^{-3}$ (blue). The full lines are for a mass of $m_X = 100$ GeV, while the dashed lines are for $m_X = 1$ TeV. Note that for $B_H = 10^{-3}$, the limit for $\tau_X \gtrsim 10^4\,$s comes from CBBN.

Here we will use as a constraint the simple interpolation for the total yield [9]

$$Y_{X+\bar{X}} \leq \begin{cases} 2\times 10^{-12}\left(\frac{\tau_X}{3\times 10^3 \mathrm{S}}\right)^{-2} & \text{for} \quad \tau_X \lesssim 10^5\mathrm{s} \\ 2\times 10^{-15} & \text{for} \quad \tau_X \geq 10^5\mathrm{s} \end{cases} \tag{A.58}$$

that lies somewhat in between. The bounds from catalysed BBN do not apply for coloured scalar relics because these should have a large branching ratio into hadrons, such that the 'conventional' BBN bounds from hadronic showers are much stronger. In passing note also that up-type squarks would mostly hadronise into neutral fermionic mesons which are lighter than the charged ones [30].

We summarise the constraints in Fig. A.7, which shows our conservative bounds in the plane of total number density vs lifetime. Note that the constraint from catalysed BBN are for the stau stronger than the hadronic ones for lifetimes longer than $\sim 10^4\,$s and exclude a light stau NLSP with a 100 GeV gravitino LSP in the CMSSM [12].

Comparing with Fig. A.6, we see that even for a charged relic that can annihilate efficiently, the BBN bounds are very strong; in particular the case of a simple abelian

[9] The catalysed BBN constraints restrict only the abundance of the negatively charged particles, but we give here the constraint for the total yield assuming $2Y_{X^-} = Y_{X+\bar{X}}$.

interaction seems to be excluded for any charged relic whose lifetime is longer than 0.1 s and produces hadronic showers with $B_H = 1$. For the coloured case the situation is less severe, but even with the Sommerfeld enhancement, which reduces the yield substantially, it is not possible to evade the bounds completely. Still all masses above approximately 50 GeV are excluded for lifetimes longer than 100 s, while for shorter lifetimes masses up to 700 GeV are allowed. A much larger number of colours than three would be needed to relax all bounds. Even the unitarity case reaches the strongest BBN constraint at masses around 700 GeV for 3 degrees of freedom or 1 TeV for a single one.

A.6 Application to the MSSM

Until now we have considered the ideal case that the relic particle has only one single interaction. In realistic models, however, more than one interaction – and hence more than one annihilation channel – is present, making the BBN bounds less stringent.

In this section, we discuss the concrete examples of a relic stau or stop in the MSSM. We use the MICROMEGAS package [47] to take into account all relevant annihilation and co-annihilation channels, but compare also with the results for Y_{ab} or Y_{nab} for the case of one single gauge interaction.

A.6.1 Relic stau

Our results for an electrically charged relic can be applied, for instance, to the case of the supersymmetric partner of the τ. We assume here that the relic stau is a right-chiral state, $\tilde{\tau}_R$, and that all other SUSY particles as well as the heavy Higgs bosons decouple.

The dependence of the yield on the stau mass is shown in Fig. A.8. For a 100 GeV $\tilde{\tau}_R$, we get $Y_{\tilde{\tau}} = 4.8 \times 10^{-13}$ at tree level from annihilation into photons (c.f. the dashed line). This is reduced by about 12% by the Sommerfeld enhancement (dashdotted line). In the full EW theory, the stau also annihilates into W^+W^-, ZZ and γZ. In fact, for $m_{\tilde{\tau}} = 100$ GeV, the $\gamma\gamma$ channel contributes about 55%, γZ about 25%, ZZ about 10% and WW about 5% to the total rate; the remaining 5% go into SM fermions. At higher stau masses, we have ∼50% $\gamma\gamma$ and ∼30% γZ. Overall this gives a reduction of

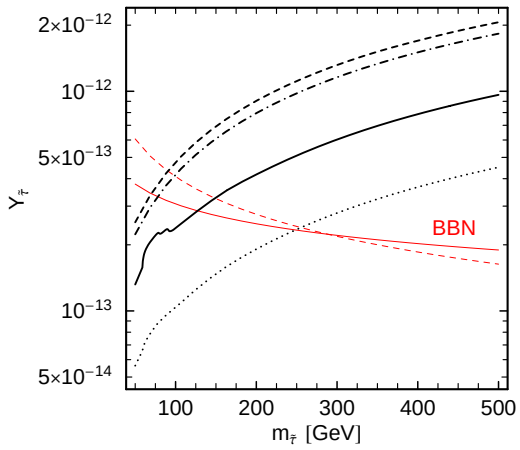

Figure A.8: Total yield Y (black lines) for a relic $\tilde{\tau}_R$ as function of the stau mass. The dashed and dashdotted curves are tree-level and Sommerfeld- corrected results, respectively, from annihilation into photons (i.e. Y_{ab}). The full line includes also annihilation into W and Z bosons, assuming all other sparticles decouple. Finally, the dotted line shows the case $m_{\tilde{B}} = 1.1 m_{\tilde{\tau}_1}$. BBN bounds are shown in red: as full line for 0.1–100 s lifetime and $B_H = 0.65$, and as dashed line for > 100 s lifetime and $B_H = 10^{-3}$. Note that if the lifetime exceeds about 10^4 s, the CBBN constraints become more important and quickly exclude number densities at the level of 10^{-13}–10^{-15}, see Fig. A.7.

Y by a factor of about 2 (solid line), leading to $Y_{\tilde{\tau}} = 2.4 \times 10^{-13}$ at $m_{\tilde{\tau}} = 100$ GeV.

Staus can also annihilate into $\tau\tau$ through t-channel neutralino exchange. We here consider only the bino contribution. Lowering the bino mass $m_{\tilde{B}}$ decreases the yield until bino-stau coannihilation takes over, increasing it again. We find a minimum yield at about $m_{\tilde{B}} \simeq (1.1 - 1.2) m_{\tilde{\tau}_1}$, shown as dotted line in Fig. A.8. It is roughly a factor 2 lower than the solid line, in agreement with [25]. Note also that the neutralino exchange leads to annihilation of same-sign stau pairs, $\tilde{\tau}_1^{\pm}\tilde{\tau}_1^{\pm} \to \tau^{\pm}\tau^{\pm}$, so this process gets Sommerfeld-*suppressed*, and the total Sommerfeld effect almost cancels.

The annihilation into W^+W^- and ZZ is considerably enhanced if the relic stau also has some $\tilde{\tau}_L$ component, $\tilde{\tau}_1 = \tilde{\tau}_R \sin\theta + \tilde{\tau}_L \cos\theta$ with $\cos\theta \neq 0$. In this case also t-channel exchange of $\tilde{\nu}_\tau$ (for W^+W^-) and $\tilde{\tau}_2$ (for ZZ) has to be taken into account in addition to the 4-vertex and s-channel γ/Z exchange, c.f. Appendix B. It turns out that these t-channel diagrams lead to a destructive interference: for given $\cos\theta$, smaller

$\tilde{\nu}_\tau$ and $\tilde{\tau}_2$ masses lead to smaller cross sections. Since the stau and sneutrino masses and stau mixing angle are related to each other, one cannot simply maximise the cross section by choosing maximal mixing ($\cos\theta = 0.7$) and very heavy $\tilde{\nu}_\tau$ and $\widetilde{\tau}_2$. However, for reasonable parameter choices, it is still possible to reduce the yield shown in Fig. A.8 by up to about an order of magnitude.Alternatively, one could rely on resonant annihilation through s-channel Higgs exchange or on coannihilation with sparticles that are close in mass to bring $Y_{\tilde{\tau}}$ below the BBN bounds.

Barring these possibilities of largely enhanced cross sections, the stau lifetime and branching ratio into hadronic modes become key parameters to decide whether the scenario is allowed. First of all, let us discuss briefly the branching ratio into hadrons. We are considering here the decay $\tilde{\tau}_R \to \tau$+LSP. The τ decays into charged mesons 65% of the time, while the remaining times into leptons only. Charged mesons have a similar effect as nucleons during BBN only at short times < 100 seconds, because later they decay before interacting with nucleons and give rise only to electromagnetic showers [40]. Therefore we will take $B_H(\tilde{\tau}) \sim 0.65$ for lifetimes up to 100 s, while it becomes much smaller for longer lifetimes, we will use $B_H(\tilde{\tau}) \sim 10^{-3}$ as reference value. This is in the central range computed recently for the stau decay into tau, gravitino and a $q\bar{q}$ pair, and we refer to that result for a more detailed analysis [48]. (A full computation including a more complete treatment of the hadronic decays of the tau for the case of a right-handed stau has been given in [42].) We have then to apply the BBN bounds discussed in the previous section corrected by these branching ratio factors, according to the time of decay.

Regarding the stau lifetime, this depends strongly on the nature of the LSP. For the case of the axino LSP, the decay rate is given by

$$\Gamma(\tilde{\tau}_R \to \tau\tilde{a}) = (25\text{ s})^{-1}\xi^2 \left(\frac{m_{\tilde{\tau}}}{10^2\text{ GeV}}\right)\left(\frac{m_{\tilde{B}}}{10^2\text{ GeV}}\right)^2 \left(\frac{10^{11}\text{ GeV}}{f_a}\right)^2 \left(1 - \frac{m_{\tilde{a}}^2}{m_{\tilde{\tau}}^2}\right) \quad \text{(A.59)}$$

where $m_{\tilde{a}}$ is the axino mass, $m_{\tilde{B}}$ is the Bino mass, f_a is the Peccei-Quinn scale, and ξ is a factor of order 1 taking into account some uncertainties in the loop computation [49]. Therefore only the weakest BBN bound applies and actually disappears completely for large stau mass: in fact even for the conservative case $m_{\tilde{B}} = 1.1\, m_{\tilde{\tau}}$ and $f_a = 10^{11}$ GeV, the lifetime becomes shorter than 0.1 s for $m_{\tilde{\tau}} \leq 590$ GeV. We are here

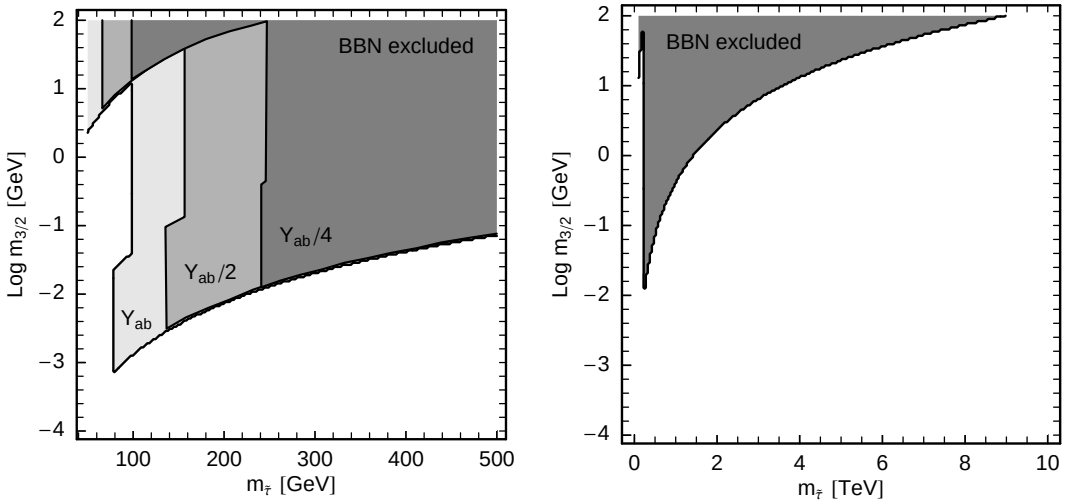

Figure A.9: BBN-excluded regions for a gravitino LSP in the plane $m_{3/2}$ vs. $m_{\tilde{\tau}}$. On the left a zoom on $m_{\tilde{\tau}} = 50$–500 GeV for $Y_{\tilde{\tau}} = Y_{ab}$ (light grey), $Y_{\tilde{\tau}} = Y_{ab}/2$ (medium grey) and $Y_{\tilde{\tau}} = Y_{ab}/4$ (dark grey). On the right for $m_{\tilde{\tau}} = 0.1$–10 TeV. Note that LEP excluded $m_{\tilde{\tau}} \leq 99.4$ GeV for a charged particle stable within the detector [50].

neglecting the case of a strong degeneracy between the stau and axino masses. We see therefore that for axino LSP a very light stau is a viable possibility and, depending on the supersymmetric spectrum, only the mass window between $125/250 - 590$ GeV is possibly excluded by the BBN constraints, as can be seen from Fig. A.8. In that region however probably a more proper computation of the stau hadronic branching ratio and its effect in the early stages of BBN is needed, as discussed in [42]. In fact comparing our exclusion region with theirs, we find that their constraints are much weaker for short lifetimes, due to an up-dated value of the Helium abundance and a larger systematic error, allowing all the stau region for an axino LSP.

For a gravitino LSP, the decay rate is given by [49]

$$\Gamma(\tilde{\tau}_R \to \tau \tilde{G}) = (5.9 \times 10^8 \text{ s})^{-1} \left(\frac{m_{\tilde{\tau}}}{100 \text{ GeV}}\right)^5 \left(\frac{100 \text{ GeV}}{m_{3/2}}\right)^2 \left(1 - \frac{m_{3/2}^2}{m_{\tilde{\tau}}^2}\right)^4 , \qquad \text{(A.60)}$$

which typically gives longer stau lifetimes than the axino case. Figure A.9 shows the BBN-excluded region in the $m_{3/2}$ vs $m_{\tilde{\tau}}$ plane. We consider a number density $Y_{\tilde{\tau}}$ equal to $1/2$ and $1/4$ times Y_{ab} to account for the possible variation depending on $m_{\tilde{B}}$. As can be seen, to avoid all bounds we need either a very light gravitino in the MeV range for

$m_{\tilde{\tau}} \sim \mathcal{O}(100)$ GeV, or a very heavy stau, e.g. $m_{\tilde{\tau}} \gtrsim 1.4$ TeV (9 TeV) for $m_{3/2} = 1$ GeV (100 GeV), corresponding to a stau lifetime shorter than 0.1 s. On the other hand, for $m_{\tilde{\tau}} \sim 100$–$250$ GeV and a lifetime longer than 100 s, $B_H \sim 10^{-3}$ can bring the effective yield below the bound of $mY \approx 5 \times 10^{-14}$ required by hadronic showers. Last but not least, note that the constraint from catalysed BBN becomes stronger than the hadronic ones for lifetimes longer than about 10^4 s and excludes a light stau NLSP for gravitino masses above 10-100 GeV.

A.6.2 Relic stop

To discuss the case of a relic stop, we assume that only $\tilde{t}_R$ is light while all other SUSY particles are heavy and decouple. Moreover, we assume that the light Higgs is SM-like with a mass of $m_h = 115$ GeV, and that the other Higgs bosons are also heavy and do not contribute to the stop annihilation.

Results for the yield as a function of the stop mass are shown in Fig. A.10. Let us first discuss the left plot, Fig. A.10(a), which shows the yield at leading order (LO). Here the full line is the pure QCD result, Y_{nab} for $SU(3)$, without Sommerfeld correction. As can be seen, $\tilde{t}\tilde{t}^* \to gg$ alone is efficient enough to avoid the BBN constraints up to stop masses of about 700 GeV. In the full theory, the stop can also annihilate into other particles, in particular into EW gauge and Higgs bosons. The yield for the QCD+EW case, still assuming heavy sparticles, is shown as the dashed line in Fig. A.10(a). The dip at $m_{\tilde{t}} \sim 120$ GeV is due to the onset of $\tilde{t}_R\tilde{t}_R^* \to hh$. Other important channels are annihilation into W^+W^- and γg, contributing about 10% each to the total annihilation cross section for $m_{\tilde{t}} \gtrsim 200$ GeV. Annihilation into ZZ contributes about 5%. Annihilation into top quarks is suppressed by the heavy gluino mass, and also by m_t. However, if $m_{\tilde{t}} > 200$ GeV and $m_{\tilde{g}} \sim 2m_{\tilde{t}}$, $\tilde{t}_R\tilde{t}_R \to tt$ further reduces the yield by 10–20%. This is shown as the dash-dotted line in Fig. A.10(a). All in all, annihilation into gluons is, however, always the dominant channel, contributing at least 50%. We therefore take $Y_{nab}/2$ as a rough limit, which is shown as the dotted line in Fig. A.10(a). Comparing with the BBN constraints we see that a relic $\tilde{t}_R$ with a lifetime of 0.1–100 s can be in agreement with BBN even for high masses of about 1 TeV.

The impact of the Sommerfeld enhancement is illustrated in Fig. A.10(b) for the

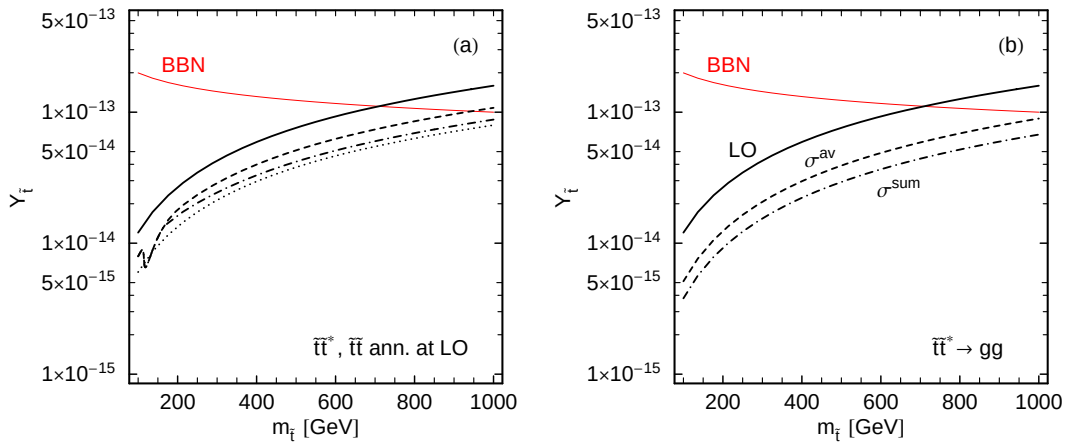

Figure A.10: Results for $Y_{\tilde{t}}$ for a relic $\tilde{t}_R$ as a function of the stop mass. In (a), tree-level results for different channels: the solid line comes from $\tilde{t}\tilde{t}^* \to gg$ only, the dashed line includes all channels into QCD+EW gauge and h bosons (case of decoupled sparticles and heavy Higgses), the dash-dotted line is the result for $m_{\tilde{g}} = 2m_{\tilde{t}_R}$, and the dotted line the limit $Y_{\tilde{t}} = Y_{nab}/2$. In (b), the effect of the Sommerfeld enhancement on the yield from $\tilde{t}\tilde{t}^* \to gg$: the full line shows the tree level result, the dashed line the result for σ^{SFav}, i.e. applying an averaged Sommerfeld factor $C^{\mathrm{av}}_{SU(3)} = 11/42$, and the dash-dotted line is for $\sigma^{\mathrm{SF}sum}$, i.e. applying a summed factor according to eq. (A.34). The BBN bound for 0.1–100 s lifetime is shown as thin red line in both plots.

case $\tilde{t}\tilde{t}^* \to gg$. As can be seen, taking the averaged Sommerfeld factor of $C^{av}_{SU(3)} = 11/42$ in eq. (A.29) reduces the LO yield by roughly a factor of 2, while a summed factor according to eq. (A.34) reduces the LO yield by roughly a factor of 3. These results are in qualitative agreement with those of [20], that considered the Sommerfeld correction in the neutralino-stop coannihilation region. Here note that for colour-singlet channels like, for instance, $\tilde{t}\tilde{t}^* \to W^+W^-$ a factor of $C = 4/3$ applies, hence leading to even larger enhancement. We leave a detailed numerical analysis of the enhancement of the various stop annihilation channels for future work. Here we just note that the overall effect can be a reduction of the yield by an order of magnitude.

Additional annihilation can take place after the QCD phase transition, when the stops are in a confined phase with the quarks. Since the lighter fermionic mesons are neutral and assuming that the annihilation process takes place without the formation

of a bound state between the mesinos, the unitarity cross section is probably a good estimate of such annihilation and allows for heavier stops to be consistent with hadronic shower constraints. We see in fact from Fig. A.6 that the unitary cross section with three degrees of freedom gives a yield well below all the BBN bounds (and below the range in Fig. A.10) for stop masses up to 700 GeV. If also bound states between the mesinos can form efficiently, the BBN constraints disappear altogether [31], but note that we do not have to rely on the enhancement coming from such processes, which are very difficult to compute, for a wide range of parameter space.

Let us briefly discuss the lifetime also for the stop case. For the case of an axino LSP, the stop decay rate is a larger than for the stau since it depends on the gluino mass and the QCD gauge coupling [3]:

$$\Gamma(\tilde{t}_R \to t\tilde{a}) = (1.3 \times 10^{-3}\,\mathrm{sec})^{-1} \xi_t^2 \left(\frac{m_{\tilde{t}}}{10^2\,\mathrm{GeV}}\right) \left(\frac{m_{\tilde{g}}}{10^2\,\mathrm{GeV}}\right)^2 \left(\frac{10^{11}\,\mathrm{GeV}}{f_a}\right)^2 \left(1 - \frac{m_{\tilde{a}}^2}{m_{\tilde{t}}^2}\right) \tag{A.61}$$

where ξ_t is again a factor of order one taking into account the uncertainties in the loop computation [49], in principle different than the one for the stau. Therefore, for the axino case, the BBN bound never applies if the decay into top is kinematically allowed, i.e. if $m_{\tilde{t}}^2 \geq (m_{\tilde{a}} + m_t)^2$. If the stop mass is smaller, the decay can proceed through a virtual top, for which we estimate a suppression of order $\mathcal{O}(1/100)$ due to the 3-body phase space. This would still give a lifetime of order 0.1 sec, so the BBN constraints are completely avoided, as long as there is not a strong degeneracy in mass between LSP and NLSP or the factor ξ_t is exceptionally large.

For a gravitino LSP, on the other hand, the same formula applies for stop as for stau, eq. (A.60) with $\tilde{\tau} \to \tilde{t}$, because the gravitino couples only to mass. Note, however, that also in this decay the width gets phase-space suppressed if $m_{\tilde{t}} < m_t + m_{\tilde{G}}$. For illustration, we show in Fig. A.11 the band of 0.1–100 s lifetime in the plane $m_{3/2}$ vs $m_{\tilde{t}}$. For lifetimes longer than 100 s, stops can still be in accord with BBN thanks to the additional annihilation during the QCD phase transition, if their annihilation reaches the unitarity one. We therefore conclude that cosmologically stops are an allowed NLSP in any mass range and in particular also for a heavy gravitino. Our results are in agreement with those for specific supersymmetric models with stop NLSP discussed in [51]. From the colliders side, note that the low mass region $m_{\tilde{t}} < 250$ GeV has been recently excluded by the search for charged massive particles at the Tevatron [52].

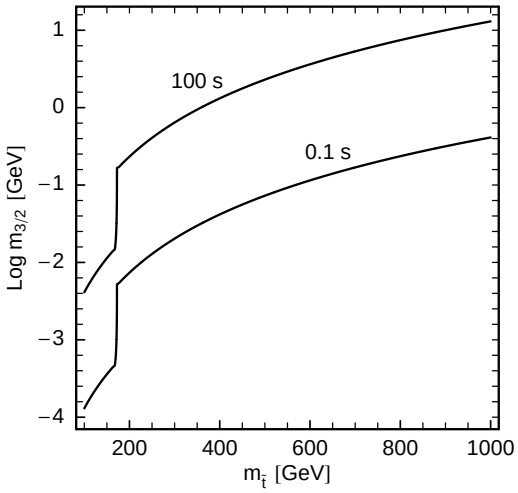

Figure A.11: Lifetime of a relic $\tilde{t}_R$ in the plane $m_{3/2}$ vs $m_{\tilde{t}}$. Recent results from the Tevatron exclude a metastable stop below 250 GeV [52].

A.7 Conclusions

We have studied the number density of a charged relic by computing the annihilation cross section into gauge bosons, including the Sommerfeld enhancement. We have found that the Sommerfeld factor increases the thermally averaged annihilation cross section by 20-50% and reduces the final yield even by a factor 2 or 3 for the $SU(3)$ case. Moreover the result is very sensitive on how the higher orders are resummed. Nevertheless the number density surviving the annihilation is still large and BBN constraints are relevant for most relics. They can be avoided completely only for very large N for particles in the fundamental representation of $SU(N)$ ($N > 100$ for $m_X \leq 10$ TeV) or for cross sections nearly fulfilling the unitarity bound. For the cases of SM gauge groups, the allowed regions only correspond to very light relic masses, where the number density is low enough, or to sufficiently heavy relic masses so that the decay takes place in the first stages of BBN. The latter allowed region depends strongly on the relic decay channel, and, in case of a gravitino LSP with conserved R-parity, also on the gravitino mass. Let us mention here that if R-parity is just marginally broken, the NLSP can decay with shorter lifetime through R-parity violating channels and the BBN constraints can be easily evaded for any NLSP while keeping the gravitino LSP as Dark Matter [53].

More specifically, for the stau NLSP the light mass window has nearly completely been excluded by direct searches at LEP, even if the annihilation cross-section is maximal $\sim 4\sigma(\tilde{\tau}\tilde{\tau}^* \to \gamma\gamma)$, unless the gravitino is lighter than a few tens of GeV, while the large mass region is unfortunately out of reach at the LHC for gravitino masses $m_{3/2} > 100$GeV. The detection of a quasi-stable stau at the LHC would then point to a scenario with relatively light gravitino mass, R-parity breaking or an axino LSP and could probably exclude the gravity mediated supersymmetry breaking scenario. In that case the determination of the stau lifetime and its decays will become crucial in distinguishing the different LSPs [7, 49].

The stop case is much less constrained thanks to the stronger annihilation cross-section, even if in this case the decay always produces mainly hadrons. We have practically no constraints if the LSP is an axino and even for a gravitino LSP, we can allow for relatively light stops up to approximately 700 GeV (1 TeV for lifetimes below 10^7 s), if the annihilation cross section reaches the unitarity one after the QCD phase transition. The window between the present Tevatron bound around 250 GeV and 1 TeV should be surely completely covered by the LHC, the signature being a quasi-stable heavy fermionic meson. The detection of such a state would call for a non-minimal SUSY breaking sector with a coloured NLSP and a very weakly interacting LSP. In this case again only the analysis of the stop decays would allow to distinguish between the lightest states.

Acknowledgements

We thank Nans Baro, Fawzi Boudjema, Lance Dixon, Koichi Hamaguchi, Wolfgang Kilian, Tom Rizzo, Masato Senami and Iain Stewart for useful discussions and communications. We thank specially Alexander Pukhov for valuable help with implementing the Sommerfeld enhancement in Micromegas.

CFB's work is supported in part by funds provided by the U.S. Department of Energy (D.O.E.) under cooperative research agreement DE-FC02-94ER40818 and by the National Science Foundation under Grant No. PHY05-51164.

LC would like to thank the Institute of Theoretical Physics of the Warsaw University for their hospitality during part of this work; the visit was supported by a Maria

Curie Transfer of Knowledge Fellowship of the European Community's Sixth Framework Programme under contract number MTKD-CT-2005-029466 (2006-2010). LC also acknowledges the support of the "Impuls- und Vernetzungsfond" of the Helmholtz Association under the contract number VH-NG-006 and of the European Network of Theoretical Astroparticle Physics ILIAS/N6 under contract number RII3-CT-2004-506222.

This work is also part of the French ANR project ToolsDMColl, BLAN07-2-194882.

.1 Annihilation into massless $SU(N)$ gauge bosons

.1.1 Amplitudes for the annihilation

We consider the case of one particle and antiparticle in the representation T_i^a and its conjugate, with momenta p_1, p_2 and mass m annihilating into two massless gauge bosons with group indices a, b, momenta p_3, p_4 and Lorentz indices μ, ν respectively.

The process has four different contributions, corresponding to the following four Feynman diagrams:

t particle exchange in the t-channel described by the amplitude

$$\mathcal{A}_t^{\mu\nu} = ig_N^2 \left(T^b T^a\right)_{ji} \frac{(2p_1 - p_3)^\mu (2p_2 - p_4)^\nu}{t - m^2}\,; \tag{62}$$

u particle exchange in the u-channel described by the amplitude

$$\mathcal{A}_u^{\mu\nu} = ig_N^2 \left(T^a T^b\right)_{ji} \frac{(2p_1 - p_4)^\nu (2p_2 - p_3)^\mu}{u - m^2}\,; \tag{63}$$

note that this contribution is identical to the t-channel under interchange of $a \leftrightarrow b$, $\mu \leftrightarrow \nu$, $(p_3, t) \leftrightarrow (p_4, u)$;

4 supersymmetric four-scalar coupling giving the amplitude:

$$\mathcal{A}_4^{\mu\nu} = ig_N^2 \left\{T^a, T^b\right\}_{ji} g^{\mu\nu}\,; \tag{64}$$

this contribution is symmetric in the exchange of a, b and therefore also μ, ν;

s off-shell gauge boson in the s-channel decaying into two bosons via the non-abelian interaction:

$$\begin{aligned}\mathcal{A}_s^{\mu\nu} &= -ig_N^2 \left[T^a, T^b\right]_{ji} \frac{1}{s} \left[g^{\mu\nu}(t-u) - (2p_4+p_3)^\mu (p_1-p_2)^\nu \right. \\ &\quad \left. +(p_1-p_2)^\mu (2p_3+p_4)^\nu\right]; \end{aligned} \tag{65}$$

this contribution is completely antisymmetric under the exchange of the gauge bosons group indices and therefore also under the exchange of their momenta and Lorentz indices.

For convenience, we can then separate the amplitude into symmetric and antisymmetric part in colours a, b; then the interference between the two parts vanishes. Using

$$T^a T^b = \frac{1}{2}\left\{T^a, T^b\right\} + \frac{1}{2}\left[T^a, T^b\right] \tag{66}$$

we have then

$$\mathcal{A}_{sym}^{\mu\nu} = \frac{ig_N^2}{2}\left\{T^a, T^b\right\}_{ji} \left[\frac{(2p_1-p_3)^\mu (2p_2-p_4)^\nu}{t-m^2} + \frac{(2p_1-p_4)^\nu (2p_2-p_3)^\mu}{u-m^2} + 2g^{\mu\nu}\right] \tag{67}$$

and

$$\begin{aligned}\mathcal{A}_{asym}^{\mu\nu} &= \frac{ig_N^2}{2}\left[T^a, T^b\right]_{ji} \left[-\frac{(2p_1-p_3)^\mu (2p_2-p_4)^\nu}{t-m^2} + \frac{(2p_1-p_4)^\nu (2p_2-p_3)^\mu}{u-m^2} \right. \\ &\quad \left. -2\frac{g^{\mu\nu}(t-u) - (2p_4+p_3)^\mu (p_1-p_2)^\nu + (p_1-p_2)^\mu (2p_3+p_4)^\nu}{s}\right]. \end{aligned} \tag{68}$$

In the Boltzmann equation, we have to insert the averaged cross-section, so first we have to sum over all the final and initial states, i.e. sum over the gauge bosons polarisations and over all the group indices.

.1.2 The matrix element

The computation for the symmetric piece is straightforward:

$$\begin{aligned}|\mathcal{A}_{sym}|^2 &= g_N^4 |\left\{T^a, T^b\right\}_{ji}|^2 \left[\frac{(t+m^2)^2}{(t-m^2)^2} + \frac{(u+m^2)^2}{(u-m^2)^2} + \frac{1}{2}\frac{(s-4m^2)^2}{(t-m^2)(u-m^2)} \right. \\ &\quad \left. +4 + \frac{s/2-4m^2-2(t-m^2)}{t-m^2} + \frac{s/2-4m^2-2(u-m^2)}{u-m^2}\right] \qquad (69) \\ &= 4g_N^4 |\left\{T^a, T^b\right\}_{ji}|^2 \left[\frac{1}{2} + \frac{2m^4}{(t-m^2)^2} + \frac{2m^2}{t-m^2}\left(1-\frac{2m^2}{s}\right)\right]. \qquad (70) \end{aligned}$$

In the antisymmetric part instead we have to take into account ghost subtraction and the total result is

$$\begin{aligned}|\mathcal{A}_{asym}|^2 &= g_N^4 |\left[T^a,T^b\right]_{ji}|^2 \left[\frac{(t+m^2)^2}{(t-m^2)^2}+\frac{(u+m^2)^2}{(u-m^2)^2}-4\right.\\ &\quad -\frac{1}{2}\frac{(s-4m^2)^2}{(t-m^2)(u-m^2)}+2\frac{(t-u)^2}{s^2}+\frac{16m^2}{s}\\ &\quad +\frac{(t-u)(3/2s-t-3m^2)+2(s-4m^2)(u-m^2)}{s(t-m^2)}\\ &\quad \left.+\frac{(u-t)(3/2s-u-3m^2)+2(s-4m^2)(t-m^2)}{s(u-m^2)}\right] \qquad (71)\\ &= 4g_N^4 |\left[T^a,T^b\right]_{ji}|^2 \left[\frac{(t-u)^2}{2s^2}+\frac{4m^2}{s}+\frac{2m^4}{(t-m^2)^2}\right.\\ &\quad \left.+\frac{2m^2}{t-m^2}\left(1+\frac{2m^2}{s}\right)\right]. \qquad (72)\end{aligned}$$

So for the total matrix element we have

$$\begin{aligned}|\mathcal{M}|^2 &= 4g_N^4 \left\{ |\left\{T^a,T^b\right\}_{ji}|^2 \left[\frac{1}{2}+\frac{2m_X^4}{(t-m_X^2)^2}+\frac{2m_X^2}{t-m_X^2}\left(1-\frac{2m_X^2}{s}\right)\right]\right.\\ &\quad +|\left[T^a,T^b\right]_{ji}|^2 \left[\frac{1}{2}\frac{(s+2(t-m_X^2))^2}{s^2}+\frac{4m_X^2}{s}+\frac{2m_X^4}{(t-m_X^2)^2}\right.\\ &\quad \left.\left.+\frac{2m_X^2}{t-m_X^2}\left(1+\frac{2m_X^2}{s}\right)\right]\right\}. \qquad (73)\end{aligned}$$

and the cross section is given in eq. (A.16).

.1.3 Comparison with QCD result

For the case of $SU(3)$ we have

$$\sum_{a,b,i,j}\left|\left\{T^a,T^b\right\}_{ji}\right|^2 = \frac{28}{3} \qquad (74)$$

and

$$\sum_{a,b,i,j}\left|\left[T^a,T^b\right]_{ji}\right|^2 = \frac{1}{2}\sum_{a,b,c} f_{abc}^2 = 12\,. \qquad (75)$$

So after the sum over colours, we get

$$\begin{aligned}|\mathcal{M}|^2 &= 4g_3^4\left[\frac{14}{3}+6\frac{(t-u)^2}{s^2}+\frac{48m^2}{s}+\frac{2m^4}{(t-m^2)^2}\left(\frac{28}{3}+12\right)\right.\\ &\left.+\frac{2m^2}{t-m^2}\left(\frac{28}{3}+12+\frac{2m^2}{s}\left(-\frac{28}{3}+12\right)\right)\right] \qquad (76)\\ &= 4g_3^4\left[\frac{32}{3}+24\frac{t-m^2}{s}+24\frac{(t-m^2)^2}{s^2}+\frac{48m^2}{s}\right.\\ &\left.+\frac{128}{3}\frac{m^4}{(t-m^2)^2}+\frac{128}{3}\frac{m^2}{t-m^2}\left(1+\frac{1}{4}\frac{m^2}{s}\right)\right]\ . \qquad (77)\end{aligned}$$

This result coincides with the one given in the literature for the QCD case [26]. Compare in general with [26]:

$$\begin{aligned}|\mathcal{M}(gg\to\tilde{q}\bar{\tilde{q}})|^2 &= 4n_f g_3^4\left[C_0\left(1-2\frac{(t-m^2)(u-m^2)}{s^2}\right)-C_K\right]\times \qquad (78)\\ &\times\left[1-2\frac{sm^2}{(t-m^2)(u-m^2)}\left(1-\frac{sm^2}{(t-m^2)(u-m^2)}\right)\right]\\ &= 4n_f g_3^4\left[C_0-C_K+2C_0\frac{t-m^2}{s}+2C_0\frac{(t-m^2)^2}{s^2}\right.\\ &+4C_0\frac{m^2}{s}+4(C_0-C_K)\frac{m^4}{(t-m^2)^2}\\ &\left.+4\frac{m^2}{t-m^2}\left(C_0-C_K+2C_K\frac{m^2}{s}\right)\right] \qquad (79)\end{aligned}$$

using again the symmetry in $u\leftrightarrow t$ and eliminating u.

We have also that

$$C_0=\sum_{a,b,c}f_{abc}^2=N(N^2-1)=24 \qquad C_K=\frac{N^2-1}{N}=\frac{8}{3} \qquad (80)$$

and for a single RH stop, we must use $2n_f=1$. Then we get

$$\begin{aligned}|\mathcal{M}(gg\to\tilde{t}_R\bar{\tilde{t}}_R)|^2 &= 4g_3^4\left[\frac{32}{3}+24\frac{t-m^2}{s}+24\frac{(t-m^2)^2}{s^2}+48\frac{m^2}{s}\right.\\ &\left.+\frac{128}{3}\frac{m^4}{(t-m^2)^2}+\frac{128}{3}\frac{m^2}{t-m^2}\left(1+\frac{1}{4}\frac{m^2}{s}\right)\right]\ , \qquad (81)\end{aligned}$$

which coincide with our result above eq. (77).

Now integrate over t and obtain

$$\begin{aligned}\sigma(m,s) &= 32\,\frac{4\pi\alpha_3^2}{s-4m^2}\left[\sqrt{1-\frac{4m^2}{s}}\left(\frac{5}{24}+\frac{31}{12}\frac{m^2}{s}\right)\right.\\ &\left.+\frac{4}{3}\frac{m^2}{s}\left(1+\frac{1}{4}\frac{m^2}{s}\right)\log\left(\frac{1-\sqrt{1-\frac{4m^2}{s}}}{1+\sqrt{1-\frac{4m^2}{s}}}\right)\right]\,, \end{aligned} \tag{82}$$

which coincides with [26] allowing for the exchange of initial and final state ($s-4m^2 \to s$ in the denominator) and the initial state averaging, i.e. a factor of 1/64 for the two gluons initial state.

.2 Annihilation into $SU(2)_L$ gauge bosons

Another important channel of annihilation for light stops or staus is into EW gauge bosons. Let us consider first the pure $SU(2)_L$ case, neglecting the gauge boson masses, but with a split $SU(2)$ multiplet. We consider here the case of one left-handed sparticle and one left-handed antisparticle of momenta p_1, p_2, mass m_1 and $SU(2)$ index 1, annihilating into 2 gauge bosons of $SU(2)_L$ index i, j, momenta p_3, p_4 and Lorentz indices μ, ν respectively. Then we can directly use the result for $SU(N)$, only taking into account that $T^a \to \sigma^i/2$, with σ^i denoting the Pauli matrices, and that in this case we have an initial state made of the upper components of the $SU(2)_L$ doublet, while the lower component is exchanged in the t- and u-channel and can have a different mass m_2.

We have then for the two amplitudes, symmetric and antisymmetric in the group and Lorentz indices,

$$\mathcal{A}^{\mu\nu}_{sym} = i\frac{g_2^2}{8}\left\{\sigma^i,\sigma^j\right\}_{11}\left[\frac{(2p_1-p_3)^\mu(2p_2-p_4)^\nu}{t-m_2^2}+\frac{(2p_1-p_4)^\nu(2p_2-p_3)^\mu}{u-m_2^2}+2g^{\mu\nu}\right] \tag{83}$$

and

$$\begin{aligned}\mathcal{A}^{\mu\nu}_{asym} &= i\frac{g_2^2}{8}[\sigma^i,\sigma^j]_{11}\left[-\frac{(2p_1-p_3)^\mu(2p_2-p_4)^\nu}{t-m_2^2}+\frac{(2p_1-p_4)^\nu(2p_2-p_3)^\mu}{u-m_2^2}\right.\\ &\left.-2\frac{g^{\mu\nu}(t-u)-(2p_4+p_3)^\mu(p_1-p_2)^\nu+(p_1-p_2)^\mu(2p_3+p_4)^\nu}{s}\right]. \end{aligned} \tag{84}$$

To compute the annihilation cross section, we have to sum over all the final states and initial states; this means that we have to sum over the W polarisations and over the $SU(2)_L$ indices i, j, but in this case the initial state group indices are fixed.

The symmetric piece gives

$$\begin{aligned}
|\mathcal{A}_{sym}|^2 &= \frac{g_2^4}{16}|\left\{\sigma^i,\sigma^j\right\}_{11}|^2\left[\frac{(t+m_1^2)^2}{(t-m_2^2)^2}+\frac{(u+m_1^2)^2}{(u-m_2^2)^2}+\frac{1}{2}\frac{(s-4m_1^2)^2}{(t-m_2^2)(u-m_2^2)}\right.\\
&\left.+4+\frac{s/2-4m_1^2-2(t-m_1^2)}{t-m_2^2}+\frac{s/2-4m_1^2-2(u-m_1^2)}{u-m_2^2}\right] \qquad (85)\\
&= \frac{g_2^4}{4}|\left\{\sigma^i,\sigma^j\right\}_{11}|^2\left[\frac{1}{2}+\frac{1}{2}\frac{(m_1^2+m_2^2)^2}{(t-m_2^2)^2}\right. \qquad (86)\\
&\left.+\frac{1}{t-m_2^2}\left(\frac{3m_2^2+m_1^2}{2}-\frac{(m_1^2+m_2^2)^2}{s+2m_2^2-2m_1^2}\right)\right].
\end{aligned}$$

In the antisymmetric part instead gives

$$\begin{aligned}
|\mathcal{A}_{asym}|^2 &= \frac{g_2^4}{16}|[\sigma^i,\sigma^j]_{11}|^2\left[\frac{(t+m_1^2)^2}{(t-m_2^2)^2}+\frac{(u+m_1^2)^2}{(u-m_2^2)^2}-4\right. \qquad (87)\\
&-\frac{1}{2}\frac{(s-4m_1^2)^2}{(t-m_2^2)(u-m_2^2)}+2\frac{(t-u)^2}{s^2}+\frac{16m_1^2}{s}\\
&+\frac{(t-u)(3/2s-t-3m_1^2)+2(s-4m_1^2)(u-m_1^2)}{s(t-m_2^2)}\\
&\left.+\frac{(u-t)(3/2s-u-3m_1^2)+2(s-4m_1^2)(t-m_1^2)}{s(u-m_2^2)}\right]\\
&= \frac{g_2^4}{4}|[\sigma^i,\sigma^j]_{11}|^2\left[\frac{(t-u)^2}{2s^2}+\frac{5m_1^2-m_2^2}{s}+\frac{1}{2}\frac{(m_1^2+m_2^2)^2}{(t-m_2^2)^2}\right. \qquad (88)\\
&\left.+\frac{1}{t-m_2^2}\left(\frac{m_2^2+3m_1^2}{2}+\frac{(m_2^2+m_1^2)^2}{s+2m_2^2-2m_1^2}-\frac{(m_2^2-m_1^2)^2}{s}\right)\right].
\end{aligned}$$

.2.1 $SU(2)_L$ sum and total matrix element

In this case the sum over the indices i, j is simple. We have that

$$\sum_{i,j}\frac{1}{4}|\left\{\sigma^i,\sigma^j\right\}_{11}|^2 = \sum_{i,j}\frac{1}{4}|2\delta_i^j I_{11}|^2 = \sum_i \delta_i^i = 2+1 \qquad (89)$$

where we have considered the annihilation into $W^{1,2}$ separately from that into W_3. In fact the intermediate particle has a different mass in the two cases.

On the other hand the antisymmetric product gives

$$\sum_{i,j}\frac{1}{4}|[\sigma^i,\sigma^j]_{11}|^2 = \sum_{i,j}\frac{1}{4}|2\epsilon_{ijk}\sigma^k_{11}|^2 = \sum_{i,j}|\epsilon_{ij3}|^2 = 2 \qquad (90)$$

since in this case only W^3 can be exchanged in the s-channel for $W^{1,2}$ in the final state.

Then the matrix element for annihilation into $W^{1,2}$ gauge bosons is given by

$$|\mathcal{M}_{W12}|^2 = g_2^4\left[1+\frac{(t-u)^2}{s^2}+\frac{10m_1^2-2m_2^2}{s}+2\frac{(m_1^2+m_2^2)^2}{(t-m_2^2)^2} +\frac{4}{t-m_2^2}\left(m_2^2+m_1^2-\frac{(m_2^2-m_1^2)^2}{2s}\right)\right], \tag{91}$$

while the annihilation into W^3 has only the abelian contribution with the presence of a single mass m_1

$$|\mathcal{M}_{W3}|^2 = g_2^4\left[\frac{1}{2}+\frac{2m_1^4}{(t-m_1^2)^2}+\frac{2m_1^2}{t-m_1^2}\left(1-\frac{2m_1^2}{s}\right)\right].$$

The cross section for the first case is then

$$\begin{aligned}\sigma_{W12} = \frac{2\pi\alpha_2^2}{s-4m_1^2}\Bigg[&\sqrt{1-\frac{4m_1^2}{s}}\left(\frac{2}{3}+\frac{13}{3}\frac{m_1^2}{s}-\frac{m_2^2}{s}+\frac{(m_1^2+m_2^2)^2}{sm_2^2+(m_2^2-m_1^2)^2}\right)\\ &+2\left(\frac{m_2^2+m_1^2}{s}-\frac{(m_2^2-m_1^2)^2}{2s^2}\right)\times\\ &\times\log\left(\frac{s+2(m_2^2-m_1^2)-\sqrt{s(s-4m_1^2)}}{s+2(m_2^2-m_1^2)+\sqrt{s(s-4m_1^2)}}\right)\Bigg],\end{aligned} \tag{92}$$

while the annihilation into W^3 is identical to the abelian one in eq. (A.9) for $e_X = 1/2$.

.2.2 Annihilation into physical W^+W^-

Let us now consider the case of a broken $SU(2)_L$ symmetry like the Standard Model and massive gauge bosons which mix to give the physical W^+, W^-, Z, γ. At the same time let us consider a general initial state given by the light stau mass eigenstate $\tilde{\tau}_1 = \tilde{\tau}_L\cos\theta_{\tilde{\tau}} + \tilde{\tau}_R\sin\theta_{\tilde{\tau}}$ and its antiparticle. In this case the intermediate particle exchanged in the t- and u-channel can be only a left-handed sneutrino and therefore we can neglect the mixing for the intermediate state.

Then the annihilation into W^+W^- is given by the following channels:

t sneutrino exchange in the t-channel described by the amplitude

$$\mathcal{A}_t^{\mu\nu} = i\frac{g_2^2}{2}\cos^2\theta_{\tilde{\tau}}\frac{(2p_1-p_3)^\mu(2p_2-p_4)^\nu}{t-m_{\tilde{\nu}}^2}; \tag{93}$$

u NO u-channel since W^+ and W^- are different particles !

4 supersymmetric four-scalar coupling giving the amplitude:

$$\mathcal{A}_4^{\mu\nu} = i\frac{g_2^2}{2}\cos^2\theta_{\tilde{\tau}} g^{\mu\nu}\,; \tag{94}$$

this contribution is symmetric in the exchange of μ, ν;

s off-shell Z/γ in the s-channel decaying into two WW via the non-abelian interaction:

$$\begin{aligned}\mathcal{A}_s^{\mu\nu} &= i\frac{g_2^2}{2}\cos^2\theta_{\tilde{\tau}}\left(1-\frac{4}{3}\frac{\sin^2\theta_W}{\cos^2\theta_{\tilde{t}}}\right)\frac{1}{s-M_Z^2}\,[g^{\mu\nu}(t-u) \qquad (95)\\ &\quad -(2p_4+p_3)^\mu(p_1-p_2)^\nu+(p_1-p_2)^\mu(2p_3+p_4)^\nu]\\ &\quad +ie^2\frac{2}{3}\frac{1}{s}\,[g^{\mu\nu}(t-u)-(2p_4+p_3)^\mu(p_1-p_2)^\nu\\ &\quad +(p_1-p_2)^\mu(2p_3+p_4)^\nu]\\ &= i\frac{g_2^2}{2}\cos^2\theta_{\tilde{\tau}}\left(1-\frac{4}{3}\frac{\sin^2\theta_W}{\cos^2\theta_{\tilde{\tau}}}\frac{M_Z^2}{s}\right) \qquad (96)\\ &\quad \frac{g^{\mu\nu}(t-u)-(2p_4+p_3)^\mu(p_1-p_2)^\nu+(p_1-p_2)^\mu(2p_3+p_4)^\nu}{s-M_Z^2}\,;\end{aligned}$$

this contribution is completely antisymmetric under the exchange of the W momenta and Lorentz indices. Note that the photon contribution is proportional to $e^2 = g_2^2\sin^2\theta_W$ and cancels exactly with the second term due to the Z-boson in the case of equal mass. In that limit in fact the $U(1)_Y$ factor decouples and does not participate in the non-abelian interaction.

s-H off-shell h/H in the s-channel decaying into two WW via the non-abelian interaction; in this case we have to consider both neutral Higgses:

$$\mathcal{A}_{sH}^{\mu\nu} = i\frac{g_2^2}{2}\cos^2\theta_{\tilde{\tau}} g^{\mu\nu}\frac{M_W^2}{s}\left[\frac{C_H s}{s-M_H^2}+\frac{C_h s}{s-M_h^2}\right]\,; \tag{97}$$

where $C_{H/h}$ is coming from the product of the coupling of the staus to the Higgses and of the Higgses to the WW pair. These constants depend on the whole SUSY breaking parameters. For the staus these couplings are probably negligible. We

have in fact

$$\begin{aligned} C_{H/h} &= \frac{(Z_{1H/h})^2 - (Z_{2H/h})^2 \tan^2\beta}{(1+\tan^2\beta)\cos^4\theta_W}\left(1 - \frac{4}{3}\sin^2\theta_W(1-\tan^2\theta_{\tilde{\tau}})\right) \\ &+4\,\frac{Y_\tau^2 \tan\beta Z_{2H/h}(Z_{1H/h} + Z_{2H/h}\tan\beta)}{g_2^2\cos^2\theta_W(1+\tan^2\beta)}\left(1+\tan^2\theta_{\tilde{\tau}}\right) \\ &-\tan\theta_{\tilde{\tau}}\frac{\sqrt{2}(Z_{1H/h} + Z_{2H/h}\tan\beta)}{g_2\cos^2\theta_W M_W\sqrt{1+\tan^2\beta}} \times \\ &\times\left(Z_{2H/h}A_\tau + Z_{1H/h}(A'_\tau + \mu^\star Y_\tau) + h.c.\right)\ , \end{aligned} \tag{98}$$

where Z is the matrix which diagonalises the Higgs mass matrix, Y_τ is the tau Yukawa coupling, A_τ, A'_τ are the SUSY breaking trilinear terms and μ the Higgs supersymmetric mass parameter. This contribution is suppressed by M_W^2/s for large s. We can include it easily into the 4-vertex contribution by substituting

$$1 \to 1 + \frac{C_H M_W^2}{s - M_H^2} + \frac{C_h M_W^2}{s - M_h^2} = 1 + K_H(s)\ . \tag{99}$$

Now we can write the t-channel as the sum of a symmetric and antisymmetric part, adding and subtracting a fictitious u-channel, as

$$\begin{aligned} \frac{(2p_1-p_3)^\mu(2p_2-p_4)^\nu}{t-m_{\tilde{\nu}}^2} &= \frac{1}{2}\left[\frac{(2p_1-p_3)^\mu(2p_2-p_4)^\nu}{t-m_{\tilde{\nu}}^2} + \frac{(2p_1-p_4)^\nu(2p_2-p_3)^\mu}{u-m_{\tilde{\nu}}^2}\right] \\ &+ \frac{1}{2}\left[\frac{(2p_1-p_3)^\mu(2p_2-p_4)^\nu}{t-m_{\tilde{\nu}}^2} - \frac{(2p_1-p_4)^\nu(2p_2-p_3)^\mu}{u-m_{\tilde{\nu}}^2}\right] \end{aligned} \tag{100}$$

so that we can make contact with the previous computation and find for the symmetric and antisymmetric amplitudes respectively:

$$\begin{aligned} \mathcal{A}_{sym}^{\mu\nu} &= +i\frac{g_2^2}{4}\cos^2\theta_{\tilde{\tau}}\left[\frac{(2p_1-p_3)^\mu(2p_2-p_4)^\nu}{t-m_{\tilde{\nu}}^2}\right. \\ &\left.+\frac{(2p_1-p_4)^\nu(2p_2-p_3)^\mu}{u-m_{\tilde{\nu}}^2} + 2g^{\mu\nu}(1+K_H(s))\right] \end{aligned} \tag{101}$$

and

$$\begin{aligned} \mathcal{A}_{asym}^{\mu\nu} &= i\frac{g_2^2}{4}\cos^2\theta_{\tilde{\tau}}\left[\frac{(2p_1-p_3)^\mu(2p_2-p_4)^\nu}{t-m_{\tilde{\nu}}^2}\right. \\ &-\frac{(2p_1-p_4)^\nu(2p_2-p_3)^\mu}{u-m_{\tilde{\nu}}^2} + 2\left(1-G_Z(s)\right)\times \\ &\left.\times\frac{g^{\mu\nu}(t-u) - (2p_4+p_3)^\mu(p_1-p_2)^\nu + (p_1-p_2)^\mu(2p_3+p_4)^\nu}{s-M_Z^2}\right]. \end{aligned} \tag{102}$$

where $G_Z(s) = \frac{4}{3}\frac{\sin^2\theta_W}{\cos^2\theta_{\tilde{\tau}}}\frac{M_Z^2}{s}$ vanishes in the limit of zero Z mass. This coincides with the previous result for $K_H, G_Z, M_Z = 0$, a part for a sign, which just corresponds in exchanging $i \leftrightarrow j$.

.2.3 Polarisation sum

The sum over the W polarisation in this case is given by the polarisation tensor

$$\Pi^{\mu\mu'} = -g^{\mu\mu'} + \frac{p_3^\mu p_3^{\mu'}}{M_W^2} \tag{103}$$

where p_3 is the gauge boson momentum.

We have then for the matrix element

$$|\mathcal{M}|^2 = \mathcal{A}^*_{\mu\nu}\mathcal{A}^{\mu\nu} - \frac{|p_3^\mu A_{\mu\nu}|^2}{M_W^2} - \frac{|p_4^\nu A_{\mu\nu}|^2}{M_W^2} + \frac{|p_3^\mu p_4^\nu A_{\mu\nu}|^2}{M_W^4}\ ; \tag{104}$$

in this case neither amplitude vanishes when contracted with the gauge boson's momentum. Note that the second and third contributions are related again by the symmetry $p_3 \leftrightarrow p_4; \nu \leftrightarrow \mu$ and are equal since the final state has two particle with the same mass.

.2.4 Symmetric part

We must compute the four contributions, and we have then

$$\begin{aligned}
\mathcal{A}^*_{\mu\nu}\mathcal{A}^{\mu\nu} &= \frac{g_2^4\cos^4\theta_{\tilde{\tau}}}{2}\left[1 + \frac{(m_{\tilde{\nu}}^2 + m_{\tilde{\tau}}^2 - M_W^2/2)^2}{(t-m_{\tilde{\nu}}^2)^2} + 2K_H(s)(1+K_H(s))\right. \qquad (105)\\
&\quad + \frac{1}{2}\frac{1}{t-m_{\tilde{\nu}}^2}\left(4(m_{\tilde{\nu}}^2 + m_{\tilde{\tau}}^2) - 2M_W^2 + s - 4(m_{\tilde{\nu}}^2 + m_{\tilde{\tau}}^2) + 2M_W^2\right.\\
&\quad \left.\left. - \frac{(s - 4m_{\tilde{\tau}}^2 + M_W^2)^2}{s + 2(m_{\tilde{\nu}}^2 - m_{\tilde{\tau}}^2 - M_W^2)} + K_H(s)(s - 4m_{\tilde{\nu}}^2 - 4m_{\tilde{\tau}}^2 + 2M_W^2)\right)\right]\\
&= \frac{g_2^4\cos^4\theta_{\tilde{\tau}}}{2}\left[1 + \frac{(m_{\tilde{\nu}}^2 + m_{\tilde{\tau}}^2 - M_W^2/2)^2}{(t-m_{\tilde{\nu}}^2)^2} + 2K_H(s)(1+K_H(s))\right. \qquad (106)\\
&\quad + \frac{1}{t-m_{\tilde{\nu}}^2}\left(m_{\tilde{\nu}}^2 + 3m_{\tilde{\tau}}^2 - 2M_W^2 - \frac{1}{2}\frac{(2m_{\tilde{\tau}}^2 + 2m_{\tilde{\nu}}^2 - 3M_W^2)^2}{s + 2(m_{\tilde{\nu}}^2 - m_{\tilde{\tau}}^2 - M_W^2)}\right.\\
&\quad \left.\left. + \frac{K_H(s)}{2}(s - 4m_{\tilde{\nu}}^2 - 4m_{\tilde{\tau}}^2 + 2M_W^2)\right)\right]\ ,
\end{aligned}$$

which in the limit of vanishing M_W and $m_{\tilde{\nu}} = m_{\tilde{\tau}}$ coincides with our old result.

The other pieces give instead

$$\begin{aligned}\frac{|p_3^\mu A_{\mu\nu}|^2}{M_W^2}+\frac{|p_4^\nu A_{\mu\nu}|^2}{M_W^2} &= \frac{g_2^4\cos^4\theta_{\tilde\tau}}{4}\left[\frac{(m_{\tilde\nu}^2-m_{\tilde\tau}^2)^2}{M_W^2}\left(\frac{2m_{\tilde\nu}^2+2m_{\tilde\tau}^2-M_W^2}{(t-m_{\tilde\nu}^2)^2}\right.\right. \\ &\left.+\frac{2}{t-m_{\tilde\nu}^2}\frac{2m_{\tilde\nu}^2+2m_{\tilde\tau}^2-3M_W^2)^2}{s+2(m_{\tilde\nu}^2-m_{\tilde\tau}^2-M_W^2)}\right) \\ &\left.-4K_H(s)\frac{m_{\tilde\nu}^2-m_{\tilde\tau}^2}{M_W^2}\left(1+\frac{m_{\tilde\nu}^2-m_{\tilde\tau}^2+s/2}{t-m_{\tilde\nu}^2}\right)+2K_H^2(s)\right]\end{aligned} \tag{107}$$

and the last part:

$$\begin{aligned}\frac{|p_3^\mu p_4^\nu A_{\mu\nu}|^2}{M_W^4} &= \frac{g_2^4\cos^4\theta_{\tilde\tau}}{4}\left[\frac{(m_{\tilde\nu}^2-m_{\tilde\tau}^2)^2}{M_W^4}\left(1+\frac{1}{2}\frac{(m_{\tilde\nu}^2-m_{\tilde\tau}^2)^2}{(t-m_{\tilde\nu}^2)^2}\right.\right. \\ &\left.+2\frac{m_{\tilde\nu}^2-m_{\tilde\tau}^2}{t-m_{\tilde\nu}^2}\left(1-\frac{1}{4}\frac{m_{\tilde\nu}^2-m_{\tilde\tau}^2}{s+2(m_{\tilde\nu}^2-m_{\tilde\tau}^2+M_W^2)}\right)\right) \\ &+K_H(s)\frac{m_{\tilde\nu}^2-m_{\tilde\tau}^2}{M_W^2}\left(\frac{s}{M_W^2}-2\right)\left(1+\frac{m_{\tilde\nu}^2-m_{\tilde\tau}^2}{t-m_{\tilde\nu}^2}\right) \\ &\left.+\frac{1}{4}K_H^2(s)\left(\frac{s}{M_W^2}-2\right)^2\right]\ .\end{aligned} \tag{108}$$

Both these contributions vanish in the limit of equal stau and sneutrino masses and zero gauge boson mass as they should.

So summing all together the result is

$$
\begin{aligned}
|\mathcal{M}_{sym}|^2 &= \frac{g_2^4\cos^4\theta_{\tilde{\tau}}}{2}\left[1+\frac{(m_{\tilde{\nu}}^2+m_{\tilde{\tau}}^2-M_W^2/2)^2}{(t-m_{\tilde{\nu}}^2)^2}\right. \\
&+\frac{1}{t-m_{\tilde{\nu}}^2}\left(m_{\tilde{\nu}}^2+3m_{\tilde{\tau}}^2-2M_W^2-\frac{1}{2}\frac{(2m_{\tilde{\tau}}^2+2m_{\tilde{\nu}}^2-3M_W^2)^2}{s+2(m_{\tilde{\nu}}^2-m_{\tilde{\tau}}^2-M_W^2)}\right) \\
&-\frac{(m_{\tilde{\nu}}^2-m_{\tilde{\tau}}^2)^2}{M_W^2(t-m_{\tilde{\nu}}^2)}\left(\frac{m_{\tilde{\nu}}^2+m_{\tilde{\tau}}^2-M_W^2/2}{t-m_{\tilde{\nu}}^2}+\frac{2m_{\tilde{\tau}}^2+2m_{\tilde{\nu}}^2-3M_W^2}{s+2(m_{\tilde{\nu}}^2-m_{\tilde{\tau}}^2-M_W^2)}\right) \\
&+\frac{1}{2}\frac{(m_{\tilde{\nu}}^2-m_{\tilde{\tau}}^2)^2}{M_W^4}\left(1+\frac{1}{2}\frac{(m_{\tilde{\nu}}^2-m_{\tilde{\tau}}^2)^2}{(t-m_{\tilde{\nu}}^2)^2}\right. \\
&\left.+2\frac{m_{\tilde{\nu}}^2-m_{\tilde{\tau}}^2}{t-m_{\tilde{\nu}}^2}\left(1-\frac{1}{4}\frac{m_{\tilde{\nu}}^2-m_{\tilde{\tau}}^2}{s+2(m_{\tilde{\nu}}^2-m_{\tilde{\tau}}^2+M_W^2)}\right)\right) \\
&+K_H(s)\left(2-3\frac{m_{\tilde{\nu}}^2-m_{\tilde{\tau}}^2}{M_W^2}+\frac{s}{2M_W^2}\frac{m_{\tilde{\nu}}^2-m_{\tilde{\tau}}^2}{M_W^2}\right) \\
&+\frac{K_H(s)}{t-m_{\tilde{\nu}}^2}\left(\frac{s}{2}-2m_{\tilde{\nu}}^2-2m_{\tilde{\tau}}^2+M_W^2\right. \\
&\left.-\frac{m_{\tilde{\nu}}^2-m_{\tilde{\tau}}^2}{M_W^2}\left(s+3(m_{\tilde{\nu}}^2-m_{\tilde{\tau}}^2)(1-\frac{s}{2M_W^2})\right)\right) \\
&\left.+K_H^2(s)\left(\frac{7}{2}-\frac{s}{2M_W^2}+\frac{s^2}{8M_W^4}\right)\right] .
\end{aligned}
\tag{109}
$$

Note that the in the limit of large s, $sK_H(s)$ remains finite and therefore there is no problem with unitarity.

.2.5 Antisymmetric part

The antisymmetric piece is more involved. We have

$$
\begin{aligned}
\mathcal{A}_{\mu\nu}^*\mathcal{A}^{\mu\nu} &= \frac{g_2^4\cos^4\theta_{\tilde{\tau}}}{4}\left[2+2\frac{(m_{\tilde{\nu}}^2+m_{\tilde{\tau}}^2-M_W^2/2)^2}{(t-m_{\tilde{\nu}}^2)^2}\right. \\
&+\frac{1}{t-m_{\tilde{\nu}}^2}\left(4(m_{\tilde{\nu}}^2+m_{\tilde{\tau}}^2)-2M_W^2+\frac{(s-4m_{\tilde{\tau}}^2+M_W^2)^2}{s+2(m_{\tilde{\nu}}^2-m_{\tilde{\tau}}^2-M_W^2)}\right) \\
&+(1-G_Z(s))^2\,\frac{5/2(t-u)^2-4(s-4m_{\tilde{\tau}}^2)(s+M_W^2/2)}{(s-M_Z^2)^2} \\
&-(1-G_Z(s))\,\frac{2(t-u)+4(s-4m_{\tilde{\tau}}^2)}{s-M_Z^2} \\
&+(1-G_Z(s))\,\frac{(t-u)(3s-2m_{\tilde{\nu}}^2-6m_{\tilde{\tau}}^2+2M_W^2)}{(s-M_Z^2)(t-m_{\tilde{\nu}}^2)} \\
&\left.-(1-G_Z(s))\,\frac{4(s+m_{\tilde{\nu}}^2-m_{\tilde{\tau}}^2)(s-4m_{\tilde{\tau}}^2)}{(s-M_Z^2)(t-m_{\tilde{\nu}}^2)}\right]
\end{aligned}
\tag{110}
$$

which in the limit of vanishing M_W, M_Z and $m_{\tilde{\nu}} = m_{\tilde{\tau}}$ coincides with our old result.

The other pieces give instead

$$\begin{aligned}
&\frac{|p_3^\mu A_{\mu\nu}|^2}{M_W^2} + \frac{|p_4^\nu A_{\mu\nu}|^2}{M_W^2} = \frac{g_2^4 \cos^4\theta_{\tilde{\tau}}}{2} \times \qquad (111)\\
\times\ &\left[\frac{1}{2}\frac{(t-u)^2}{(s-M_Z^2)^2}\left(1-G_Z(s)\right)\left(\frac{M_Z^2}{M_W^2}-\frac{1}{2}-G_Z(s)\left(\frac{s}{M_W^2}-\frac{1}{2}\right)\right)\right.\\
&-\frac{(s-4m_{\tilde{\tau}}^2)M_W^2}{(s-M_Z^2)^2}\left(\frac{M_Z^2}{M_W^2}-1-G_Z(s)(\frac{s}{M_W^2}-1)\right)^2\\
&-\frac{m_{\tilde{\nu}}^2-m_{\tilde{\tau}}^2}{s-M_Z^2}\frac{t-u-2(s-4m_{\tilde{\tau}}^2)}{t-m_{\tilde{\nu}}^2}\left(\frac{M_Z^2}{M_W^2}-1-G_Z(s)(\frac{s}{M_W^2}-1)\right)\\
&-\frac{(m_{\tilde{\nu}}^2-m_{\tilde{\tau}}^2)^2}{M_W^2(s-M_Z^2)}\left(1-G_Z(s)\right)\frac{t-u}{t-m_{\tilde{\nu}}^2}\\
&\left.+\frac{(m_{\tilde{\nu}}^2-m_{\tilde{\tau}}^2)^2}{M_W^2(t-m_{\tilde{\nu}}^2)}\left(1+\frac{s-4m_{\tilde{\tau}}^2+M_W^2}{s+2(m_{\tilde{\nu}}^2-m_{\tilde{\tau}}^2-M_W^2)}+\frac{m_{\tilde{\nu}}^2+m_{\tilde{\tau}}^2-M_W/2}{t-m_{\tilde{\nu}}^2}\right)\right]\ ;
\end{aligned}$$

in the limit of vanishing $m_{\tilde{\nu}}^2 - m_{\tilde{\tau}}^2, M_Z, M_W$ masses keeping $M_Z/M_W \to 1$ we have

$$\frac{|p_3^\mu A_{\mu\nu}|^2}{M_W^2} + \frac{|p_4^\nu A_{\mu\nu}|^2}{M_W^2} \to \frac{g_2^4 \cos^4\theta_{\tilde{\tau}}}{4}\frac{(t-u)^2}{2s}\ , \qquad (112)$$

as expected from the QCD result.

The last part gives instead

$$\begin{aligned}
\frac{|p_3^\mu p_4^\nu A_{\mu\nu}|^2}{M_W^4} \ &=\ \frac{g_2^4\cos^4\theta_{\tilde{\tau}}}{16M_W^4}\left[\frac{(t-u)^2}{(s-M_Z^2)^2}\left(M_Z^2-G_Z(s)s\right)^2\right. \qquad (113)\\
&-4(m_{\tilde{\nu}}^2-m_{\tilde{\tau}}^2)^2\frac{t-u}{(t-m_{\tilde{\nu}}^2)(s-M_Z^2)}\left(M_Z^2-G_Z(s)s\right)\\
&\left.+2\frac{(m_{\tilde{\nu}}^2-m_{\tilde{\tau}}^2)^4}{(t-m_{\tilde{\nu}}^2)}\left(\frac{1}{(t-m_{\tilde{\nu}}^2)}+2\frac{1}{s+2(m_{\tilde{\nu}}^2-m_{\tilde{\tau}}^2-M_W^2)}\right)\right]\ .
\end{aligned}$$

Note that this contribution does not vanish in the limit of equal stop and sbottom masses and massless gauge bosons.In fact keeping $M_Z/M_W \to 1$, we have

$$\frac{|p_3^\mu p_4^\nu A_{\mu\nu}|^2}{M_W^4} \to \frac{g_2^4\cos^4\theta_{\tilde{\tau}}}{8}\frac{(t-u)^2}{2s}\ , \qquad (114)$$

which gives the annihilation into the Goldstone part of the Higgs field.

We can now put all together to give

$$
\begin{aligned}
|\mathcal{M}_{asym}|^2 \;=\; & \frac{g_2^4\cos^4\theta_{\tilde{\tau}}}{2}\left[1+\frac{(m_{\tilde{\nu}}^2+m_{\tilde{\tau}}^2-M_W^2/2)^2}{(t-m_{\tilde{\nu}}^2)^2}\right. \\
& +\frac{1}{t-m_{\tilde{\nu}}^2}\left(2(m_{\tilde{\nu}}^2+m_{\tilde{\tau}}^2)-M_W^2+\frac{1}{2}\frac{(s-4m_{\tilde{\tau}}^2+M_W^2)^2}{s+2(m_{\tilde{\nu}}^2-m_{\tilde{\tau}}^2-M_W^2)}\right) \\
& +\frac{1}{2}\left(1-G_Z(s)\right)^2\frac{5/2(t-u)^2-4(s-4m_{\tilde{\tau}}^2)(s+M_W^2/2)}{(s-M_Z^2)^2} \\
& -\left(1-G_Z(s)\right)\frac{(t-u)+2(s-4m_{\tilde{\tau}}^2)}{s-M_Z^2} \\
& +\frac{1}{2}\left(1-G_Z(s)\right)\frac{(t-u)(3s-2m_{\tilde{\nu}}^2-6m_{\tilde{\tau}}^2+2M_W^2)}{(s-M_Z^2)(t-m_{\tilde{\nu}}^2)} \\
& -\left(1-G_Z(s)\right)\frac{2(s+m_{\tilde{\nu}}^2-m_{\tilde{\tau}}^2)(s-4m_{\tilde{\tau}}^2)}{(s-M_Z^2)(t-m_{\tilde{\nu}}^2)} \\
& -\frac{(t-u)^2}{2(s-M_Z^2)^2}\left(1-G_Z(s)\right)\left(\frac{M_Z^2}{M_W^2}-\frac{1}{2}-G_Z(s)\left(\frac{s}{M_W^2}-\frac{1}{2}\right)\right) \\
& +\frac{M_W^2(s-4m_{\tilde{\tau}}^2)}{(s-M_Z^2)^2}\left(\frac{M_Z^2}{M_W^2}-1-G_Z(s)(\frac{s}{M_W^2}-1)\right)^2 \\
& +\frac{m_{\tilde{\nu}}^2-m_{\tilde{\tau}}^2}{s-M_Z^2}\left(\frac{M_Z^2}{M_W^2}-1-G_Z(s)(\frac{s}{M_W^2}-1)\right)\frac{t-u-2(s-4m_{\tilde{\tau}}^2)}{t-m_{\tilde{\nu}}^2} \\
& +\frac{(m_{\tilde{\nu}}^2-m_{\tilde{\tau}}^2)^2}{M_W^2(s-M_Z^2)}\left(1-G_Z(s)\right)\frac{t-u}{t-m_{\tilde{\nu}}^2} \\
& -\frac{(m_{\tilde{\nu}}^2-m_{\tilde{\tau}}^2)^2}{M_W^2(t-m_{\tilde{\nu}}^2)^2}\left(m_{\tilde{\nu}}^2+m_{\tilde{\tau}}^2-M_W/2\right) \\
& -\frac{(m_{\tilde{\nu}}^2-m_{\tilde{\tau}}^2)^2}{M_W^2(t-m_{\tilde{\nu}}^2)}\left(1+\frac{s-4m_{\tilde{\tau}}^2+M_W^2}{s+2(m_{\tilde{\nu}}^2-m_{\tilde{\tau}}^2-M_W^2)}\right) \\
& +\frac{(t-u)^2}{8(s-M_Z^2)^2}\left(\frac{M_Z^2}{M_W^2}-G_Z(s)\frac{s}{M_W^2}\right)^2 \\
& -\frac{1}{2}\frac{(m_{\tilde{\nu}}^2-m_{\tilde{\tau}}^2)^2}{M_W^2}\frac{t-u}{(t-m_{\tilde{\nu}}^2)(s-M_Z^2)}\left(\frac{M_Z^2}{M_W^2}-G_Z(s)\frac{s}{M_W^2}\right) \\
& \left.+\frac{1}{4}\frac{(m_{\tilde{\nu}}^2-m_{\tilde{\tau}}^2)^4}{M_W^4(t-m_{\tilde{\nu}}^2)}\left(\frac{1}{(t-m_{\tilde{\nu}}^2)}+2\frac{1}{s+2(m_{\tilde{\nu}}^2-m_{\tilde{\tau}}^2-M_W^2)}\right)\right]\,.
\end{aligned}
\tag{115}
$$

Note that to reduce these expressions in terms of only the t variable, we have used the simple decompositions, i.e. from $s+t+u=2m_{\tilde{t}}^2+2M_W^2$ one obtains

$$
\frac{1}{(t-m_{\tilde{\nu}}^2)(u-m_{\tilde{\nu}}^2)}=-\frac{1}{s+2(m_{\tilde{\nu}}^2-m_{\tilde{\tau}}^2-M_W^2)}\left(\frac{1}{t-m_{\tilde{\nu}}^2}+\frac{1}{u-m_{\tilde{\nu}}^2}\right). \tag{116}
$$

.2.6 Results for the cross section

We can integrate the matrix element to obtain the cross section in the two cases:

$$
\begin{aligned}
\sigma_{sym}(s) \;=\; & \frac{g_2^4\cos^4\theta_{\tilde\tau}}{32\pi(s-4m_{\tilde\tau}^2)}\sqrt{\left(1-\frac{4m_{\tilde\tau}^2}{s}\right)\left(1-\frac{4M_W^2}{s}\right)}\left[1+\frac{1}{2}\frac{(m_{\tilde\nu}^2-m_{\tilde\tau}^2)^2}{M_W^4}\right.\\
& +\frac{(m_{\tilde\nu}^2+m_{\tilde\tau}^2-M_W^2/2)^2}{m_{\tilde\nu}^2(s+m_{\tilde\nu}^2-2m_{\tilde\tau}^2-2M_W^2)+(m_{\tilde\tau}^2-M_W^2)^2}\times\\
& \times\left(1-\frac{(m_{\tilde\nu}^2-m_{\tilde\tau}^2)^2}{M_W^2(2m_{\tilde\nu}^2+2m_{\tilde\tau}^2-M_W^2)}\right)^2\\
& +K_H(s)\left(2-3\frac{m_{\tilde\nu}^2-m_{\tilde\tau}^2}{M_W^2}+\frac{s}{2M_W^2}\frac{m_{\tilde\nu}^2-m_{\tilde\tau}^2}{M_W^2}\right)\\
& +K_H^2(s)\left(\frac{7}{2}-\frac{s}{2M_W^2}+\frac{s^2}{8M_W^4}\right)\\
& +\frac{Ln(s)}{\sqrt{(s-4m_{\tilde\tau}^2)\,(s-4M_W^2)}}\left(m_{\tilde\nu}^2+3m_{\tilde\tau}^2-2M_W^2\right.\\
& -\frac{1}{2}\frac{(2m_{\tilde\tau}^2+2m_{\tilde\nu}^2-3M_W^2)^2}{s+2(m_{\tilde\nu}^2-m_{\tilde\tau}^2-M_W^2)}-\frac{(m_{\tilde\nu}^2-m_{\tilde\tau}^2)^2}{M_W^2}\frac{2m_{\tilde\tau}^2+2m_{\tilde\nu}^2-3M_W^2}{s+2(m_{\tilde\nu}^2-m_{\tilde\tau}^2-M_W^2)}\\
& +\frac{(m_{\tilde\nu}^2-m_{\tilde\tau}^2)^3}{M_W^4}\left(1-\frac{1}{4}\frac{m_{\tilde\nu}^2-m_{\tilde\tau}^2}{s+2(m_{\tilde\nu}^2-m_{\tilde\tau}^2-M_W^2)}\right)\\
& +K_H(s)\left(\frac{s}{2}-2m_{\tilde\nu}^2-2m_{\tilde\tau}^2+M_W^2-\frac{s(m_{\tilde\nu}^2-m_{\tilde\tau}^2)}{M_W^2}\right.\\
& \left.\left.\left.-3\frac{(m_{\tilde\nu}^2-m_{\tilde\tau}^2)^2}{M_W^2}\left(1-\frac{s}{2M_W^2}\right)\right)\right)\right]\;.
\end{aligned}
$$

where

$$
Ln(s) \;=\; \ln\left[\frac{s+2(m_{\tilde\nu}^2-m_{\tilde\tau}^2-M_W^2)-\sqrt{(s-4m_{\tilde\tau}^2)\,(s-4M_W^2)}}{s+2(m_{\tilde\nu}^2-m_{\tilde\tau}^2-M_W^2)+\sqrt{(s-4m_{\tilde\tau}^2)\,(s-4M_W^2)}}\right] \qquad (117)
$$

The antisymmetric part gives instead:

$$
\begin{aligned}
\sigma_{asym}(s) \;=\; & \frac{g_2^4\cos^4\theta_{\tilde\tau}}{32\pi(s-4m_{\tilde\tau}^2)}\sqrt{\left(1-\frac{4m_{\tilde\tau}^2}{s}\right)\left(1-\frac{4M_W^2}{s}\right)}\times \\
& \times\left[1+(1-G_Z(s))\,\frac{s-2m_{\tilde\nu}^2+2m_{\tilde\tau}^2+2M_W^2}{s-M_Z^2}\right. \\
& -(1-G_Z(s))^2\,\frac{(s-4m_{\tilde\tau}^2)(2s+M_W^2)}{(s-M_Z^2)^2} \\
& +\frac{M_W^2(s-4m_{\tilde\tau}^2)}{(s-M_Z^2)^2}\left(\frac{M_Z^2}{M_W^2}-1-G_Z(s)(\frac{s}{M_W^2}-1)\right)^2 \\
& +2\frac{m_{\tilde\nu}^2-m_{\tilde\tau}^2}{s-M_Z^2}\left(\frac{M_Z^2}{M_W^2}-1-G_Z(s)(\frac{s}{M_W^2}-1)\right) \\
& +2\frac{(m_{\tilde\nu}^2-m_{\tilde\tau}^2)^2}{M_W^2(s-M_Z^2)}\,(1-G_Z(s)) \\
& -\frac{(m_{\tilde\nu}^2-m_{\tilde\tau}^2)^2}{M_W^2(s-M_Z^2)}\left(\frac{M_Z^2}{M_W^2}-G_Z(s)\frac{s}{M_W^2}\right) \\
& +\frac{(m_{\tilde\nu}^2+m_{\tilde\tau}^2-M_W^2/2)^2}{m_{\tilde\nu}^2(s+m_{\tilde\nu}^2-2m_{\tilde\tau}^2-2M_W^2)+(m_{\tilde\tau}^2-M_W^2)^2}\times \\
& \times\left(1-\frac{(m_{\tilde\nu}^2-m_{\tilde\tau}^2)^2}{M_W^2(2m_{\tilde\nu}^2+2m_{\tilde\tau}^2-M_W^2)}\right)^2 \\
& +\frac{(s-4m_{\tilde\tau}^2)(s-4M_W^2)}{24\,(s-M_Z^2)^2}\left(10(1-G_Z(s))^2+\frac{M_Z^4}{M_W^4}\left(1-G_Z(s)\frac{s}{M_Z^2}\right)^2\right. \\
& \left.\left.-4\,(1-G_Z(s))\left(\frac{M_Z^2}{M_W^2}-\frac{1}{2}-G_Z(s)\left(\frac{s}{M_W^2}-\frac{1}{2}\right)\right)\right) \\
& +\frac{1}{2}\frac{Ln(s)}{\sqrt{(s-4m_{\tilde\tau}^2)\,(s-4M_W^2)}}\left(\frac{(s-4m_{\tilde\tau}^2+M_W^2)^2}{s+2(m_{\tilde\nu}^2-m_{\tilde\tau}^2-M_W^2)}+4(m_{\tilde\nu}^2+m_{\tilde\tau}^2)\right. \\
& -2M_W^2-(1-G_Z(s))\,\frac{s(s-20m_{\tilde\tau}^2+8M_W^2)}{s-M_Z^2} \\
& -4\,(1-G_Z(s))\,\frac{M_W^2(4m_{\tilde\tau}^2-M_W^2)+m_{\tilde\nu}^2(m_{\tilde\nu}^2-m_{\tilde\tau}^2)}{s-M_Z^2} \\
& -2\frac{m_{\tilde\nu}^2-m_{\tilde\tau}^2}{s-M_Z^2}\left(\frac{M_Z^2}{M_W^2}-1-G_Z(s)(\frac{s}{M_W^2}-1)\right)(s-2m_{\tilde\nu}^2-6m_{\tilde\tau}^2+2M_W^2) \\
& +2\frac{(m_{\tilde\nu}^2-m_{\tilde\tau}^2)^2}{M_W^2(s-M_Z^2)}\,(1-G_Z(s))\,(s+2m_{\tilde\nu}^2-2m_{\tilde\tau}^2-2M_W^2) \\
& -2\frac{(m_{\tilde\nu}^2-m_{\tilde\tau}^2)^2}{M_W^2}\left(1+\frac{s-4m_{\tilde\tau}^2+M_W^2}{s+2(m_{\tilde\nu}^2-m_{\tilde\tau}^2-M_W^2)}\right) \\
& -\frac{(m_{\tilde\nu}^2-m_{\tilde\tau}^2)^2}{M_W^2}\frac{s+2(m_{\tilde\nu}^2-m_{\tilde\tau}^2-M_W^2)}{s-M_Z^2}\left(\frac{M_Z^2}{M_W^2}-G_Z(s)\frac{s}{M_W^2}\right) \\
& \left.\left.+\frac{(m_{\tilde\nu}^2-m_{\tilde\tau}^2)^4}{M_W^4(s+2(m_{\tilde\nu}^2-m_{\tilde\tau}^2-M_W^2))}\right)\right]\,.
\end{aligned}
\tag{118}
$$

References

[1] For a compilation of bounds on charged or coloured relics, see the Particle Data Group, W.-M. Yao et al., J. Phys. G 33, 1 (2006)

[2] L. Covi, J. E. Kim and L. Roszkowski, Phys. Rev. Lett. **82** (1999) 4180 [arXiv:hep-ph/9905212]; L. Covi, H. B. Kim, J. E. Kim and L. Roszkowski, JHEP **0105** (2001) 033 [arXiv:hep-ph/0101009]; L. Covi, L. Roszkowski, R. Ruiz de Austri and M. Small, JHEP **0406** (2004) 003 [arXiv:hep-ph/0402240].

[3] L. Covi, L. Roszkowski and M. Small, JHEP **0207** (2002) 023 [arXiv:hep-ph/0206119].

[4] A. Brandenburg and F. D. Steffen, JCAP **0408** (2004) 008 [arXiv:hep-ph/0405158]. K. Y. Choi, L. Roszkowski and R. Ruiz de Austri, JHEP **0804** (2008) 016 [arXiv:0710.3349 [hep-ph]]. H. Baer and H. Summy, arXiv:0803.0510 [hep-ph].

[5] J. L. Feng, A. Rajaraman and F. Takayama, Phys. Rev. Lett. **91** (2003) 011302 [arXiv:hep-ph/0302215]; J. R. Ellis, K. A. Olive, Y. Santoso and V. C. Spanos, Phys. Lett. B **588** (2004) 7 [arXiv:hep-ph/0312262]; J. L. Feng, S. f. Su and F. Takayama, Phys. Rev. D **70** (2004) 063514 [arXiv:hep-ph/0404198]; D. G. Cerdeno, K. Y. Choi, K. Jedamzik, L. Roszkowski and R. Ruiz de Austri, JCAP **0606** (2006) 005 [arXiv:hep-ph/0509275]. J. L. Feng, B. T. Smith and F. Takayama, Phys. Rev. Lett. **100** (2008) 021302 [arXiv:0709.0297 [hep-ph]].

[6] J. L. Feng, S. f. Su and F. Takayama, Phys. Rev. D **70** (2004) 075019 [arXiv:hep-ph/0404231]; L. Roszkowski, R. Ruiz de Austri and K. Y. Choi, JHEP **0508** (2005) 080 [arXiv:hep-ph/0408227].

[7] W. Buchmuller, K. Hamaguchi, M. Ratz and T. Yanagida, Phys. Lett. B **588** (2004) 90 [arXiv:hep-ph/0402179]; K. Hamaguchi, Y. Kuno, T. Nakaya and M. M. Nojiri, Phys. Rev. D **70** (2004) 115007 [arXiv:hep-ph/0409248]; J. L. Feng and B. T. Smith, Phys. Rev. D **71** (2005) 015004 [Erratum-ibid. D **71** (2005) 0109904] [arXiv:hep-ph/0409278]; H. U. Martyn, Eur. Phys. J. C **48** (2006) 15 [arXiv:hep-ph/0605257]; J. R. Ellis, A. R. Raklev and O. K. Oye, JHEP **0610**

(2006) 061 [arXiv:hep-ph/0607261]; K. Hamaguchi, M. M. Nojiri and A. de Roeck, JHEP **0703** (2007) 046 [arXiv:hep-ph/0612060].

[8] M. Fairbairn, A. C. Kraan, D. A. Milstead, T. Sjostrand, P. Skands and T. Sloan, Phys. Rept. **438** (2007) 1 [arXiv:hep-ph/0611040].

[9] See e.g. the review by B. Fields and S. Sarkar, in W. M. Yao *et al.* [Particle Data Group], J. Phys. G **33** (2006) 1 [arXiv:astro-ph/0601514].

[10] D. Lindley, Astrophys. J. **294** (1985) 1; M. H. Reno and D. Seckel, Phys. Rev. D **37** (1988) 3441; S. Dimopoulos, R. Esmailzadeh, L. J. Hall and G. D. Starkman, Astrophys. J. **330** (1988) 545; R. J. Scherrer and M. S. Turner, Astrophys. J. **331** (1988) 19 [Astrophys. J. **331** (1988) 33]; J. R. Ellis, G. B. Gelmini, J. L. Lopez, D. V. Nanopoulos and S. Sarkar, Nucl. Phys. B **373** (1992) 399.

[11] M. Pospelov, Phys. Rev. Lett. **98** (2007) 231301 [arXiv:hep-ph/0605215]; K. Kohri and F. Takayama, Phys. Rev. D **76** (2007) 063507 [arXiv:hep-ph/0605243]; M. Kaplinghat and A. Rajaraman, Phys. Rev. D **74** (2006) 103004 [arXiv:astro-ph/0606209].

[12] R. H. Cyburt, J. R. Ellis, B. D. Fields, K. A. Olive and V. C. Spanos, JCAP **0611** (2006) 014 [arXiv:astro-ph/0608562]; J. Pradler and F. D. Steffen, Phys. Lett. B **648** (2007) 224 [arXiv:hep-ph/0612291]; M. Kawasaki, K. Kohri and T. Moroi, Phys. Lett. B **649** (2007) 436 [arXiv:hep-ph/0703122]; J. Pradler and F. D. Steffen, arXiv:0710.2213 [hep-ph]; J. Kersten and K. Schmidt-Hoberg, JCAP **0801** (2008) 011 [arXiv:0710.4528 [hep-ph]]; F. D. Steffen, arXiv:0806.3266 [hep-ph].

[13] S. Wolfram, Phys. Lett. **B82** (1979) 65;

[14] E. Nardi and E. Roulet, Phys. Lett. B **245** (1990) 105.

[15] K. Griest and M. Kamionkowski, Phys. Rev. Lett. **64** (1990) 615.

[16] M. Cirelli, A. Strumia and M. Tamburini, Nucl. Phys. B **787** (2007) 152 [arXiv:0706.4071 [hep-ph]];

[17] A. Sommerfeld, *Atombau und Spektrallinien, Band 2*, Vieweg & Sohn (1939);
A. D. Sakharov, Zh. Eksp. Teor. Fiz. **18**, 631 (1948) [Sov. Phys. Usp. **34**, 375

(1991)]; J. S. Schwinger, *Particles, sources, and fields. Vol. 2,* Addison-Wesley (1989) (Advanced book classics series).

[18] A. Arvanitaki, C. Davis, P. W. Graham, A. Pierce and J. G. Wacker, Phys. Rev. D **72** (2005) 075011 [arXiv:hep-ph/0504210].

[19] J. Hisano, S. Matsumoto, M. Nagai, O. Saito and M. Senami, Phys. Lett. B **646** (2007) 34 [arXiv:hep-ph/0610249].

[20] A. Freitas, Phys. Lett. B **652** (2007) 280 [arXiv:0705.4027 [hep-ph]];

[21] N. Baro, F. Boudjema and A. Semenov, Phys. Lett. B **660** (2008) 550 [arXiv:0710.1821 [hep-ph]]; J. March-Russell, S. M. West, D. Cumberbatch and D. Hooper, arXiv:0801.3440 [hep-ph].

[22] A. Strumia, arXiv:0806.1630 [hep-ph].

[23] E. W. Kolb and M. S. Turner, *The Early Universe,* Front. Phys. **69** (1990) 1.

[24] P. Gondolo and G. Gelmini, Nucl. Phys. B **360** (1991) 145.

[25] T. Asaka, K. Hamaguchi and K. Suzuki, Phys. Lett. B **490** (2000) 136 [arXiv:hep-ph/0005136].

[26] W. Beenakker, R. Hopker, M. Spira and P. M. Zerwas, Nucl. Phys. B **492**, 51 (1997) [arXiv:hep-ph/9610490].

[27] S. Raby, Phys. Lett. B **422** (1998) 158 [arXiv:hep-ph/9712254]; H. Baer, K. m. Cheung and J. F. Gunion, Phys. Rev. D **59** (1999) 075002 [arXiv:hep-ph/9806361].

[28] A. H. Hoang, Phys. Rev. D **56**, 7276 (1997) [arXiv:hep-ph/9703404]; A. H. Hoang, A. V. Manohar, I. W. Stewart and T. Teubner, Phys. Rev. D **65**, 014014 (2002) [arXiv:hep-ph/0107144].

[29] J. Kublbeck, H. Eck and R. Mertig, Nucl. Phys. Proc. Suppl. **29A**, 204 (1992).

[30] S. J. J. Gates and O. Lebedev, Phys. Lett. B **477** (2000) 216 [arXiv:hep-ph/9912362].

[31] J. Kang, M. A. Luty and S. Nasri, arXiv:hep-ph/0611322.

[32] J. Dunkley *et al.* [WMAP Collaboration], arXiv:0803.0586 [astro-ph].

[33] See R. Lamon and R. Durrer, Phys. Rev. D **73** (2006) 023507 [arXiv:hep-ph/0506229] and references therein.

[34] See K. Abazajian, G. M. Fuller and W. H. Tucker, Astrophys. J. **562** (2001) 593 [arXiv:astro-ph/0106002]; A. Boyarsky, A. Neronov, O. Ruchayskiy and M. Shaposhnikov, Mon. Not. Roy. Astron. Soc. **370** (2006) 213 [arXiv:astro-ph/0512509]; G. Bertone, W. Buchmuller, L. Covi and A. Ibarra, JCAP **0711** (2007) 003 [arXiv:0709.2299 [astro-ph]]; H. Yuksel and M. D. Kistler, Phys. Rev. D **78** (2008) 023502 [arXiv:0711.2906 [astro-ph]] and references therein.

[35] T. Yamagata, Y. Takamori and H. Utsunomiya, Phys. Rev. D **47** (1993) 1231.

[36] P. F. Smith, J. R. J. Bennett, G. J. Homer, J. D. Lewin, H. E. Walford and W. A. Smith, Nucl. Phys. B **206** (1982) 333.

[37] T. K. Hemmick *et al.*, Phys. Rev. D **41** (1990) 2074.

[38] P. Verkerk, G. Grynberg, B. Pichard, M. Spiro, S. Zylberajch, M. E. Goldberg and P. Fayet, Phys. Rev. Lett. **68** (1992) 1116.

[39] E. B. Norman, R. B. Chadwick, K. T. Lesko, R. M. Larimer and D. C. Hoffman, Phys. Rev. D **39** (1989) 2499.

[40] M. Kawasaki, K. Kohri and T. Moroi, Phys. Rev. D **71** (2005) 083502 [arXiv:astro-ph/0408426].

[41] K. Jedamzik, Phys. Rev. D **74** (2006) 103509 [arXiv:hep-ph/0604251].

[42] M. Kawasaki, K. Kohri and T. Moroi, Phys. Lett. B **649** (2007) 436 [arXiv:hep-ph/0703122]; M. Kawasaki, K. Kohri, T. Moroi and A. Yotsuyanagi, arXiv:0804.3745 [hep-ph].

[43] C. Bird, K. Koopmans and M. Pospelov, arXiv:hep-ph/0703096; T. Jittoh, K. Kohri, M. Koike, J. Sato, T. Shimomura and M. Yamanaka, Phys. Rev. D

76 (2007) 125023 [arXiv:0704.2914 [hep-ph]]; K. Jedamzik, Phys. Rev. D **77** (2008) 063524 [arXiv:0707.2070 [astro-ph]]. T. Jittoh, K. Kohri, M. Koike, J. Sato, T. Shimomura and M. Yamanaka, arXiv:0805.3389 [hep-ph]; D. Cumberbatch, K. Ichikawa, M. Kawasaki, K. Kohri, J. Silk and G. D. Starkman, Phys. Rev. D **76** (2007) 123005 [arXiv:0708.0095 [astro-ph]]; M. Kusakabe, T. Kajino, R. N. Boyd, T. Yoshida and G. J. Mathews, Phys. Rev. D **76** (2007) 121302 [arXiv:0711.3854 [astro-ph]].

[44] K. Jedamzik, JCAP **0803** (2008) 008 [arXiv:0710.5153 [hep-ph]].

[45] K. Hamaguchi, T. Hatsuda, M. Kamimura, Y. Kino and T. T. Yanagida, Phys. Lett. B **650** (2007) 268 [arXiv:hep-ph/0702274].

[46] J. Pradler and F. D. Steffen, arXiv:0710.2213 [hep-ph].

[47] G. Belanger, F. Boudjema, A. Pukhov and A. Semenov, Comput. Phys. Commun. **149** (2002) 103 [arXiv:hep-ph/0112278], Comput. Phys. Commun. **174** (2006) 577 [arXiv:hep-ph/0405253], Comput. Phys. Commun. **176** (2007) 367 [arXiv:hep-ph/0607059].

[48] F. D. Steffen, JCAP **0609** (2006) 001 [arXiv:hep-ph/0605306].

[49] A. Brandenburg, L. Covi, K. Hamaguchi, L. Roszkowski and F. D. Steffen, Phys. Lett. B **617** (2005) 99 [arXiv:hep-ph/0501287].

[50] LEPSUSYWG, ALEPH, DELPHI, L3 and OPAL experiments, note LEPSUSYWG/02-05.1 (http://lepsusy.web.cern.ch/lepsusy/Welcome.html).

[51] J. L. Diaz-Cruz, J. R. Ellis, K. A. Olive and Y. Santoso, JHEP **0705** (2007) 003 [arXiv:hep-ph/0701229].

[52] J. Nachtman, talk at the symposium "The Hunt for Dark Matter", Fermilab, 10–12 May 2007.

[53] F. Takayama and M. Yamaguchi, Phys. Lett. B **485** (2000) 388 [arXiv:hep-ph/0005214]; W. Buchmuller, L. Covi, K. Hamaguchi, A. Ibarra and T. Yanagida, JHEP **0703** (2007) 037 [arXiv:hep-ph/0702184].